PENETRATION OF NUCLEAR RADIATION INTO SHAFTS, TUNNELS AND ENTRANCEWAYS

by

B.W. Vanzant
R.C. DeHart

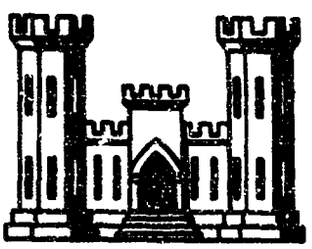

June 1966

for

Department of the Army
Office of the Chief of Engineers
Washington, D.C.

Contract No. DA 49-129-Eng.-504

by

Southwest Research Institute
San Antonio, Texas

3

DEPARTMENT OF THE ARMY
OFFICE OF THE CHIEF OF ENGINEERS
WASHINGTON, D.C. 20315

IN REPLY REFER TO

ENGMC-EM 26 September 1966

SUBJECT: Report on Penetration of Nuclear Radiation into Shafts, Tunnels and Entranceways by Southwest Research Institute

TO: DISTRIBUTION LIST

1. The attached report records the results of an attempt to utilize existing laboratory experimental data and empirical relationships to calculate the penetration of gamma and neutron radiation from nuclear weapons into protective structures. The study was prompted by a need for practical procedures for design.

2. The objective was to find relationships among the variables and to secure quantitative data to enable an engineer to compute the total dose within an open shaft or tunnel when exposed to the burst of a nuclear weapon.

3. Expressions for transmission factors which had been developed from laboratory experiments and theory were examined for possible practical application. It was found that the empirical expressions had been developed from point source data or from idealized distributions located at the mouths of small scale ducts. An attempt was made to modify these expressions for application to full scale situations. This was done with considerable reservation since no data was available to justify the assumptions which were made.

4. Comparison of the results of calculations using the developed expressions with limited measurements from full scale tests and with data from simulated full scale tests conducted at the Oak Ridge Tower Shielding Facility was disappointing.

5. The difficulties encountered in trying to utilize the results of the many laboratory experiments and the resulting poor agreement with full scale tests and simulated full scale experiments point out the limitations of the laboratory research programs using point sources and idealized distributions at the mouth of openings. Experiments of the type conducted at the Oak Ridge Tower Shielding Facility appear to be the best source of

ENGMC-EM 26 Sep 66

Subject: Report on Penetration of Nuclear Radiation into Shafts, Tunnels and Entranceways by Southwest Research Institute

data for practical application and for verification of theoretical computational techniques. We agree with the authors that with available methods and data, it is not possible to calculate, with any degree of certainty, the amount of radiation from a nuclear weapon that penetrates openings. Comments on the attached report are solicited.

FOR THE CHIEF OF ENGINEERS:

H. B. JACKRISON, SR.
Chief, Engineering Division
Military Construction

1 Incl
Report by SRI

DISTRIBUTION:

ARMY

2 Commanding Officer, U. S. Army Nuclear Defense Laboratory
ATTN: Mr. M. J. Schumchyk
ATTN: Dr. H. Donnert
Edgewood Arsenal, Maryland 21040

2 Director, U. S. Army Engineer Waterways Experiment Station
ATTN: Mr. Klaus Donat
ATTN: Library
Vicksburg, Mississippi 39180

1 Director, Ballistic Research Laboratories
ATTN: Mr. A. Budka
Aberdeen Proving Ground, Maryland 21005

1 Chief of Research and Development, Department of the Army
ATTN: Atomic Office, Washington, D. C. 20310

2 Commanding Officer, U. S. Army Engineer Research and Development Center, ATTN: Information Resources Branch,
Fort Belvoir, Virginia 22060

1 Commanding Officer, U. S. Army Combat Developments Command, Nuclear Group, ATTN: Major J. T. Gibson
Fort Bliss, Texas 79906

2 Commanding General, U. S. Army Materiel Command
ATTN: AMCPM-MBT; AMCRD-DN, Washington, D. C.

1 Director of Civil Defense, Office of the Secretary of the Army,
ATTN: Assistant Director for Research, Washington, D. C. 20310

1 Director of Civil Defense, Office of the Secretary of the Army,
ATTN: Dr. J. Buchanan, Washington, D. C. 20310

1 Division Engineer, Missouri River, Omaha Nebraska 68101

1 District Engineer, Omaha, Nebraska 68102

1 District Engineer, Mobile Alabama 36601

DISTRIBUTION (Cont'd)

NAVY

1 Chief, Naval Facilities Engineer Command, ATTN: Asst. Chief for Planning and Design, Department of the Navy, Washington, DC 20360
1 Chief, Naval Facilities Engineer Command, ATTN: Asst. Chief for RDT&E, Department of the Navy, Washington, D. C. 20360
1 Chief of Naval Research (Code 104), Department of the Navy, Washington, D. C. 20350
1 Commanding Officer and Director, U. S. Naval Civil Engineering Laboratory, ATTN: Dr. C. M. Huddleston, Port Hueneme, California 93041
1 Director, U. S. Naval Ordnance Laboratory, White Oak, Maryland
1 Commanding Officer and Director, U. S. Naval Radiological Defense Laboratory, ATTN: Dr. J. Ferguson, San Francisco, California 94135
1 Chief, Naval Facilities Engineer Command, ATTN: Code 74, Department of the Navy, Washington, D. C. 20390
1 Chief, Bureau of Ships, Department of the Navy, ATTN: Mr. L. Sieffert, Washington, D. C. 20360
1 Chief of Naval Operations, Department of the Navy, ATTN: OP-754, Washington, D. C. 20350

AIR FORCE

1 Research and Technology Division, Air Force Weapons Laboratory, Air Force Systems Command, Kirtland Air Force Base, New Mexico
1 Director, Air Force Nuclear Engineering Facility, Air Force Institute of Technology, Wright Patterson Air Force Base, Dayton, Ohio 45433
1 Chief of Staff, U. S. Air Force, ATTN: (AFRDPF) Major W. Dunn, Washington, D. C. 20330

OTHER GOV'T AGENCIES

3 Director, Defense Atomic Support Agency, ATTN: Chief, Nuclear Branch Washington, D. C. 20301
1 Commander, Field Command, Defense Atomic Support Agency, Sandia Base, Albuquerque, New Mexico
1 Radiation Shielding Information Center, Oak Ridge National Laboratory, P. O. Box X, Oak Ridge, Tennessee
1 Director, Oak Ridge National Laboratory, ATTN: Dr. Charles E. Clifford, P. O. Box X, Oak Ridge, Tennessee
1 Radiation Physics Laboratory, ATTN: Mr. Charles M. Eisenhauer, National Bureau of Standards, Washington, D. C. 20324
20 Defense Documentation Center, Cameron Station, Alexandria, Virginia 22314

DISTRIBUTION (Cont'd)

OTHERS

1 University of Illinois, Department of Civil Engineering, ATTN: Prof. A. B. Chilton, Urbana, Illinois 61803
1 Radiation Research Associates, Inc., ATTN: Dr. M. B. Wells, 1506 West Terrell Avenue, Fort Worth, Texas
1 IIT Research Institute, ATTN: Mr. C. W. Terrell 10 West 35th Street, Chicago, Illinois 60613
1 Stanford Research Institute, 333 Raven Wood, Menlo Park, California 94025
1 General American Transportation Corporation, 7501 North Natchez Avenue, Niles, Illinois 60648
1 Broadview Research Corporation, 1811 Trousdale Drive, Burlingame, California
1 Technical Operations Research, ATTN: Dr. Hans Tiller, Burlington, Massachusetts 01804
1 Ottawa University, Department of Physics, ATTN: Dr. L. V. Spencer, Ottawa, Kansas 66067
1 United Nuclear Corporation, 5 New Street, White Plains, N. Y. 10600
1 General Dynamics Corporation, General Atomic Division, P. O. Box 5, Old San Diego Station, San Diego, California 92100
1 Director, Applied Physics Laboratory, Johns Hopkins University, 8621 Georgia Avenue, Silver Spring, Maryland 20900
1 Los Alamos Scientific Laboratory, Los Alamos, New Mexico 87544
1 The Rand Corporation, 1700 Main Street, Santa Monica, Calif 90406
1 Applied Experiments Division, Sandia Corporation, Sandia Base, Albuquerque, New Mexico 87115
1 University of California, Lawrence Radiation Laboratory, Technical Information Division, Livermore, California 94551
1 Ammann and Whitney, Consulting Engineer, 111 Eighth Avenue, New York, N. Y.
1 Black & Veatch, Consulting Engineers, 1500 W. Meadow Lake Parkway, Kansas City, Missouri 64114

SOUTHWEST RESEARCH INSTITUTE
8500 Culebra Road, San Antonio, Texas 78206

PENETRATION OF NUCLEAR RADIATION INTO SHAFTS, TUNNELS AND ENTRANCEWAYS

B. W. Vanzant
R. C. DeHart

FINAL REPORT

SwRI Project No. 03-1238
Contract No. DA49-129-Eng-504

for

Department of the Army
Office of the Chief of Engineers
Washington 25, D. C.

June 1966

APPROVED:

Robert C. DeHart

Robert C. DeHart, Director
Department of Structural
Research

SUMMARY

It is important to designers of shelters to be able to determine the amount of radiation from a nuclear weapon detonation that penetrates shafts, tunnels and entranceways of the shelter. In this report, existing procedures available to designers are discussed, and a comparison is made between calculated results with those determined experimentally. This comparison clearly indicates that the agreement between experiment and calculation is not as close as is desirable. It is noted that consistent and complete laboratory experiments have not been undertaken for the purpose of determining transmission characteristics of radiation (gamma and neutron) from a nuclear weapon into tunnels with standardized cross sections, bends and intersections. Such a program would require the use of gamma and neutron radiation sources of appropriate energy levels placed at varying distances and angles from the tunnel opening. Most of the available empirical data were not directly applicable to the problem under consideration. When an appropriate source configuration was used, the tunnel configuration at the bend or intersection was not a practical one. When the tunnel configuration was appropriate, the source was clouded with background shielding, etc. In most cases, an empirical relation can be obtained for the measured data and a reasonable theoretical explanation can be given; but, there is little agreement between the various sets of data. Even in full-scale tests, there was little agreement between two types of measuring devices at the same point. In short, the existing data and procedures are lacking in agreement to such an extent that it appears at this time that the shelter designer cannot with any degree of certainty calculate the amount of nuclear radiation penetrating shafts, tunnels and entranceways.

It is believed that, if a laboratory program were to be undertaken with the purpose of providing consistent design curves for determining the transmission of radiation from nuclear weapon detonation into standard tunnel geometries, specific studies should be conducted so that it will be possible to obtain:

(1) Doses incident at given distances from the center of detonation of both fission and fusion weapons for air and ground bursts.

(2) The effect of distance and burst angle on source configuration across a tunnel opening as determined by clear and dusty environments for various energy levels.

(3) The effect of energy level and angle of burst on penetration into barrier material such as earth, concrete, iron and water.

(4) The effect of source configuration (point or plane) on transmission into square and round tunnels and around 90° bends with concrete and earthen tunnel walls.

(5) Experimental confirmation of procedures for transforming data obtained with point sources at various energy levels into data which would be obtained if a plane source were used.

(6) The effect of energy level and wall material on transmission characteristics around corners with various bend angles.

(7) The effect of the configuration of the tunnel intersection on transmission factors (square-round intersections, square-rectangular intersections and round-rectangular intersections).

(8) The effect of angle of burst on transmission into rectangular tunnels with the angle of burst being determined relative to both the long dimension and short dimension of the cross section of the opening.

(9) Directional characteristics of radiation from a weapon.

(10) The ability of water traps to increase neutron attenuation in tunnels.

(11) Design data for the efficiency of corner traps.

(12) The usefulness of baffled tunnels in decreasing the transmission of radiation into tunnels.

(13) The adherance of radioactive particles to various type surfaces and material.

(14) Experimental data on secondary gamma production in tunnels.

TABLE OF CONTENTS

TABLE OF CONTENTS (Cont'd)

TABLE OF CONTENTS (Cont'd)

TABLE OF CONTENTS (Cont'd)

SECTION 1. INTRODUCTION

This report discusses general design considerations pertinent to the calculation of nuclear radiation transmitted into shafts, tunnels, ducts and entrances of shelters and points out the limitations of existing design procedures. It should be noted that it is not possible, with available methods and data, to calculate with any degree of certainty, the amount of radiation that penetrates openings into shelters.

Openings into shelters may range in size from a 4-inch diameter for an air duct to a 25-ft. width for a two lane truck path. Penetration of gamma rays and neutrons associated with the initial radiation from a nuclear weapon detonation as well as the penetration of gamma radiation from fallout debris into these openings are of concern in this report. Alpha and beta radiations are not of interest since they do not penetrate materials more than a few millimeters and shielding against them presents minor problems. The weapon yields of interest vary from 1 KT to 100 MT, burst at distances corresponding to air blast overpressures from 1 to 1000 psi at the entrance to an opening.

The primary variables necessary for appropriate design are:

(1) The nature of the radioactive source

(2) Directional distribution and energy of the radiation incident at the face of the opening

(3) Type of material in the tunnel walls

(4) Tunnel length, width and height, and

(5) Angle and number of bends within the tunnel.

It is necessary to anticipate the radiated intensity and spectrum range incident in the tunnel vicinity in order to determine penetration and transmission of radiation into the tunnel proper. Wall material is important, of course, in that different materials produce different scattering effects on the incident radiation. Tunnel geometry is of consequence since appropriate configurations such as bending (lengthening and/or reducing the size of the tunnel opening) can minimize transmission of radiation through the tunnel. The total radiation at a point in a shaft or tunnel is the sum of the radiation that is transmitted through the entrance opening plus that which penetrates the walls. The latter will usually be negligible because of the attenuating effect of the over-burden. Possible configurations will, quite naturally, be limited by the intended use of the ducts or tunnels--air exhaust

or entry, etc. The following entrance configurations are deemed of importance for design considerations in calculating transmission of nuclear radiation into the main shelter area:

(1) Shelters with a straight horizontal or vertical tunnel (Fig. 1).

(2) Shelters with an entranceway having single or multiple bends (Fig. 2).

(3) Shelters with multiple entranceways or tunnels (Fig. 3).

The fundamental parameters of:

(1) Burst height and slant range of weapon,

(2) Weapon energy yield and total amount of initial gamma radiation and neutrons

should be considered when determining the nature of the radiation incident on the tunnel opening. It is not convenient, however, to consider other fundamental parameters, owing to their indeterminancy in specific situations. Among these are:

(1) Air density, humidity and velocity,

(2) Ascent velocity of radiating cloud, and

(3) Distribution of radiation sources within the cloud.

The rapid growth of nuclear science within recent years has resulted in the creation of new terms and evolution of existing terms such that they have new specialized meanings. Consequently, in Appendix H, specific terms and concepts are defined according to the connotation with which they are used in the report.

PLAN

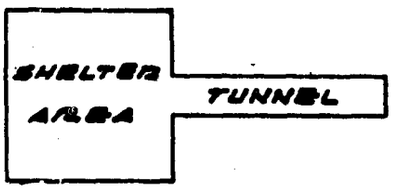

PLAN

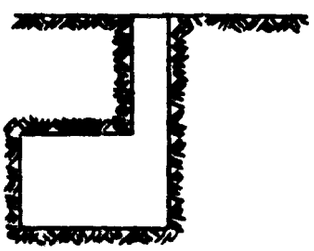

SECTION

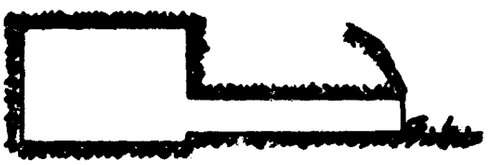

SECTION

FIGURE 1. SHELTERS WITH A STRAIGHT HORIZONTAL OR VERTICAL TUNNEL

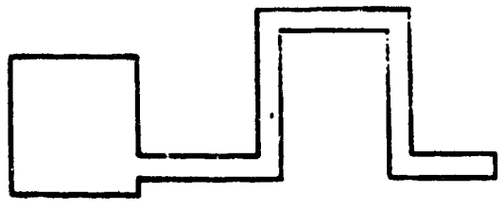

PLAN

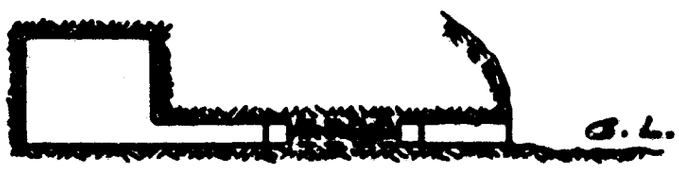

SECTION

FIGURE 2. SHELTER WITH ENTRANCEWAY HAVING SINGLE OR MULTIPLE BENDS (MULTIPLE SHOWN)

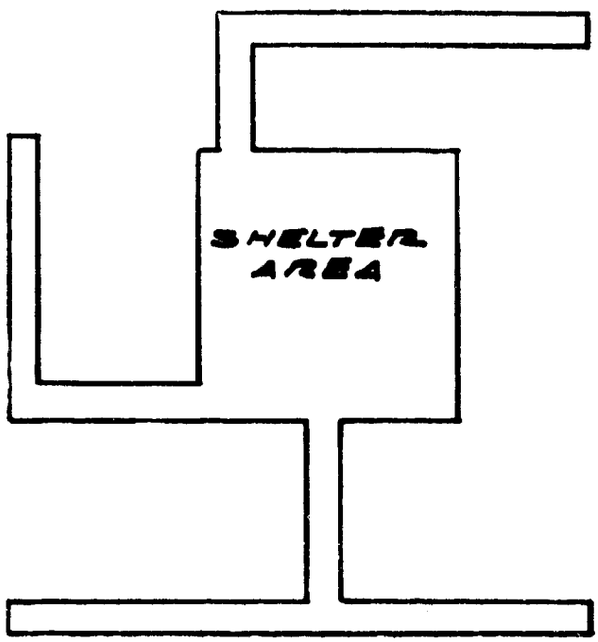

PLAN

FIGURE 3. SHELTER WITH MULTIPLE ENTRANCEWAYS OR TUNNELS

SECTION 2. GAMMA AND NEUTRON RADIATION FROM NUCLEAR WEAPONS

A. General

Radiation hazards from nuclear explosions exist not only within the first minute or so after detonation but also present problems for longer intervals due to contamination of fallout material. The radiation emitted within the first minute after detonation is termed initial radiation and consists of both gamma rays and neutrons. This is the only interval for which neutrons are a problem. Radiation hazards from fallout are limited to gamma rays.

Although the total of initial and fallout radiation is detrimental to human health, it is convenient to discuss the separate sources of initial gamma, neutron, and fallout radiation. Exposure to radiation is usually termed dose or dosage and is measured in several units (see Appendix C) among which are roentgens, rads and rems. It is interesting to note tha rems (roentgens equivalent man) is not a directly measurable physical quantity.[1]

B. Initial Gamma Radiation

Detailed information of initial radiation at given distances from ground zero is, in general, classified information due to its direct relation to type of weapon. Representative curves of initial radiation, however, are available. Initial gamma radiation at given distances from ground zero of a surface burst is shown in Figure 4. Since the radiation at a given distance from a surface burst is only two-thirds of that incident at the same distance from an air burst of a similar weapon due to the extra dust and debris, the value of Figure 4 can be multiplied by 1.5 to give values for initial gamma radiation from an air burst.[2] It is to be noted that the gamma radiation incident at various distances from a 100-MT weapon is not available from References 2 or 3.

C. Neutron Radiation

Neutrons emitted during weapon detonation have a range of energies but are predominantly in the high energy region. These high energy neutrons are called fast neutrons. Those neutrons having energies in excess of 0.5 Mev may be arbitarily considered to be fast neutrons. Thermal neutrons in contrast are, by definition, those in thermal equilibrium with their surroundings. They have very low energies - a fraction of an electron volt, often treated as a single value of about 0.025 ev. Despite their low energy, when they are captured (as in a shield or wall materials), the process results in release of highly energetic gamma rays.

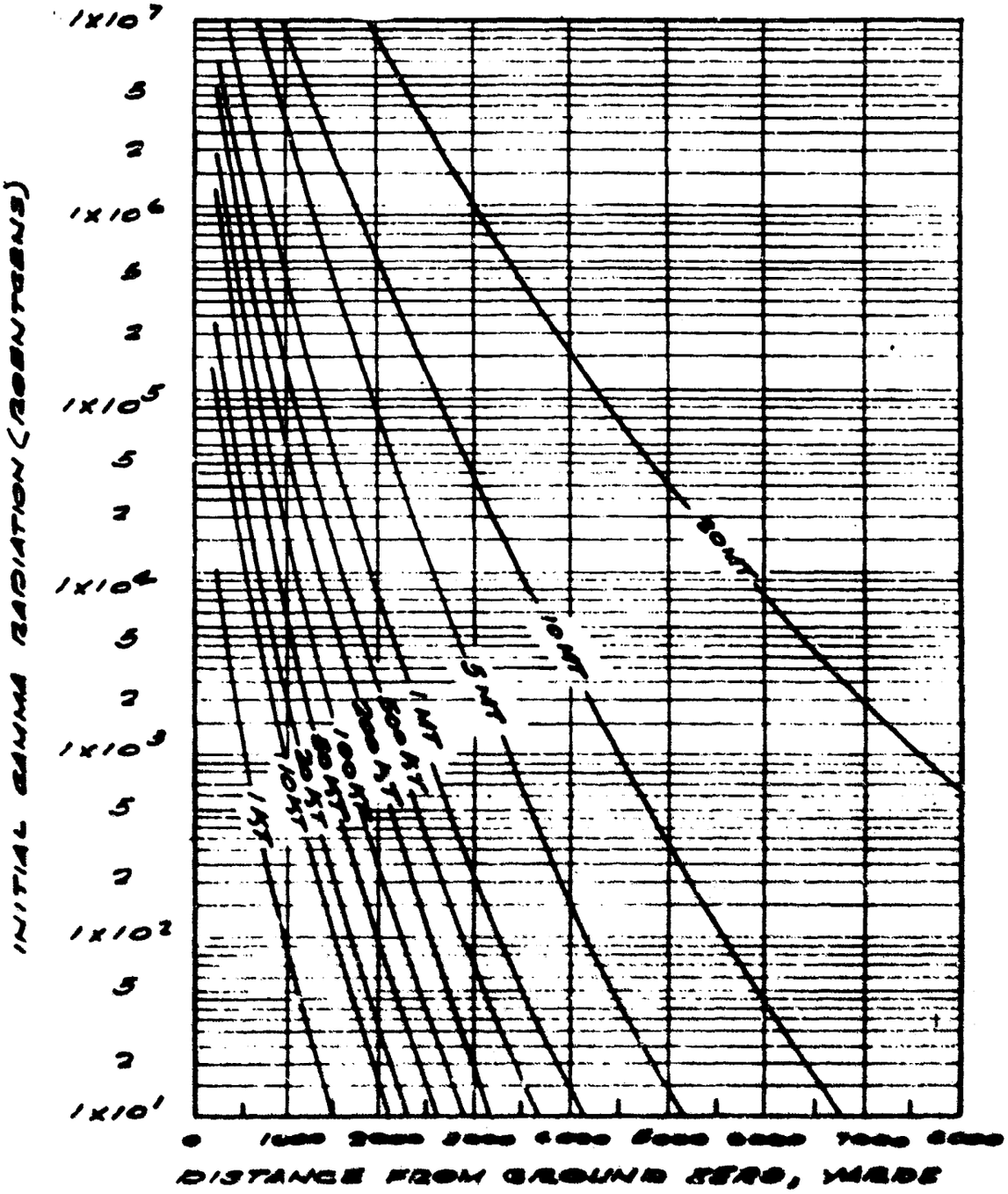

FIGURE 4. INITIAL GAMMA RADIATION, SURFACE BURST, 0.9 AIR DENSITY[3]

Neutron flux is a means of expressing neutron intensity and is measured in terms of the number of neutrons passing through a unit area in a unit time, or

$$\phi = \rho V_s \quad \frac{\text{neutrons/cm}^2}{\text{sec}}$$

(See Appendix B for nomenclature.) Integrated neutron flux is the time integral of the above product, or

$$\phi_T = \int \rho V_s dt \quad \frac{\text{neutrons}}{\text{cm}^2}$$

It should be notedthat, since the average velocity is used, the integrated flux represents neutrons at all energy levels received at a point during a time interval.

Neutron emission varies between weapons of different types, i.e., fission or fusion. Since the relative biological effectiveness (RBE) is considered to be unity, the rad (unit of absorbed radiation) is numerically equivalent to the rem, which is useful for expressing relative magnitude of biological destructiveness. The relation between neutron dose and distance is given for fission weapons (less than 100 KT) in Figure 5. Similar relations for fusion weapons are shown in Figure 6. Variations which occur among different weapons of either the fission of fusion type are not within the scope of this report.

D. Fallout Radiation

Residual radiation is usually considered to be that which is emitted later than one minute after the initiation of the explosion. This radiation results from fission fragments or neutron induced activity and manifests itself as a hazard in the form of gamma rays from fallout particles.

It is convenient to discuss radiation from fallout in terms of dose rate at unit time, commonly called unit-time reference dose rate of H + 1. Although a time reference base of one hour has been chosen, it should be remembered that near ground zero the initial dose rate may be considerably higher than the H + 1 rate and that at greater distances the time of arrival is longer than one hour. The time of arrival must be known in order to calculate the total dose.

Fallout patterns can be depicted by a series of contours or isodose-rate lines, as shown in Figure 7, for a megaton fission burst. Alternatively, the dose rate contours may be presented in tabular form, as shown in Figure 8, for a 20-KT surface burst. From these figures, it is possible to estimate the dose rate and arrival time downwind from an explosion, and, from Figure 9, the accumulated dose may be determined. For example,

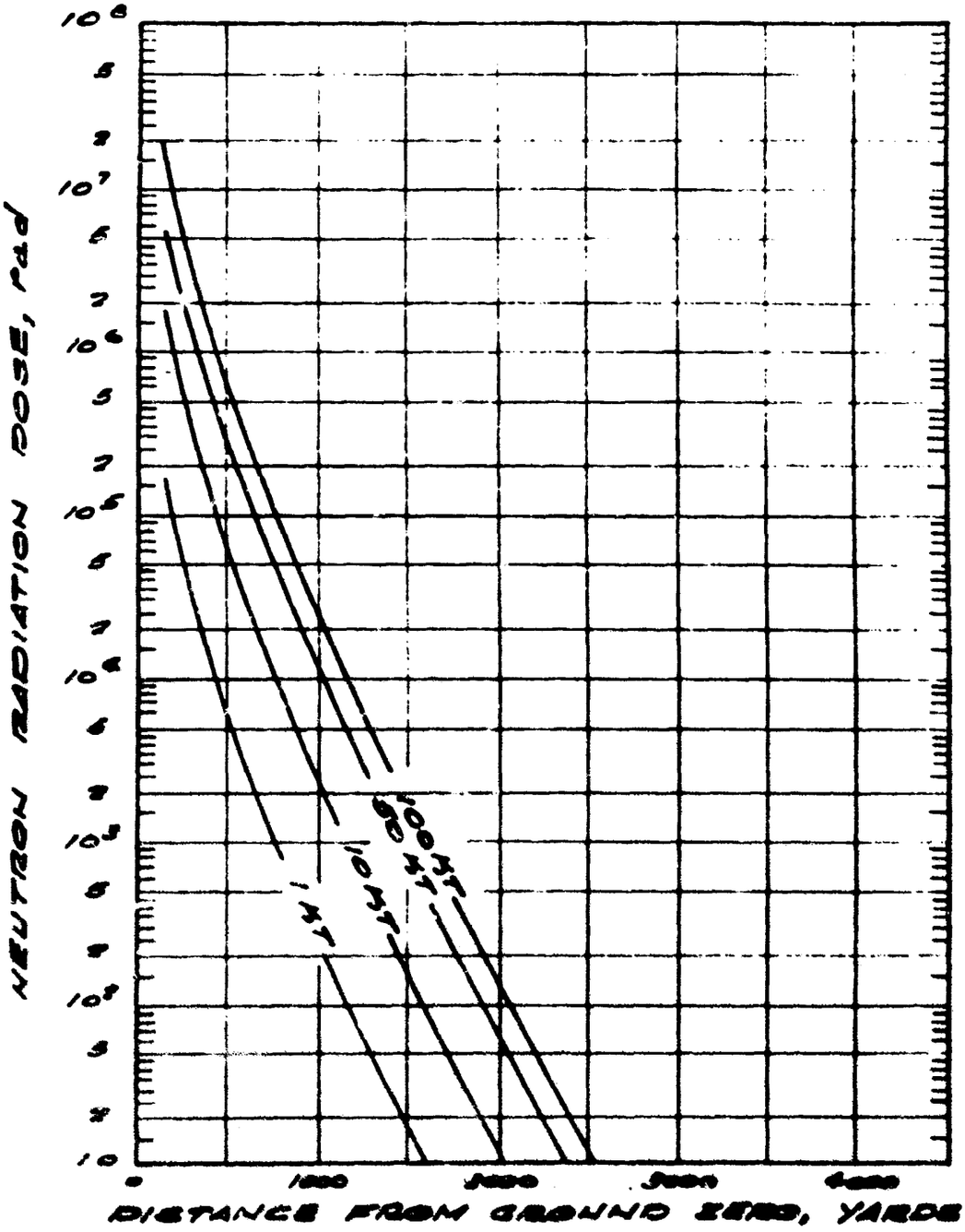

FIGURE 5. NEUTRON RADIATION DOSE, SURFACE BURST, FISSION WEAPON, 0.9 AIR DENSITY[3]

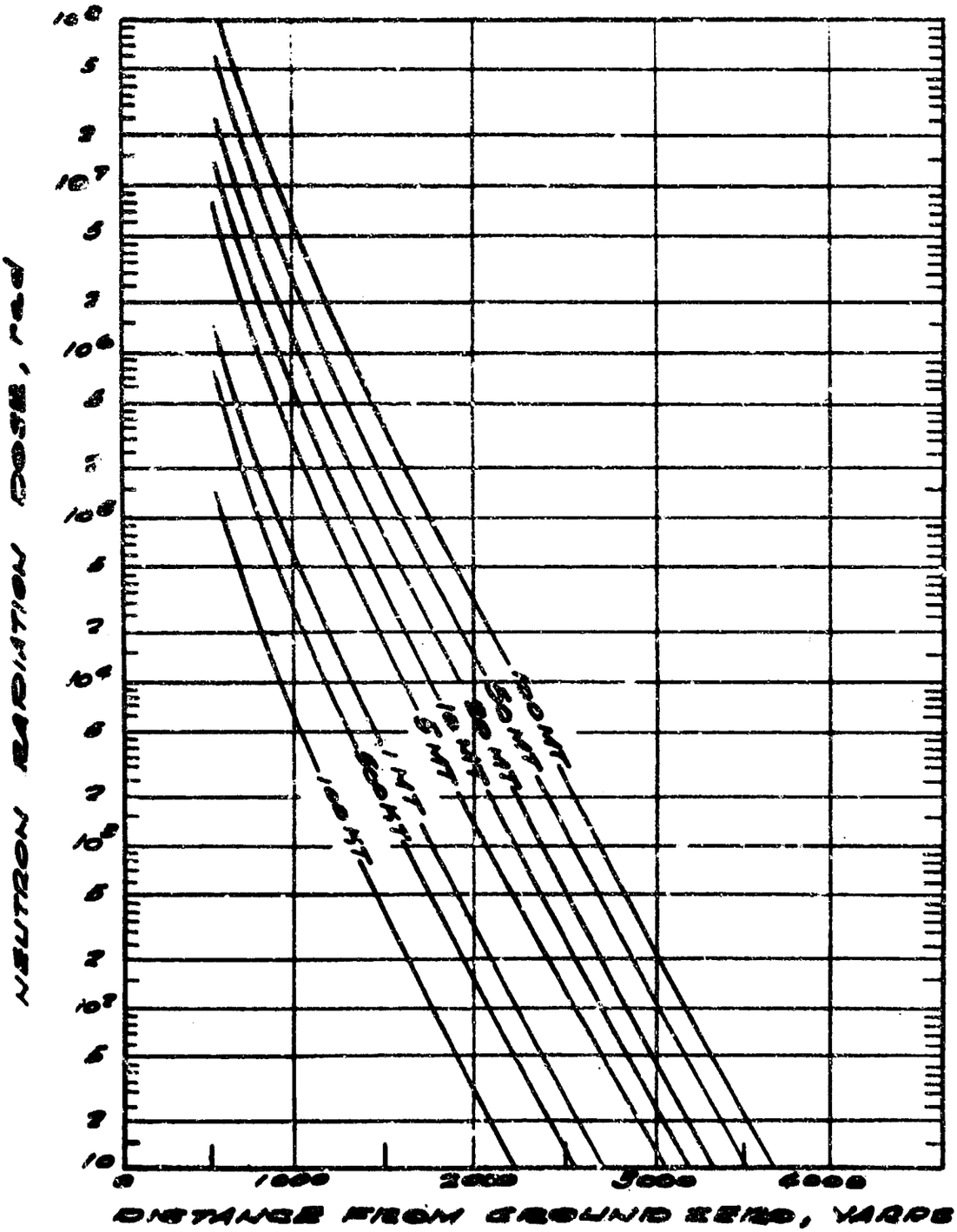

FIGURE 6. NEUTRON RADIATION DOSE, SURFACE BURST, FUSION WEAPON, 0.9 AIR DENSITY[3]

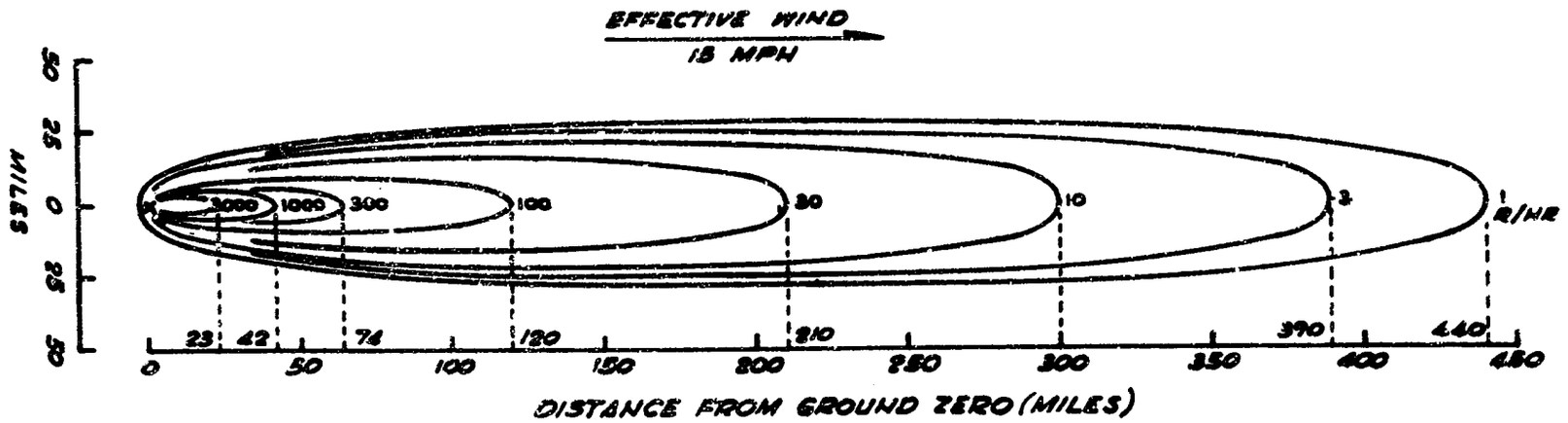

FIGURE 7. IDEALIZED UNIT-TIME REFERENCE DOSE RATE PATTERN FOR EARLY FALLOUT FROM A 1-MEGATON FISSION YIELD SURFACE BURST, 15 MPH EFFECTIVE WIND SPEED (UNIT TIME OF 1 HOUR AFTER BURST)[2]

GRAPHIC REPRESENTATION

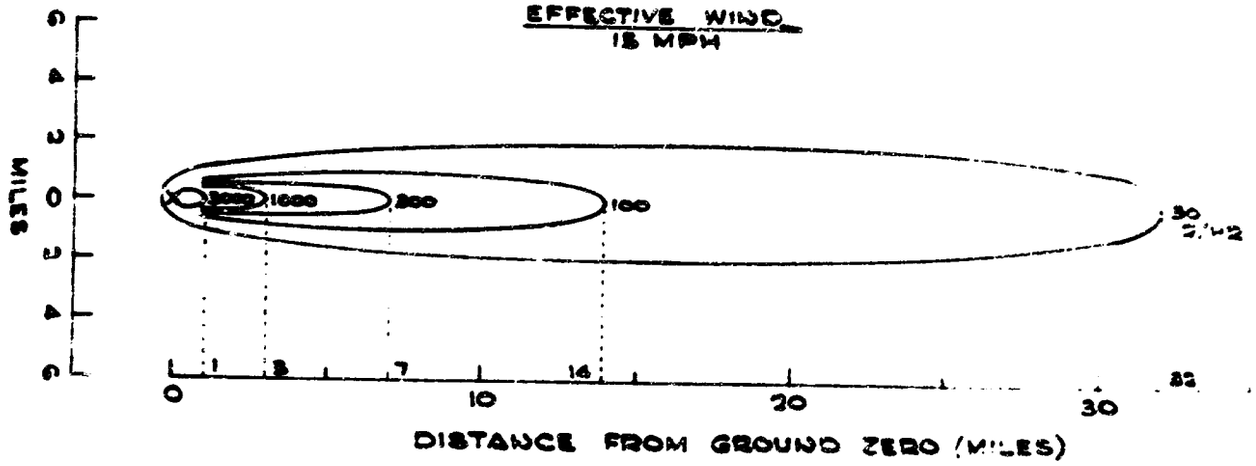

TABULAR REPRESENTATION

REFERENCE DOSE RATE (ROENTGENS / HOUR)	DOWNWIND DISTANCE (STATUTE MILES)	MAXIMUM WIDTH (STATUTE MILES)
3000	1	< 0.5
1000	3	< 1.0
300	7	1
100	14	2
30	32	4
10	60	6
3	100	11
1	150	16

FIGURE 8. GRAPHIC AND TABULAR REPRESENTATION OF DOWNWIND EXTENT OF UNIT-TIME REFERENCE DOSE RATE CONTOURS FOR 20-KT SURFACE BURST WITH 15-MPH WIND (UNIT TIME OF 1 HOUR AFTER BURST)(2)

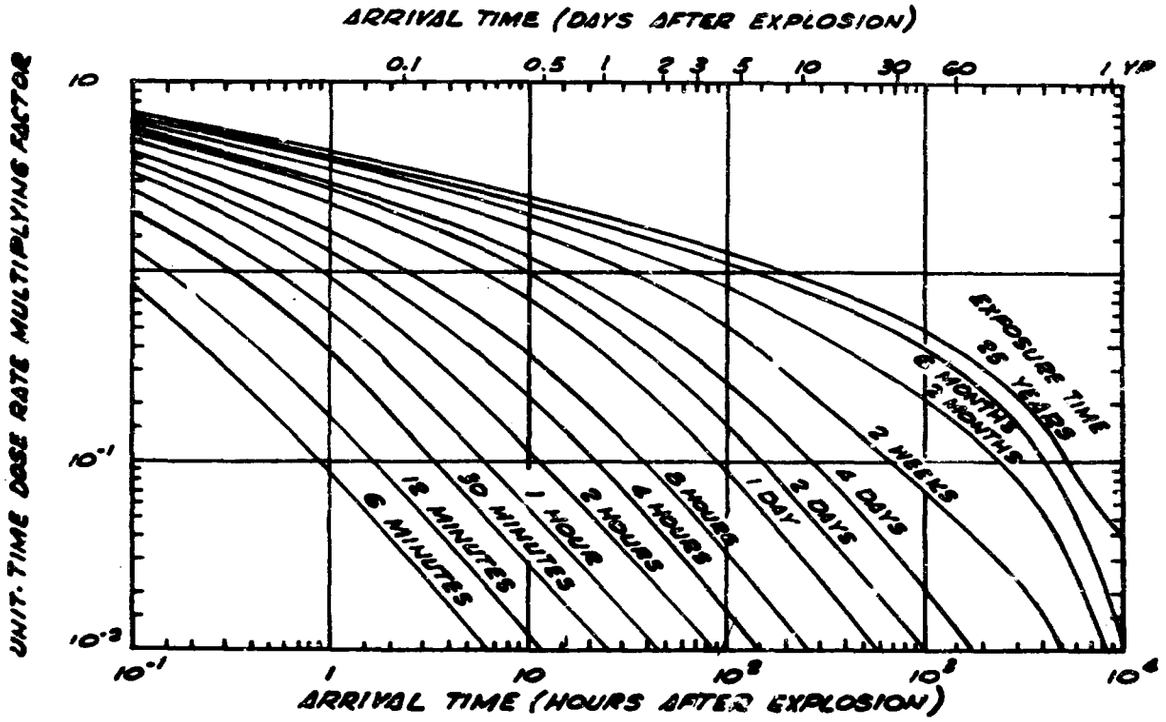

FIGURE 9. TOTAL RADIATION DOSE FROM EARLY FALLOUT BASED ON UNIT-TIME REFERENCE DOSE RATE (UNIT TIME OF 1 HOUR AFTER BURST)(2)

consider a 10-megaton surface burst with a fission yield of 50 percent in an effective wind of 25 mph averaged from the surface to 80,000 feet. Figure 7 is scaled approximately by multiplying the contours (dose rate) by 15/25 or 15/v and the downwind distance from ground zero by 25/15 or v/15, where v is the effective velocity in the situation under consideration. Plotting the scaled values of reference dose rate versus downwind distance on log-log paper, it is seen that the reference dose rate 100 miles downwind is 270 roentgens per hour, and at 200 miles downwind it is 60 roentgens per hour. Since the fission yield is 5 megatons, the reference values obtained must be multiplied by 5 to obtain the unit-time reference dose rates of 1350 roentgens/hr at 100 miles and 300 roentgens/hr at 200 miles.

The fallout obviously arrives 4 hours after burst 100 miles downrange and 8 hours after burst at 200 miles. These values may be considered as effective arrival times in Figure 9, from which it is seen that the total accumulated dose two days after the arrival of fallout is 2.2×1350, or about 2970 roentgens 100 miles downwind and around 1.8×300, or 540 roentgens 200 miles downwind.

The above data are from unclassified sources. More precise delineation, especially for close-in distances, is available from Reference 4.

After total fallout has occurred, and if the fallout is not being spatially displaced by winds, the ratios of dose rates (D) at corresponding times can be expressed as (5)

$$\frac{D_2}{D_1} = \left(\frac{t_2}{t_1}\right)^{-1.2}$$

where the t's represent elapsed times following the explosion. The total exposure dose E for some time interval $t_2 - t_1$ can be obtained from(5)

$$E = 5t_1D_1\left[1 - \left(\frac{t_2}{t_1}\right)^{-0.2}\right]$$

Values of these functions as related to the ratio t_2/t_1 are shown in Figure 10. For example, if the dose rate is measured to be 32 roentgens/hr 4 hours after an explosion, the rate in 2 days, or at $t_2/t_1 = 12$, is found to be 0.053×32, or around 1.7 roentgens per hour. The corresponding total dosage is seen to be 5×4 hours $\times 32 \times (0.39)$, or 250 roentgens.

E. Source Configuration

Source configuration refers to the paths taken by rays or particles emanating from the detonation of a nuclear device. The number of "collisions" encountered by the radiation between the source and the point of interest is

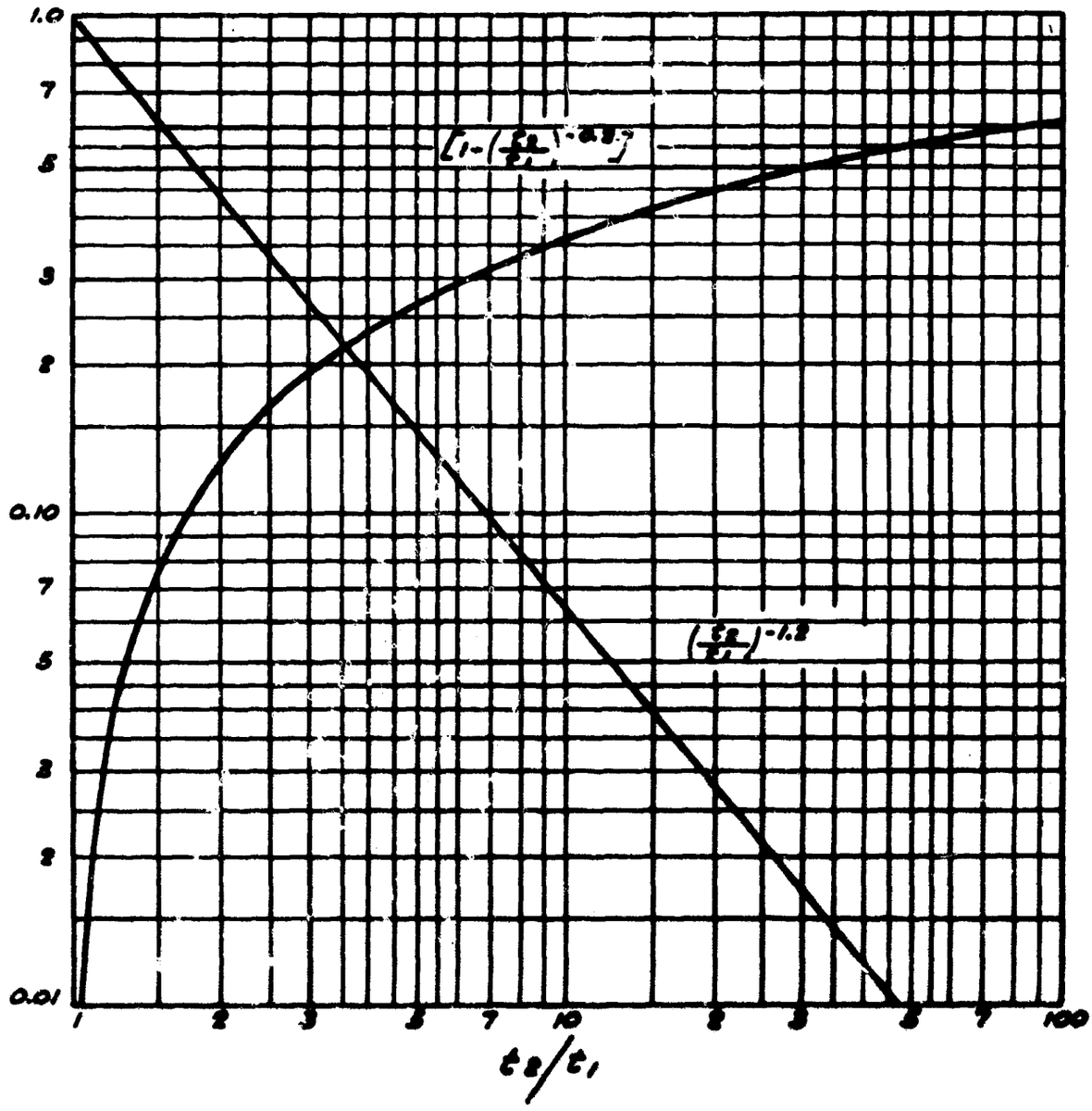

FIGURE 10. FUNCTIONS FOR OBTAINING THE RADIATION DOSE RATES AND CUMULATIVE DOSE AT DIFFERENT TIMES AFTER FISSION(5)

of consequence in determining how the source appears if observed from the point of interest. Actually, it is only possible to speculate as to how source configuration is affected by height of burst and distance from point of detonation, since these determinations have not been made in full-scale tests.

Usually, the ability of a particular type of radiation to penetrate a given structural configuration is experimentally determined with a finite source of radioactive material. It is then necessary to relate the effects measured from the known source to those that would be anticipated in a full-scale test. In this sense, source configurations are of theoretical consequence in that they determine the transformations necessary to relate laboratory data to full-scale effects.

1. Point Isotropic Source

A point isotropic source is the simplest type of source (Figure 11a). It consists of a small round source (or point) from which radiation is uniformly radially emitted. The intensity at a given distance from the source varies inversely with the surface area of a sphere encompassing that distance.

Point sources are of interest in both theoretical and experimental studies. For example, the methods of Section 9 were derived by considering a point isotropic source at the tunnel mouth; and the empirical relations of Section 8 were developed from experiments with a point source at a known distance from the tunnel mouth.

2. Plane Isotropic Source

A plane isotropic source (Figure 11b) is a plane array of point isotropic sources. Radiation paths from such a source have no predominant direction relative to the source plane. It is convenient at times to treat an interface through which radiation emerges as a source. Initial radiation incident on a tunnel opening can be considered to form a plane isotropic source across the tunnel opening if the burst angle is greater than 40°. The burst angle is defined to be the angle formed by the line of sight to the point of burst and the tunnel centerline. It is shown in Section 6C that a reasonable estimate of the radiation transmitted into a tunnel can be obtained by assuming a plane isotropic source at the tunnel opening.

As mentioned above, gamma radiation from fallout approximates that from a plane isotropic source.

3. Broadbeam Parallel Source

A broadbeam parallel source (Figure 11c) is considered to be a source which emanates radiation in parallel rays or paths. Initial gamma

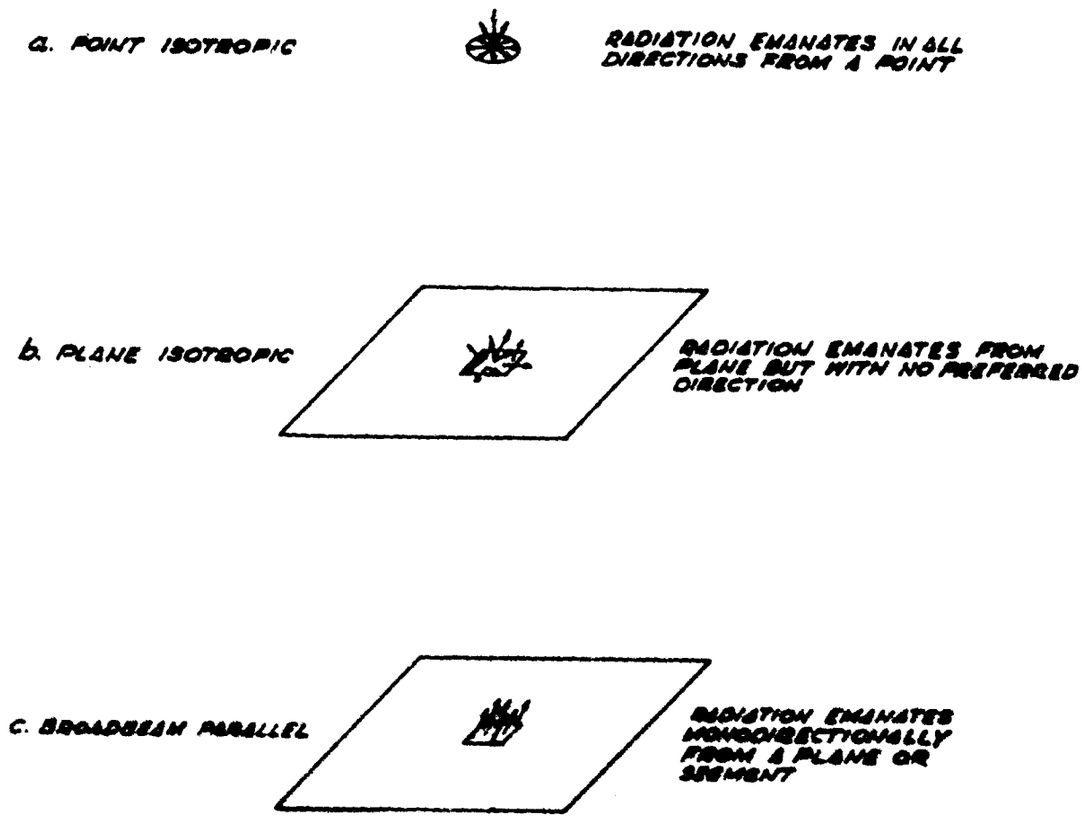

FIGURE 11. IDEALIZED SOURCE GEOMETRIES

radiation incident at burst angles less than 40° may be considered to arrive in parallel rays at the tunnel opening, in which instance no attenuation is considered to occur in the first leg of the tunnel. This type of source at a tunnel opening is not considered to be applicable to neutrons owing to their short mean free path in air.

4. Cosine Source

A cosine source or distribution is mathematically useful in describing the escape and scatter of neutrons at a surface. It has been experimentally observed[6] that the intensity (or number per unit solid angle) of neutrons emerging at a given angle from the normal to a unit surface area varies approximately as the cosine of that angle. This type of angular distribution, shown schematically in Figure 12, indicates that the neutron intensity per unit solid angle is greatest at 90° to the surface and is almost nonexistent at angles close to the surface. A unit solid angle is, of course, the surface area of a sphere of unit radius divided by 4π. The cosine distribution is of importance for calculating the scattering or albedo of neutrons in tunnel walls. Also, as will appear in Section 13C, it may be useful in describing incident neutron radiation.

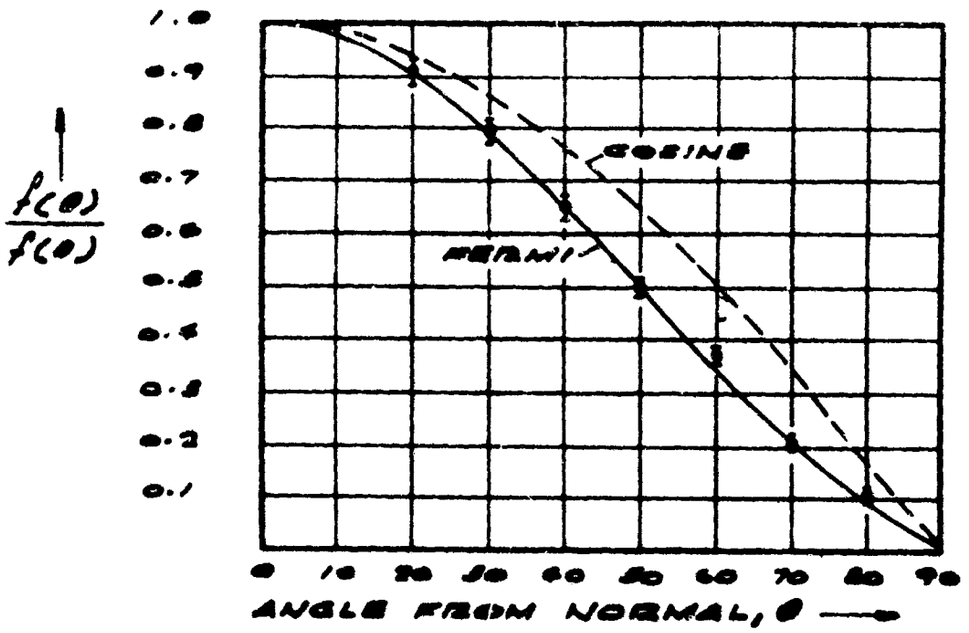

$f(\theta)$= number of neutrons emerging per unit area of surface per unit solid angle at angle θ

$f(0)$= normalising point: $\theta = 0$

Note: The curve plotted through the experimental points § is approximated by the dashed cosine curve.

FIGURE 12. COSINE DISTRIBUTION(6)

SECTION 3. RADIATION ENERGY RELATIONS AND SPECTRA

A. General

Radiation from a nuclear weapon encompasses a range of energies, but precise energy spectra are difficult to define due to variations among different weapons. Consequently, average or representative values are used to approximate the anticipated spectra. As is pointed out in Section 3D, experimental observations of energy spectra indicate that most of the radiation appears in a narrow energy range. The use of average or representative values also allows for computational expediency.

B. Energy Spectra for Initial Gamma Radiation

Initial gamma has been arbitrarily defined as that gamma radiation which is received within the first minute after detonation of a nuclear weapon. It may arise from (1) emission during fissioning, (2) induction by the neutron-nitrogen activation process, and (3) decay of fission fragments or products in the atomic cloud. However, since essentially all of the gamma emitted during the fission process is absorbed in the bomb material, the prompt emission is negligible.

Interaction of neutrons produced by the fissioning process with nitrogen in the air induces radiation termed nitrogen-capture gamma. The energy range for this radiation varies from around 4 to about 10 Mev as shown by Table I. Radiation at such a relatively high energy level is generally called hard, to distinguish it from low energy level, or soft radiation. Gamma radiation from fission products is relatively soft as shown in Table II. This source of radiation continues to emit past the arbitrary minute and is ultimately the source of fallout gamma.

C. Energy Spectra for Gamma Radiation from Fallout

The intensity of gamma radiation and its spectral distribution vary with time as shown in Figure 13. This figure indicates that during the first 30 minutes after detonation, the dominant energy range is around 0.5 Mev. Figure 14 shows specific variations within the fallout gamma spectrum at three specific times. At one hour, the total energy is fairly evenly distributed among gamma rays with photon energies between 0.5 and 2.5 Mev. By the end of the day, however, most of the radiation consists of photons with energies below 1 Mev. Energies a little greater than 1 Mev again become important after about a week. Finally, the lower energies again become prevalent. This is shown in Figure 15 where the averaged energy of emitted photons is plotted against time. Again, it is noted that the average energy approaches 0.5 Mev by the end of the day and remains close to this level thereafter.

TABLE I. NITROGEN-CAPTURE GAMMA SPECTRUM[7]

Energy (Mev)	Fraction Present
10.816	0.133
9.156	0.012
8.278	0.025
7.356	0.074
7.1[illegible]	0.025
6.318	0.119
5.554	0.200
5.287	0.306
4.485	0.106

TABLE II. FISSION-PRODUCT SPECTRUM[7]

Energy (Mev)	Fraction Present
2.55	0.023
2.10	0.030
1.65	0.002
1.35	0.212
0.75	0.682
0.35	0.051

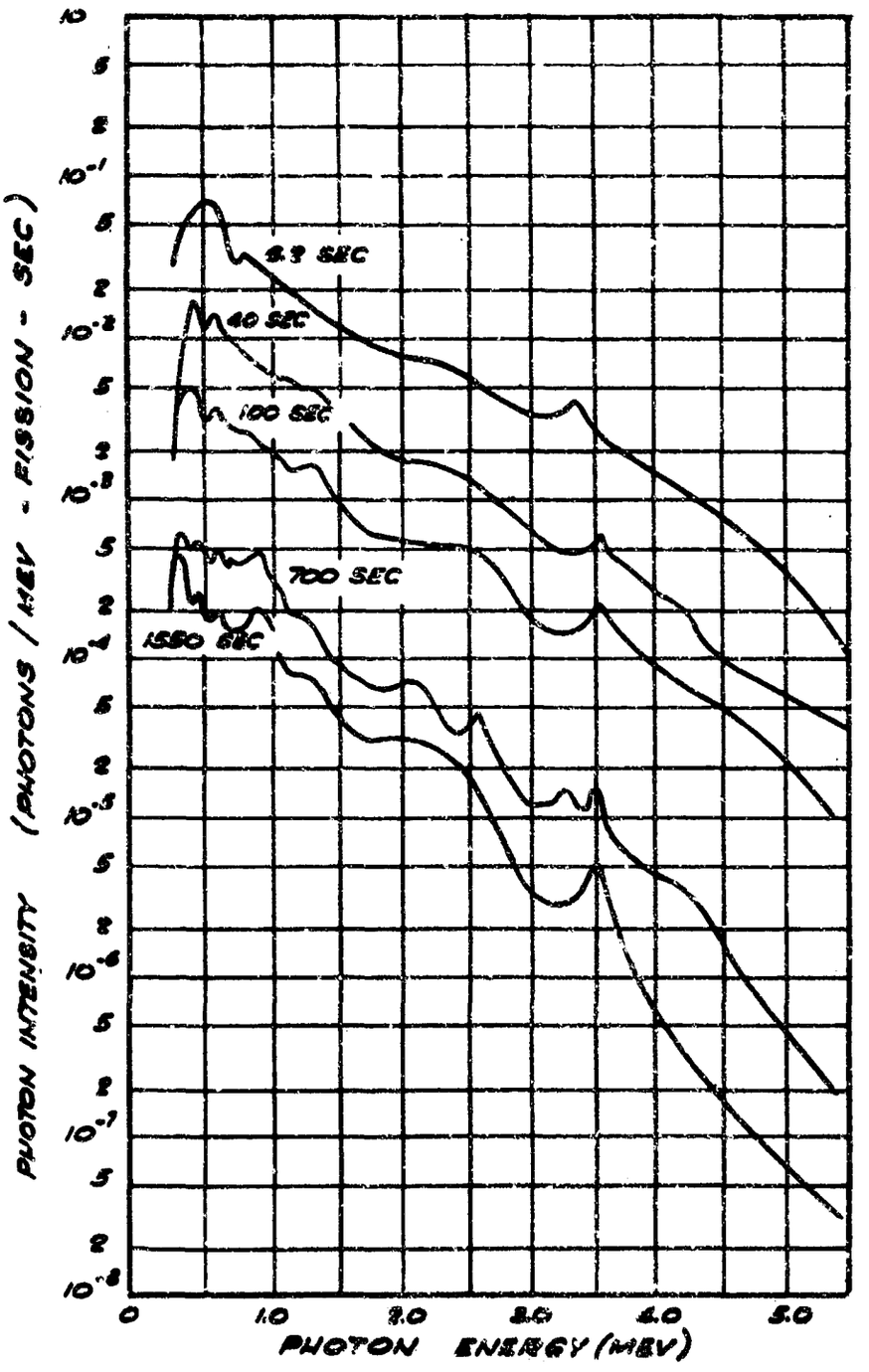

FIGURE 13. GAMMA SPECTRUM FROM THE DECAY OF FISSION PRODUCTS[6]

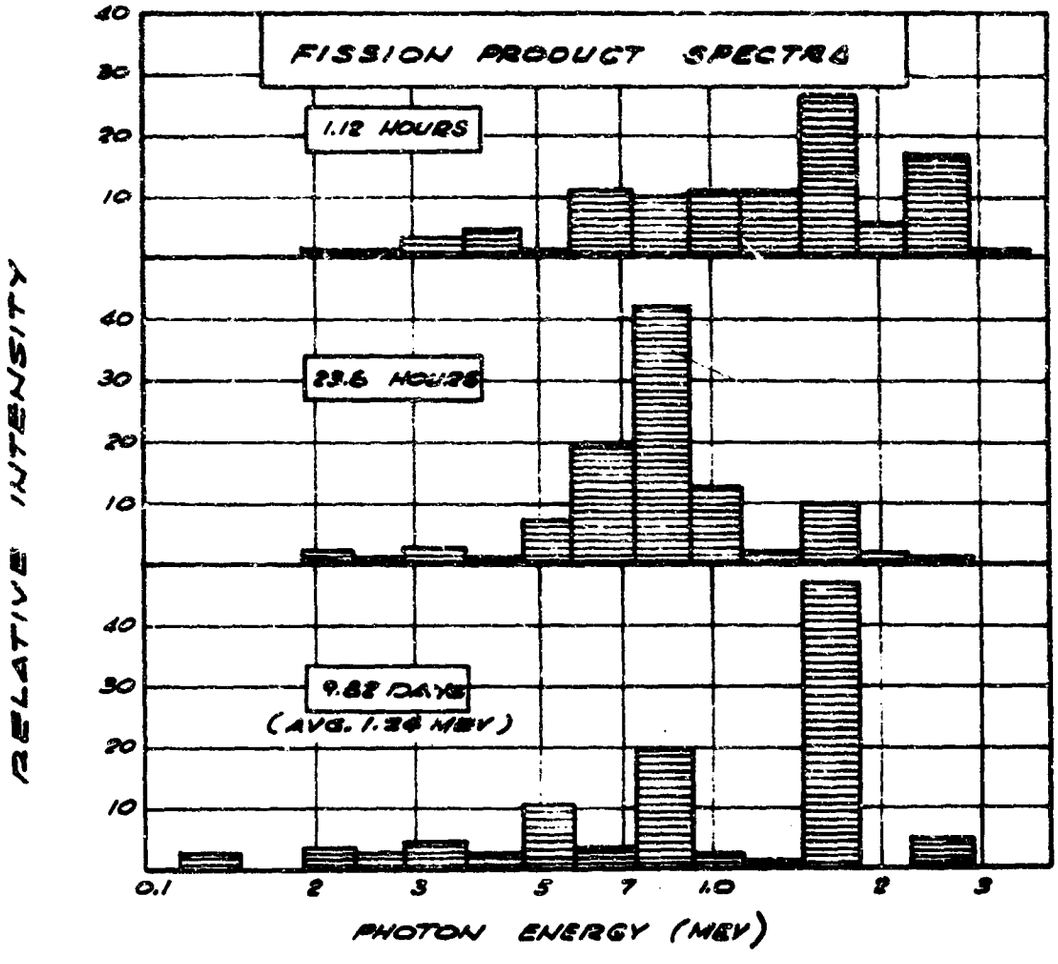

FIGURE 14. RELATIVE INTENSITIES OF DIFFERENT SPECTRAL COMPONENTS AT SEVERAL TIMES AFTER FISSION[5]

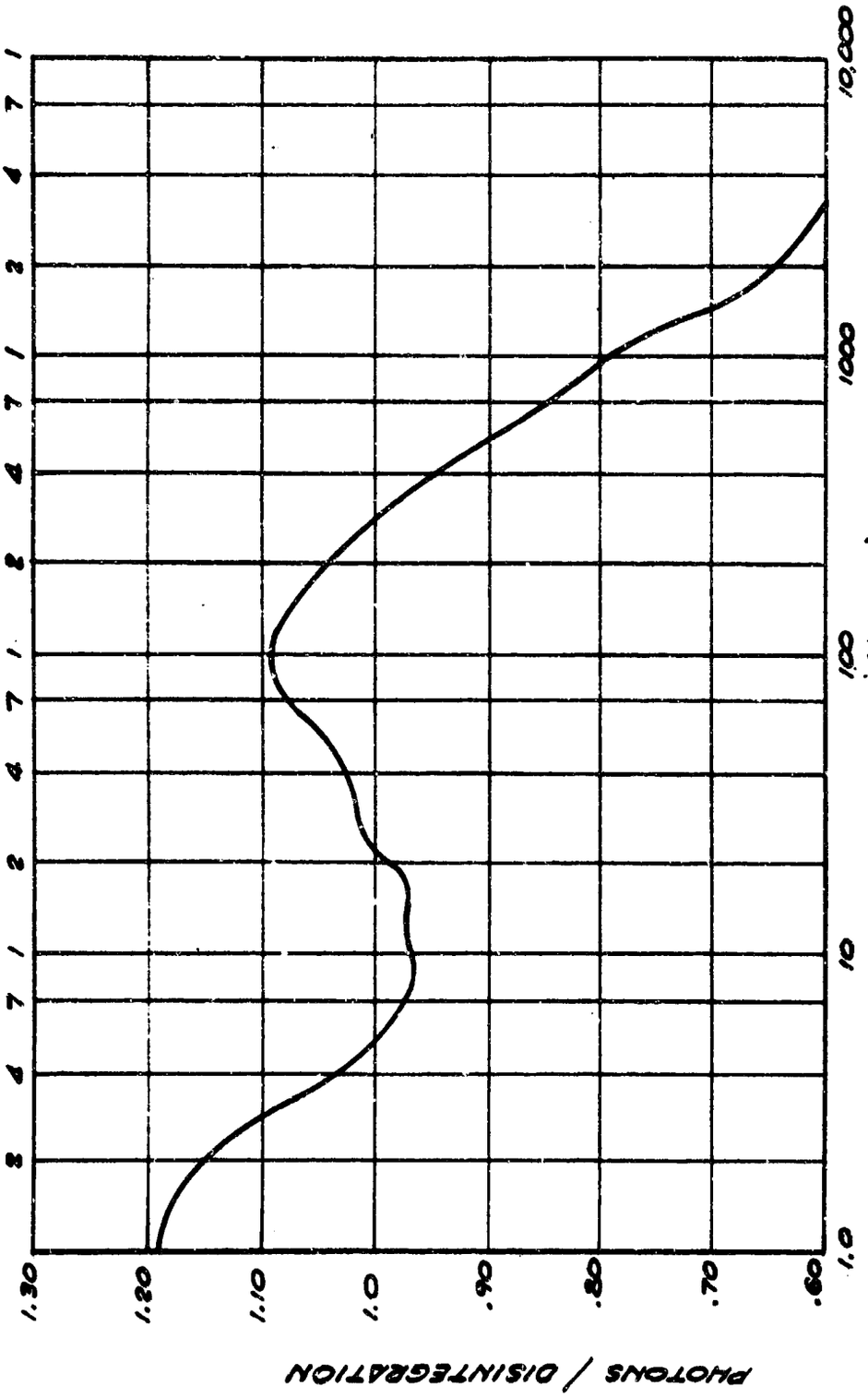

FIGURE 15. AVERAGE PHOTON ENERGY OF U^{235} FISSION PRODUCTS(9)

D. Averaged Levels of Gamma Ray Energy

It has been indicated that gamma radiation occurs in a myriad of spectra. These spectra are never precisely known, especially for enemy weapons; therefore, it is impossible to account for the various energy levels in an accurate manner. Because of the lack of more precise information, the choice of an average energy level to represent all the energy is as reasonable as any other approach that might be made. For example, in Table I, it is seen that a majority of nitrogen-capture gamma have an energy level of around 5.2-5.5 Mev. It has also been observed that penetration data are not highly sensitive to precise photon energies in the range of 4-10 Mev[10]. Consequently, there is a tendency to use 6.0 Mev as a representative energy level for the most penetrating of the initial gamma radiation from nuclear explosions, or the nitrogen-capture gamma.

Another representative energy level is 0.5 Mev as indicated by Figure 15 for times greater than one day after the time the burst has occurred. It has also been observed[10] that gamma radiation deflected by 90° (Compton Scattering) approximates this energy level, which is considered to be a representative level for fallout gamma.

Cobalt 60, a source often used in experimental work, emanates radiation at an average energy level of 1.25 Mev. Since this energy level is not only available for empirical observations but also approximates the principal energy ranges around 0.5 to 1.0 Mev in Figure 14 and Table II, it has been convenient to consider 1.25 Mev as an appropriate level for use in developing data suitable for the solution of fallout problems

It should be noted that investigators studying the penetration of nuclear radiation into shelters have found it expedient to choose representative energy levels that are relatively close to those available from laboratory sources. This allows for simulation experiments to approximate the effect of energy level on transmission of radiation from nuclear weapons into various geometric configurations. Of course, since information is not available from full-scale tests, the most reasonable approach would involve determining the "penetrability" into various geometric configurations of radiation at energy levels obtainable from laboratory sources and then summing the transmitted dose for weighted energy levels simulating the spectrum emanating from a nuclear weapon. The dose transmitted could be determined for either the worst case or a moderate case.

E. The Effect of Slant Range on Initial Gamma

The higher the energy level of gamma radiation, the longer its mean free path and the farther it is likely to travel before being absorbed. Nitrogen-capture gamma has a high energy level and penetrates farther than does fission product gamma. In Figure 16, it is seen that the percentage of nitrogen-capture gammas exceeds that of the fission product gammas except at short

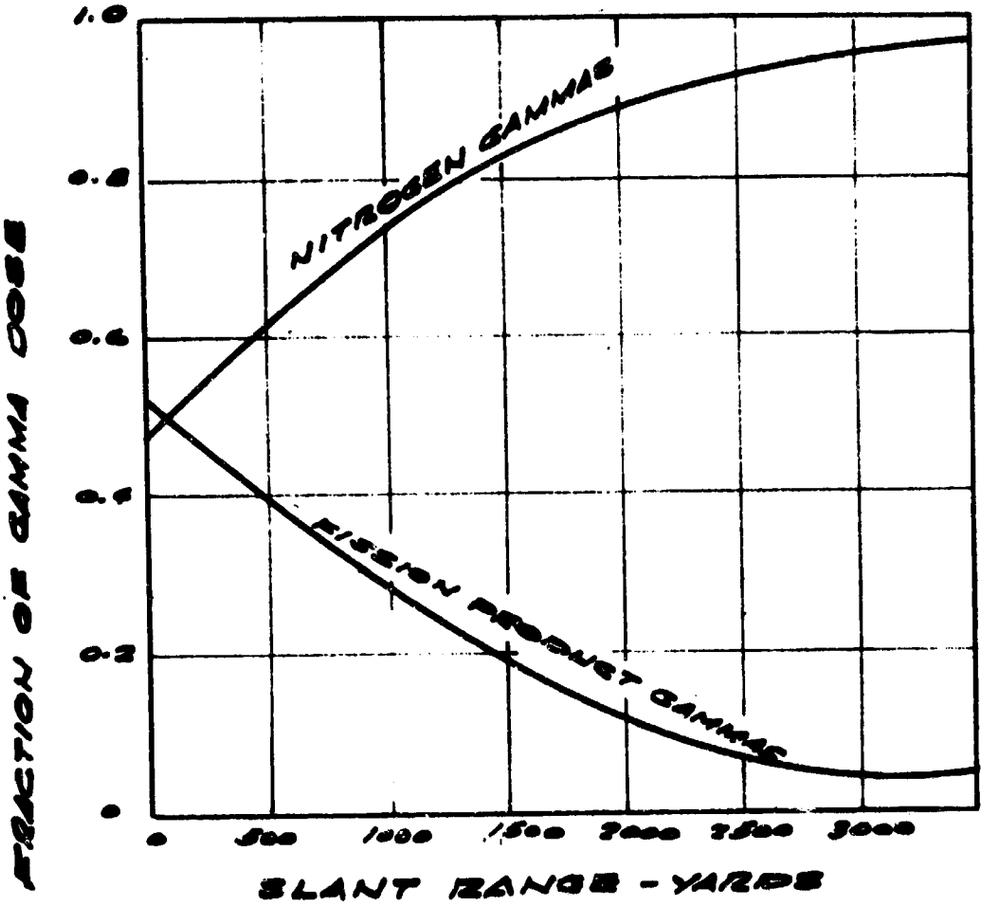

FIGURE 16. FRACTIONAL PARTITION OF INITIAL GAMMA DOSE AT SURFACE[7]

range[7]. This information has been experimentally verified for low and intermediate yields (up to 50 KT), but data for larger weapons are lacking.

That portion of nitrogen gamma which arrives at a point without having participated in a scattering reaction could perhaps be considered to arrive as broadbeam parallel radiation. The percentage of unscattered nitrogen-capture gamma arriving as broadbeam radiation at slant ranges from ground zero is shown in Table III[7] for low and intermediate yield weapons. With sufficient information, a method for partitioning the initial gamma into both a broadbeam and plane isotropic source at the tunnel opening could be developed. The need to partition gamma radiation into isotropic and broad beam parallel sources in order to significantly improve the accuracy of radiation penetration predictions could be established experimentally. It is pointed out in Section 6, however, that for engineering applications, fractional partitioning is not necessary. Also, Reference 7, which developed the method, indicates that in most instances a plane isotropic source can accurately approximate all of the initial gamma. Unshielded entranceways may, however, provide instances where this approximation is not very good.

F. Energy Spectra for Neutron Radiation

Fission neutrons emitted by the detonation of a nuclear weapon have energies ranging up to 14 Mev. Neutron energies are usually determined by threshold measurements. For example, the element sulfur becomes radioactive when it captures neutrons having energies in excess of 3 Mev. Some results of such measurements are shown in Figure 17, where it is seen that a majority of neutrons have energies less than 3.0 Mev. It should be noted that this is for fission weapons only.

This spectrum appears to remain relatively constant as the slant range increases[2]. Consequently, a representative and conservative energy level for use in determining neutron penetration into tunnels has frequently been taken to be 3.0 Mev.

As in the case of gamma, laboratory experiments are warranted to determine the transmission characteristics of neutrons with various energy levels into pertinent geometries.

TABLE III. PERCENT OF DIRECT NITROGEN GAMMA PHOTONS RECEIVED VS DISTANCE TO THE BURST POINT[7]

Slant Range to Burst, ft	% Rec'd Directly
1,000	74
2,000	57
3,000	48
4,000	38
5,000	32
6,000	28
7,000	25
8,000	23
9,000	20
10,000	18

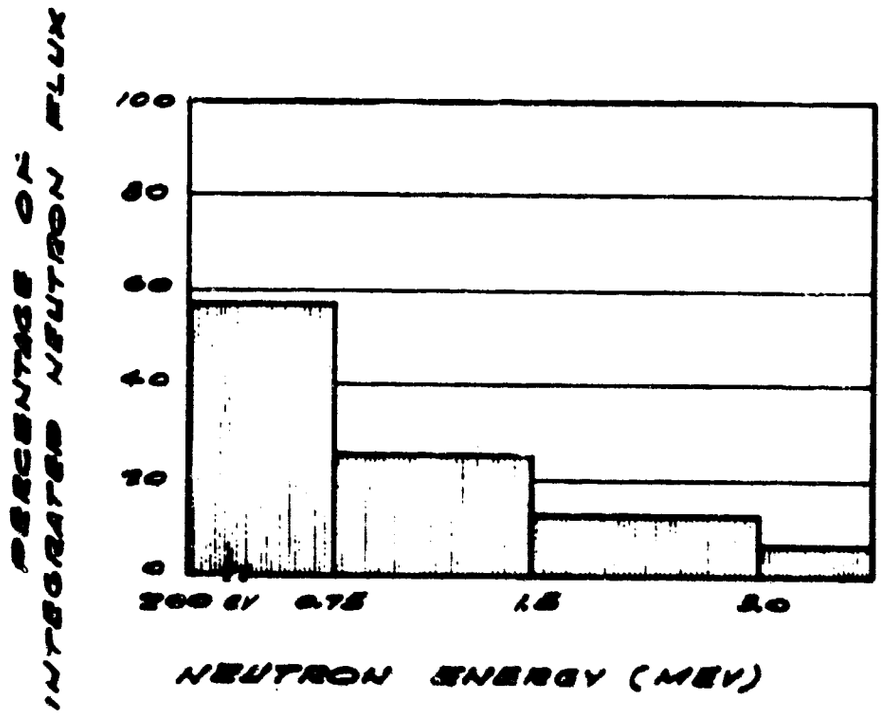

FIGURE 17. TYPICAL NEUTRON ENERGY SPECTRUM, FISSION WEAPON[2]

SECTION 4. TRANSMISSION FACTORS

A. Definition

Resistance of materials to penetration by radiation is usually discussed in terms of transmission factors. Transmission factors apply to solid materials for the case of barrier shielding and to air for the case of penetration into tunnels and entranceways. The factors are the ratios of the radiation received at a shielded point to that received at a reference point*. Symbolically,

$$T = \frac{D_p}{D_o}$$

where

T = Transmission factor for shielding material
D_p = Dose rate at a point behind a shield
D_o = Dose rate at the reference point

B. Initial Radiation

Values of transmission factors for initial radiation in various materials are shown in Figures 18 and 19. Factors for materials with densities different from earth and concrete may be estimated by density interpolation between the curves in Figure 18[3].

As an example of the application of the factors, consider a 100-KT fission burst at a slant range of 1500 yards in an 8-1/2-mph wind. From Figure 4, the initial gamma dose is about 1700 roentgen and from Figure 5, the neutron dose is close to 2000 rem. The radiation penetrating a one-foot concrete door would be $0.18 \times 1700 = 306$ roentgen for the gamma (as indicated by Figure 18) and $0.125 \times 2000 = 250$ rem for the neutrons (from Fig. 19). Thus, the total hazard from initial radiation would be 556 rems. It should be noted that the transmission factors listed in Figures 18 and 19 are for point sources with perpendicular incidence[3]. Such calculations overestimate the transmitted radiation.

Fallout from such a burst can be determined from the tabular representation of Figure 8. The downwind distance is multiplied by (8.5/15) and the contours by (15/8.5). A dose rate of 3550 roentgen/hr is obtained from a

*In most of the following sections, the reference point is taken as one unit of distance from the source.

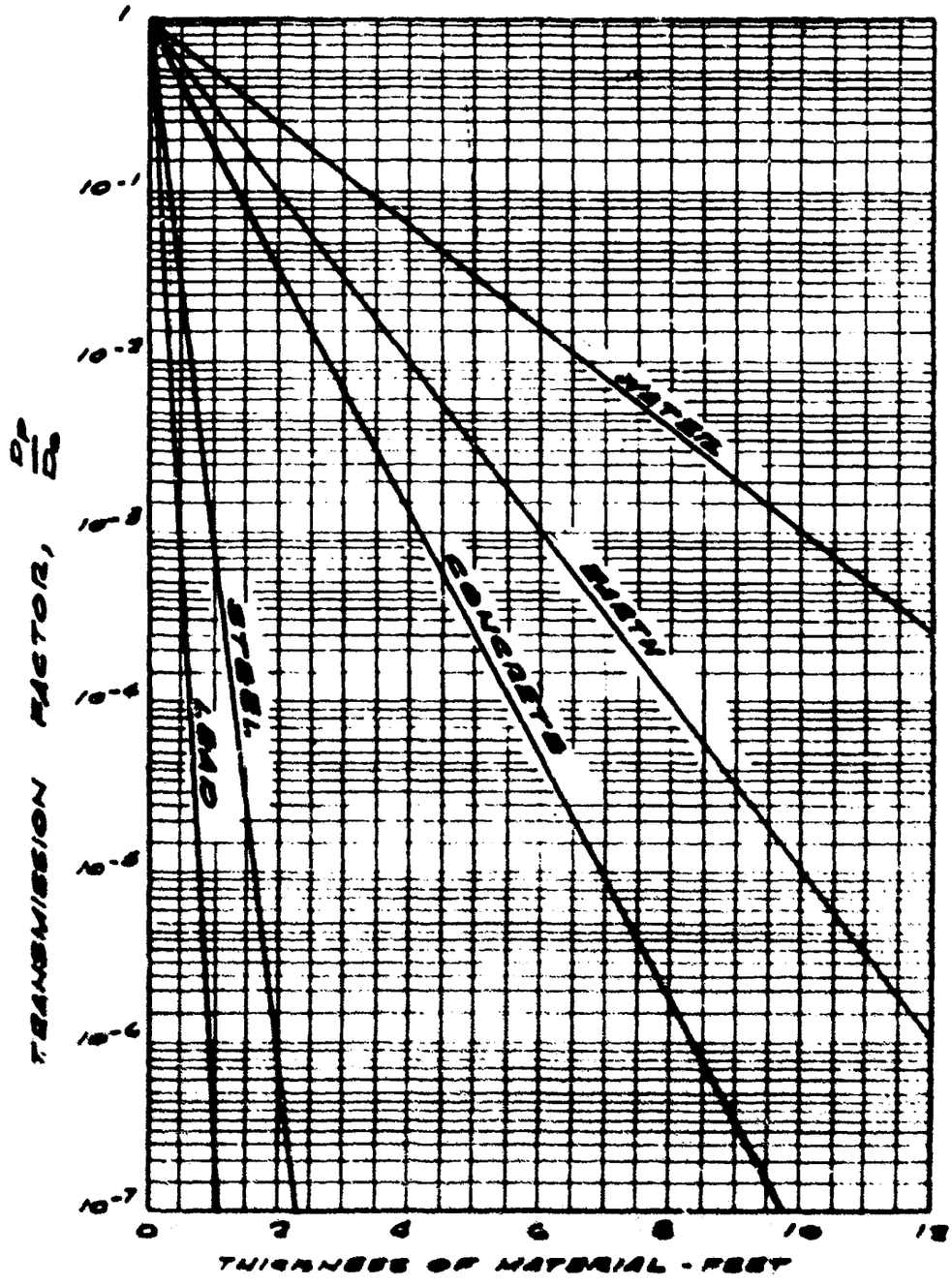

FIGURE 18. ATTENUATION OF INITIAL GAMMA RADIATION, POINT SOURCE AND NORMAL INCIDENCE[3]

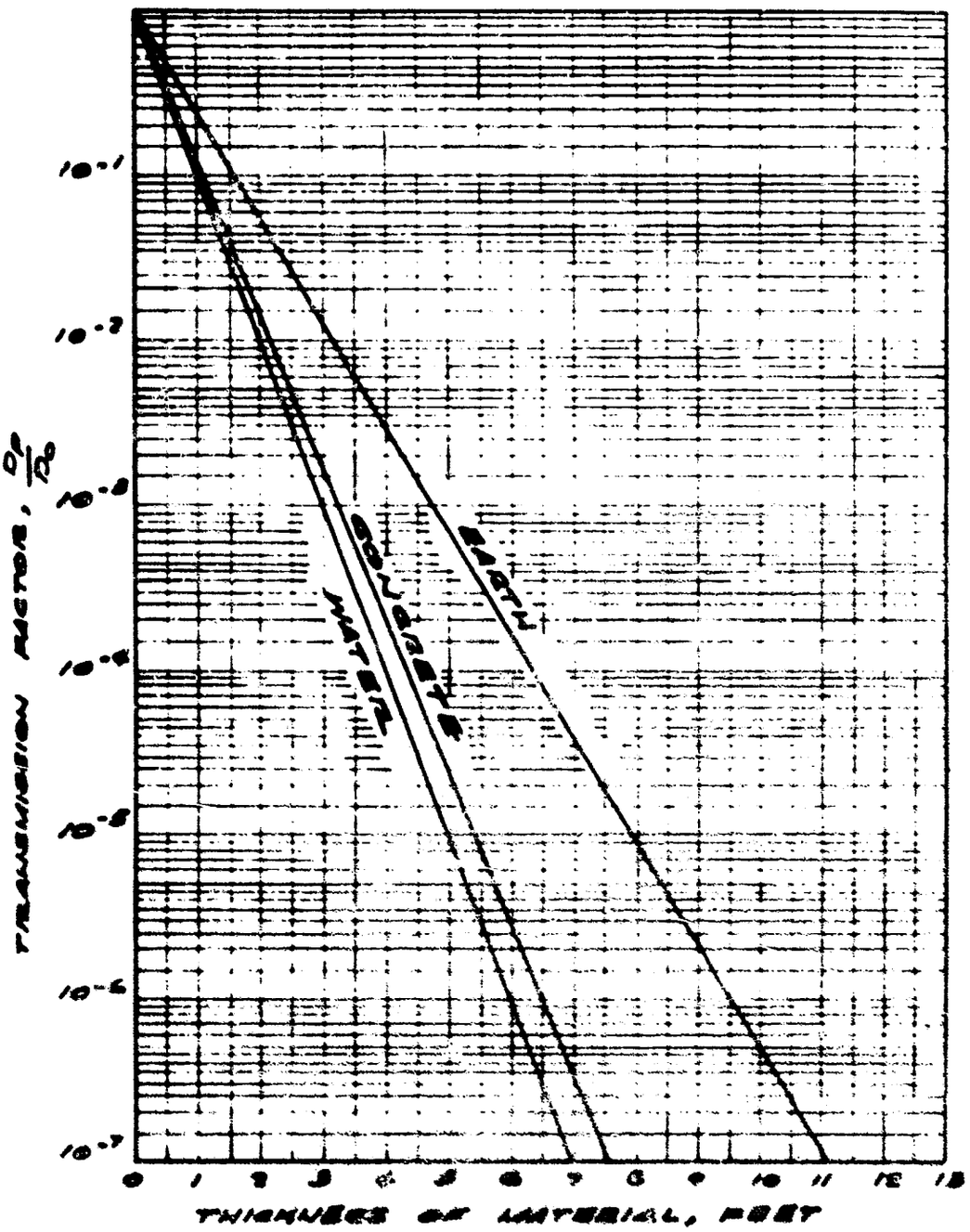

FIGURE 19. ATTENUATION OF NEUTRONS, POINT SOURCE AND NORMAL INCIDENCE[3]

log-log plot of these values, so that for the 100-KT burst the rate would be 5 X 3550 or 17,750 roentgen per hour. Of course, the fallout would arrive 6 minutes after the burst.

C. Fallout Radiation

Barrier shielding for fallout protection is fully treated in Office of Civil Defense Publications, such as Reference 11, and will not be treated here. Penetration of fallout gamma through openings can be handled on the same basis as initial gamma using isotropic sources, as the fallout is more nearly isotropic than the initial gamma.

D. Effect of Energy Level on Transmission Factor

It has been mentioned that high energy radiation is more capable of penetrating barrier materials than that at low energy. The effect of this phenomenon on transmission factors is shown in Figure 20 for the ability of water slabs to shield against neutron energies. For a plane isotropic source, the transmission factor is, from Figure 20, about 0.04 for 3-Mev neutrons incident on a 6-inch slab of water. On the other hand, from Figure 19, which is for a point isotropic source, the factor is 0.4 which is considerably more conservative. It should be noted that energy levels do not affect the transmission factor greatly for shields thinner than 6 inches[11]. Again, the lack of sufficient empirical information on energy level as it pertains to transmission characteristics is noted.

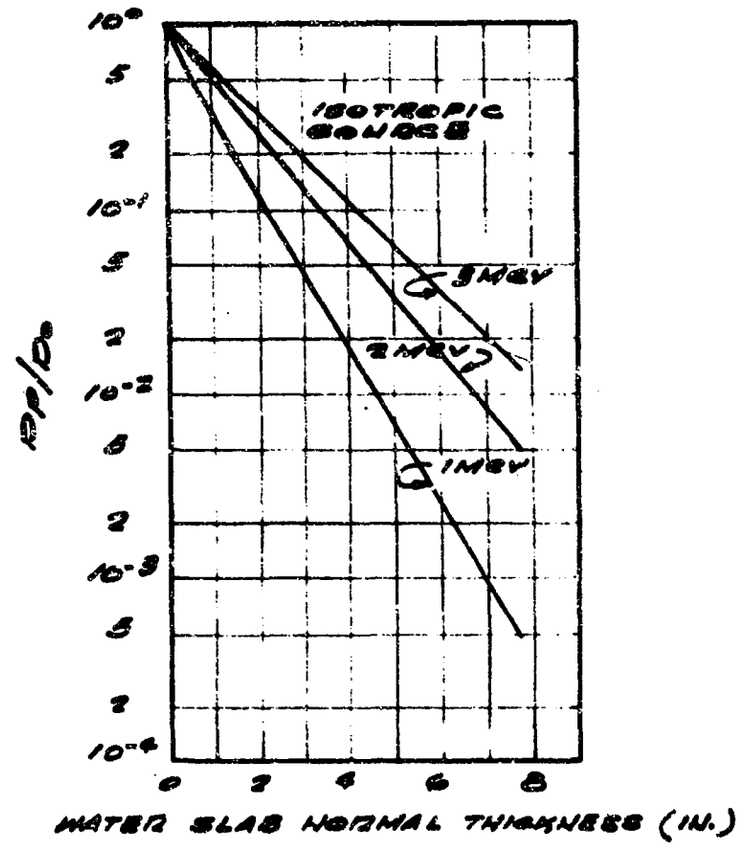

FIGURE 20. RATIO OF EMERGENT TO INCIDENT DOSE RATE FOR PLANE ISOTROPIC NEUTRON SOURCES INCIDENT ON SEMI-INFINITE SLABS OF WATER (MONTE CARLO CALCULATIONS)[12]

SECTION 5. RADIOLOGICAL ALBEDO IN TUNNELS

Radiation transmitted through a duct or tunnel to an area of concern within a shelter usually gets to this area after impinging on or scattering off the tunnel walls. The literature discusses this scattering in terms of albedo, which pertains to the fraction of incident radiation reflected by a surface. That is, albedo is a reflection coefficient.[1]

A geometrical representation of basic albedo geometry is given in Figure 21, from which the following general relationship is obtained.[1, 10, 13]

$$D_p = \frac{D_o \, a \cos \theta_o A}{r_1^2 r_2^2}$$

where

D_p = Detector response at point in question with no radiation coming straight from source, i.e., it all comes from reflecting surface

D_o = Detector response at unit distance from source with all radiation coming straight from source

ϕ = Azimuthal angle in x-y plane

θ_o = Polar angle of incidence

θ = Polar angle of reflection

A = Area of reflecting surface

r_1 = Distance from source to surface

r_2 = Distance from surface to point in question

a = Albedo

It should be noted that the albedo in this equation is a function of the incident radiation energy, the three angles defined in Figure 21, and the reflective characteristics of the target material. The fraction of the incident radiation which is reflected in a specific direction is termed differential albedo to distinguish it from the total amount of incident radiation reflected, or total albedo. If the detector response is measured in units of energy, dose, or number of photons, the albedo is accordingly called energy albedo, dose albedo, or number albedo. These values may approximate each other but are not necessarily equal[14].

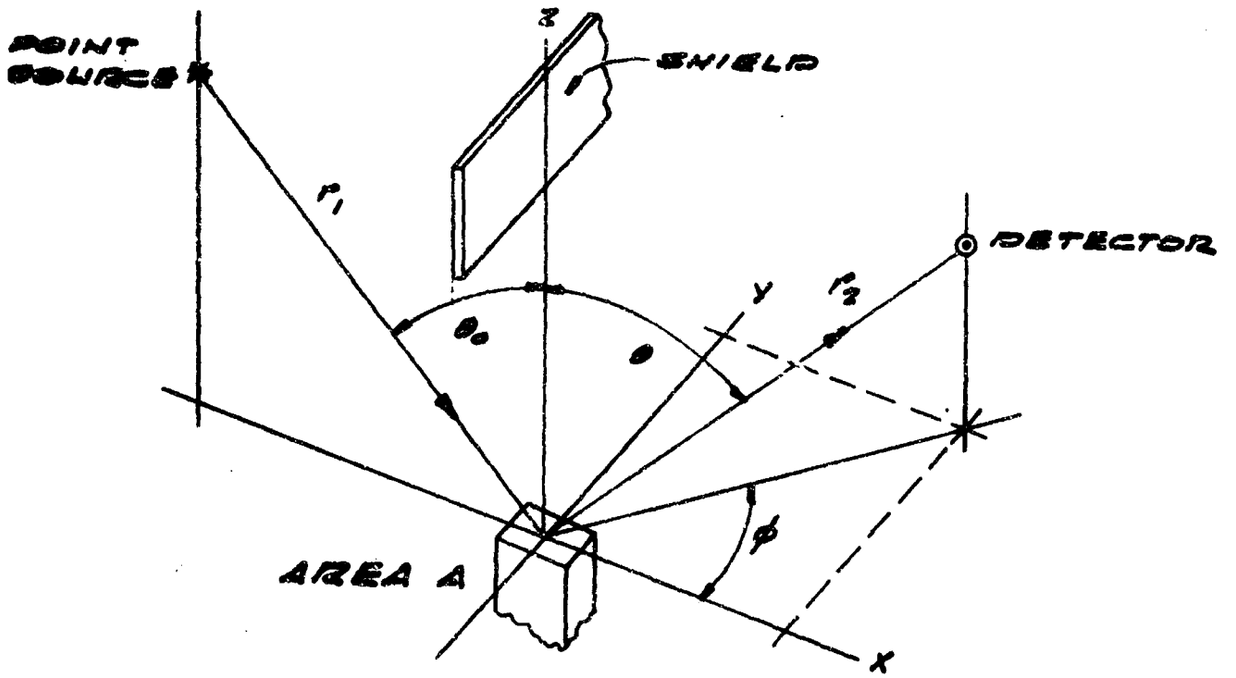

FIGURE 21. SCHEMATIC OF BASIC ALBEDO GEOMETRY(10)

In calculating anticipated transmission of radiation through tunnels, it has been convenient to use probability (Monte Carlo) procedures in addition to analytical methods to predict interaction between incident particles and barrier or tunnel materials. The probability of such an interaction is proportional to the nuclear cross section of the atoms of the material. It is this interaction that gives rise to backscattering or reflection and determines albedo. Attempts at experimental confirmation of these concepts have in some instances led to evaluation procedures based on semiempirical information, as is pointed out in the following sections. There is an apparent deficiency of empirical information concerning albedo for radiation at the energy levels of consequence during a nuclear weapon explosion.

SECTION 6. TRANSMISSION OF GAMMA RADIATION INTO STRAIGHT TUNNELS

A. General

It is desirable to reinforce analytical methods for predicting the transmission of radiation into tunnels or ducts with experimental observations. Usually, experimental studies concerning nuclear radiation are conducted with point sources because they are relatively safe to handle and are economical. Since a point source model is not directly applicable to either initial or fallout radiation from a nuclear explosion, it is necessary to consider ways in which data from such a source can be utilized.

B. Transmission of Gamma Radiation from Point Isotropic Source

Under ideal conditions, the ratio of radiation intensity at a distance L_p from a point source to that at unit distrance from the source would be[10]

$$\frac{D_p}{D_o} = \frac{1}{L_p^2}$$

This is considered to be the transmission factor for the centerline of a rectangular tunnel with nonreflecting walls if the source is placed in the center of the tunnel opening. It has been observed from experiments that reflection increases the intensity by about 40 percent so that the transmission of gamma radiation into a tunnel from a point source may be more accurately represented by[15]

$$\frac{D_p}{D_o} = \frac{1.4}{L_p^2}$$

This relation is useful for discussing the effect of source configurations on the transmission of initial gamma into tunnels. It is to be noted that fallout gamma is treated separately since its source configuration is affected by particle entrapment around the tunnel opening.

C. Transmission of Initial Gamma Radiation from a Plane Isotropic Source

The gamma radiation arriving at a point within the first minute after the detonation of a nuclear weapon arises from nitrogen-capture and fission products. It is theoretically possible to partition this incident gamma as illustrated by Figure 16. The fission product gammas would then be considered scattered and, thus, from a plane isotropic source. The fraction of nitrogen-capture gamma arriving would have to be divided into a scattered

and unscattered portion, such as is done in Table III. The unscattered nitrogen gamma would then be considered to arrive as broadbeam radiation, and the scattered portion would be added to the fission gamma from a plane isotropic source. Although such a partitioning would give an accurate prediction of the amount of radiation penetrating the tunnel, it presupposes precise knowledge concerning the nature of the radiation emitted by an enemy weapon, and safety factors would have to be included to cover the worst possible cases. Unfortunately, this information is not available for all the energy yields of interest, and scaling laws have not been experimentally verified.

With existing data, it is reasonable (and perhaps necessary) to assume that the burst angle (Section 2E2) is the only factor determining whether the initial gamma is from a plane isotropic or broadbeam source. Specifically, if the line of sight to center of burst makes an angle of greater than 40° with the centerline of the initial leg of the tunnel, initial radiation incident across the tunnel opening can be considered to be from a plane isotropic source. This simplifying assumption results in an overestimation of incident intensity and is therefore considered conservative. For example, the attenuation characteristics of gamma photons from a plane isotropic source are about the same as those from a plane collimated beam incident at 40°[7]. During Operation Plumbob, it was found that the gamma angular distribution was insensitive to both weapon design and distance from burst point[16], which implies that weapon yield does not affect source configuration at the tunnel opening. In Figure 22, it is seen that the percentage of air dose received by a collimator decreases rapidly for angles greater than 40°. Similar experimental data (Fig. 23) have been obtained with a 15° collimator[17], showing that if the burst angle to the collimator is greater than 40°, the dose stays approximately constant.

If the incident radiation at the tunnel mouth is equally distributed or isotropic, then the intensity at a given distance L down a cylindrical tunnel of radius R would be proportional to[6, 10] $\ln\left(1 + \frac{R^2}{L^2}\right)$. Equating the cross-sectional areas of circular and rectangular tunnels [$\pi R^2 = WH$], it is seen that the intensity in a rectangular tunnel would be proportional to $\ln\left(1+\frac{WH}{\pi L^2}\right)$, where W is tunnel width and H is tunnel height. The transmission factor is the ratio of dose at the point in question to the dose at unit length, or

$$T = \frac{\ln\left[1 + \frac{WH}{\pi L^2}\right]}{\ln\left[1 + \frac{WH}{\pi}\right]}$$

Noting that

$$\ln = \left[1 + \frac{WH}{\pi L^2}\right] \cong \frac{WH}{\pi L^2} \text{ for } WH << \pi L^2$$

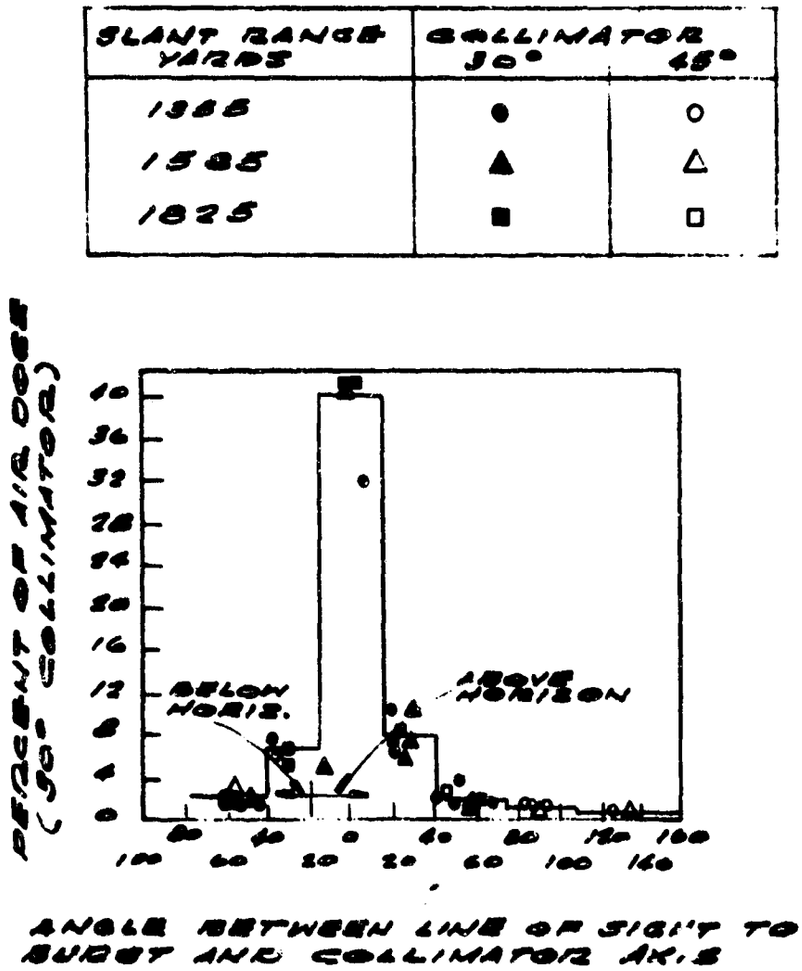

FIGURE 22. GAMMA ANGULAR DISTRIBUTION AS INDICATED BY 30° COLLIMATOR[16]

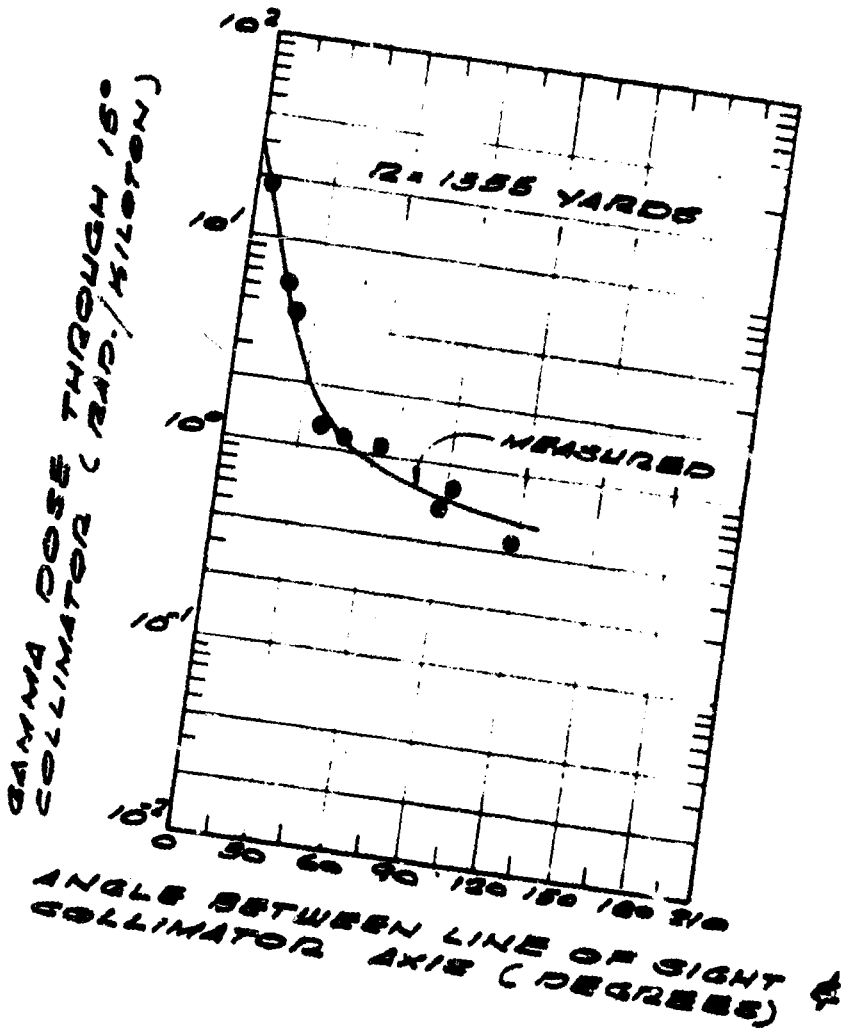

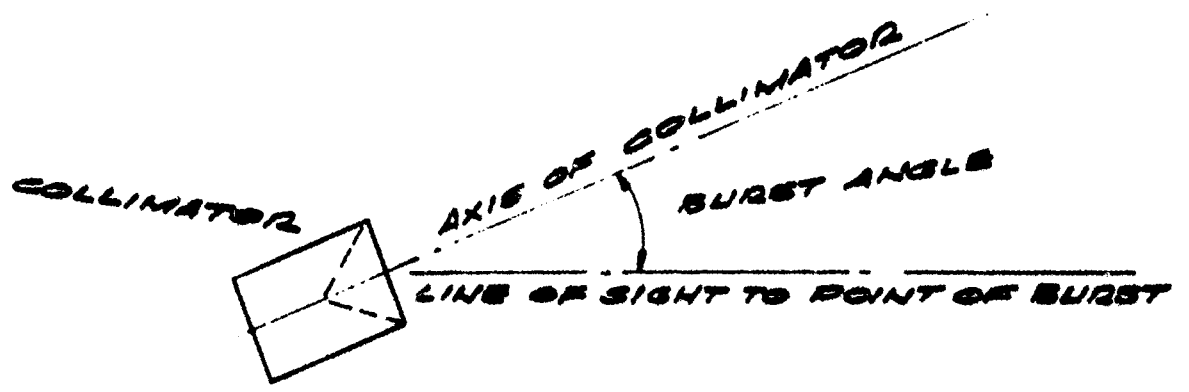

FIGURE 23. ANGULAR DISTRIBUTION OF GAMMA DOSE AS INDICATED BY 15° COLLIMATOR(17)

one obtains

$$T = \left[\frac{1}{L^2}\right]\left[\frac{WH}{\pi \ln\left(1 + \frac{WH}{\pi}\right)}\right]$$

The first bracketed expression is for a point isotropic source; and, if it is corrected for experimental observation to $\left[\frac{1.4}{L^2}\right]$, then

$$T_{\substack{\text{plane}\\ \text{isotropic}\\ \text{source}}} = \left[T_{\substack{\text{point}\\ \text{isotropic}\\ \text{source}}}\right]\left\{\frac{WH}{\pi \ln\left(1 + \frac{WH}{\pi}\right)}\right\}$$

Thus, transmission factors obtained by experiment from point sources may be multiplied by the correction factor in the braces to obtain an appropriate transmission factor for a plane isotropic source.

Experimental support for this relation is shown in Figure 24. These data were obtained in an open four-foot diameter hole 20 feet in depth with a source 100 feet from the tunnel opening placed at different positions in the vertical plane to allow for various angles of incidence. The source was a spherically symmetrical reactor modified so that radiation leakage would be similar to that from a weapon[18]. For a cylindrical tunnel, it is necessary to substitute $R^2 = \frac{WH}{\pi}$ in the above equation. Then, if D is the diameter, for L/D = 3 or L = 12, the transmission factor is calculated to be 0.024. This is compared to ratios obtained by dividing the values for L/D = 3 in Figure 24 by the values for L/D = 0. It is seen that the expression gives an equivalent transmission factor for about 45° and conservative values for greater angles. For L/D = 2, the transmission factor is calculated to be 0.054 which also agrees with experimental evidence for incidence of 45° and is conservative for larger angles. It should be remembered that the equation was derived for L large with respect to R; thus, comparison at L/D = 1 is not valid.

D. Parallel Ray Broadbeam Transmission of Gamma Radiation

If this type of incident radiation is coincident with the centerline of the tunnel, then no attenuation is attributed to tunnel length since air attenuation is considered negligible. The assumption made here is that radiation incident at angles less than 40° with the centerline of the tunnel will behave as parallel ray broadbeam radiation. In Figure 24, it is seen that the radiation incident at angles less than 40° is not drastically attenuated so that a transmission factor of unity for such cases is reasonably conservative.

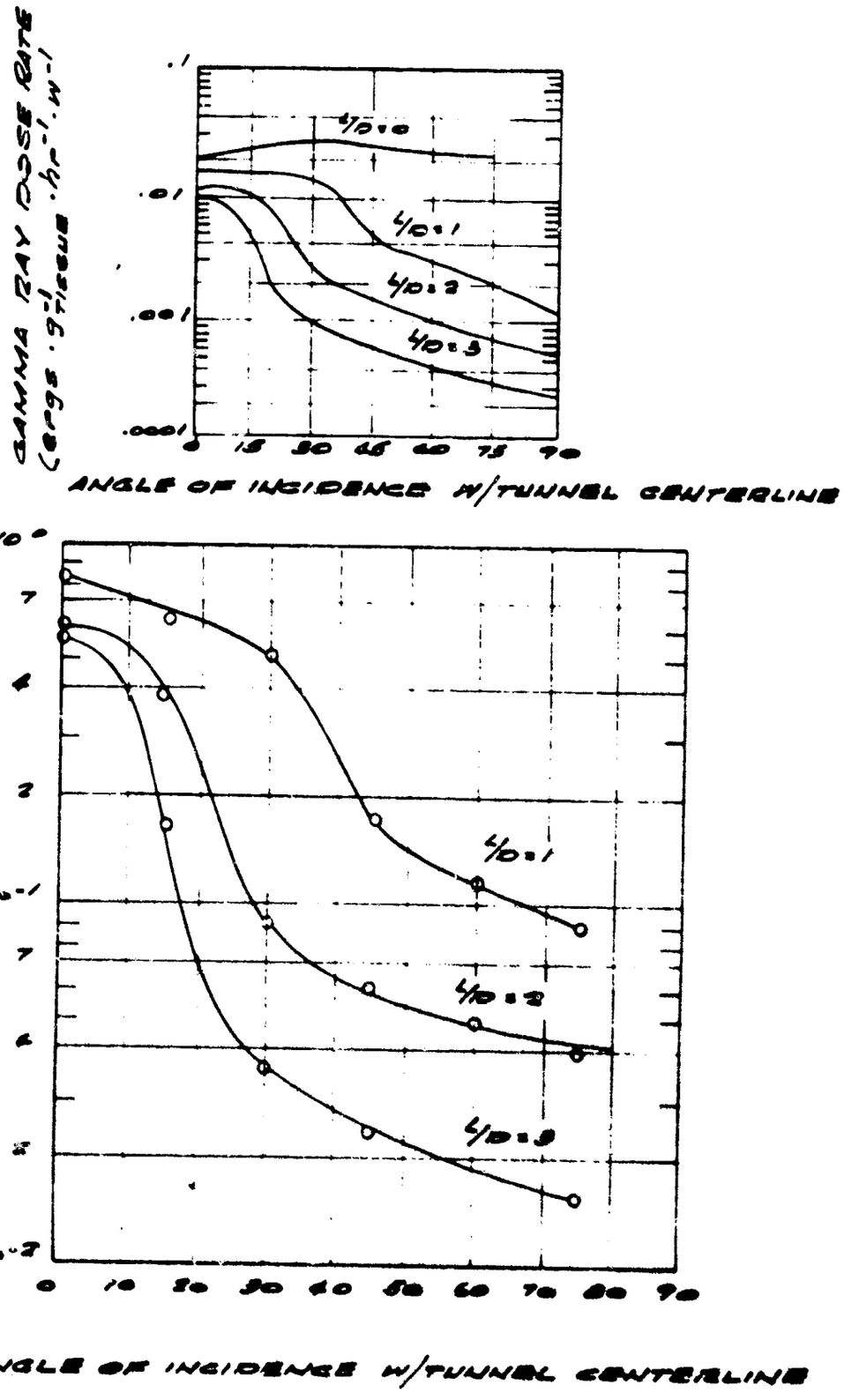

FIGURE 24. ATTENUATION OF GAMMA RADIATION IN A STRAIGHT SHAFT AS A FUNCTION OF L/D AND THE INCIDENT ANGLE (POINT ISOTROPIC SOURCE 100 FEET FROM SHAFT)[18]

SECTION 7. TRANSMISSION OF GAMMA RADIATION IN TUNNELS HAVING RIGHT-ANGLE BENDS (APPROXIMATE PROCEDURE)

A. General

Preliminary estimates using approximations are often invaluable in establishing representative values for transmission of radiation in tunnels. For example, a transmission factor of 0.1 can be used as a rough rule of thumb for each 90° bend in an average entrance[19]. In Figure 25, transmission factors for a straight tunnel are compared with those for a tunnel having a right-angle bend. It is seen that the bend attenuates the radiation by a factor close to 10. Considering experimental data given in Section 11, however, the factor of attenuation sometimes appears to deviate from 10.

Equations applicable to a plane isotropic source are developed in Section 7 B and 7 C.

B. Calculations for One Bend

The transmission factor for the first or exposed leg of a tunnel was developed in Section 6 C, using a backscatter factor equal to 40 percent. A similar expression may be developed for the second leg with a backscatter factor of 15 percent[15]. The transmission factor for a point at the end of the second leg can then be written as a product of the individual transmission factors, or (by assuming a 1/10 attenuation due to a corner)

$$T = \left[\frac{1.4\ WH}{\pi L_1^2 \ln\left(1 + \frac{WH}{\pi}\right)}\right](0.1)\left[\frac{1.15\ WH}{\pi L_2^2 \ln\left(1 + \frac{WH}{\pi}\right)}\right]$$

where L_1 is length of the first leg to the beginning of the corner and L_2 is the length of the second leg beginning at the end of the corner. This can be simplied to

$$T = \frac{0.016\ (WH)^2}{L_1^2 L_2^2 \left[\ln\left(1 + \frac{WH}{\pi}\right)\right]^2}$$

If the radiation is incident at angles less than 40°, no attenuation is attributed to the first leg, but scattering at the corner is assumed to generate a plane isotropic source for the second leg. Consequently, the transmission factor for this case is

$$T = \frac{0.115\ WH}{\pi L_2^2 \ln\left(1 + \frac{WH}{\pi}\right)}$$

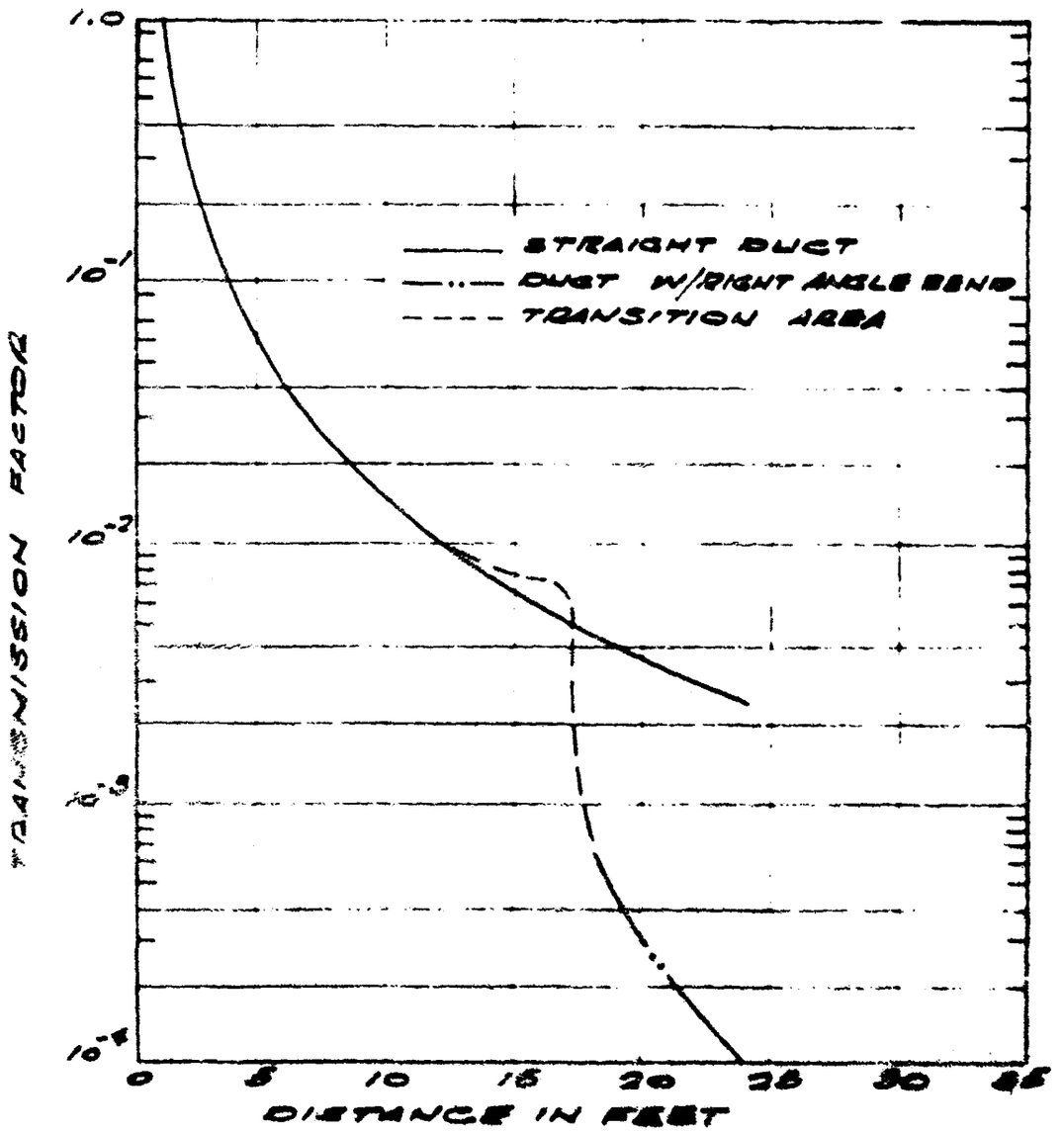

FIGURE 25. COMPARISON BETWEEN STRAIGHT TUNNEL AND TUNNEL WITH A RIGHT-ANGLE BEND (WIDTH = 6 FT, LENGTH FROM TUNNEL OPENING TO BEGINNING OF BEND = 12 FT)[15]

It is questionable as to whether a 40-percent or 15-percent backscatter should apply to the second leg when the burst angle is less than 40° for the first leg, but, for consistency, a 15-percent backscatter has been assumed in the equation.

C. Calculation for More Than One Bend

For the case of ducts having more than two legs, additonal attenuation factors would be included in the above expression. For burst angles greater than 40°, the total attenuation factor for ducts having multiple right-angle bends then becomes

$$T = 0.45[(0.037)^{n-1}]\left[\prod_{i=1}^{n}\frac{1}{L_i^2}\right]\left[\frac{WH}{\ln\left(1+\frac{WH}{\pi}\right)}\right]^n$$

where n is the number of legs and n - 1 is the number of right-angle bends. Thus, the total attenuation factor for a duct having three right-angle bends would be

$$T = 0.45[(0.037)^3]\left[\frac{1}{L_1^2L_2^2L_3^2L_4^2}\right]\left[\frac{WH}{\ln\left(1+\frac{WH}{\pi}\right)}\right]^4$$

if the radiation is incident at an angle greater than 40°.

If the burst angle is less than 40°, the expression would be

$$T = (0.037)^3\left[\frac{1}{L_2L_3L_4}\right]\left[\frac{WH}{\ln\left(1+\frac{WH}{\pi}\right)}\right]^3$$

since the factor for the first leg would be considered to be unity due to the lack of better data. For n legs and burst angles less than 40°

$$T = \left[\frac{0.037\ WH}{\ln\left(1+\frac{WH}{\pi}\right)}\right]^{n-1}\prod_{i=2}^{n}\frac{1}{L_i^2}$$

SECTION 8. EMPIRICAL RELATIONS FOR CALCULATING THE TRANSMISSION OF GAMMA RADIATION THROUGH TUNNELS HAVING RIGHT-ANGLE BENDS

A. Experimental Observations Used by Green[15] and Chapman[20]

Theoretical approaches to the scattering of radiation around a bend usually raise questions concerning the validity of assumptions, especially concerning multiple scatter and the transmission of radiation through material at the lip of the corner. Considering data from several sources, Green[15] developed the empirical relations

$$T_1 = \frac{D_1}{D_o} = 1.4\, L_1^{-2}$$

$$T_2 = \frac{D_2}{D_1} = wv(L_2/W)^{-s}$$

$$T_t = \frac{D_2}{D_o} = 1.4\, L_1^{-2}\, wv(L_2/W)^{-s}$$

where the following values apply:

Source	Energy, mev	w	s	v
Co^{60}	1.25	2	2.8	0.067
Au^{198}	0.441	2	2.8	0.067
Cs^{137}	0.667	2	2.8	0.067
Na^{24}	2.76, 1.37	2	2.8	0.033

$\frac{L_1}{W} \geq 3$ when $W \leq 1$ foot

$\frac{L_1}{W}, \frac{L_2}{W} \geq 1$

The subscript o applies to a point at unit distance from the source, while the subscripts 1 and 2 apply to points at the end of each leg.

Using a Co^{60} source and a three-foot square duct, Chapman[20] obtained the following values:

L_1, ft	Dose Rate, mr/hr $L_2 = 0$	$L_2 = 3$ ft	$L_2 = 6$ ft	s	v
4.5	2000	220	29	2.92	0.110
6	1212	87	12	2.86	0.0715
7.5	729	38	6.4	2.57	0.0526
9	482	24	4.1	2.55	0.0500

The accuracy of the dosimeters used was ± 10 percent. These values of s and v are comparable to the values obtained by Green, i.e., $s = 2.8$, $v = 0.067$.

Green apparently did not consider the dosimeter accuracy when formulating his empirical relation. Considering instrument accuracy and backscatter effects, a modified Green relation may be obtained as

$$T_t = 1.1(1.4)L_1^{-2}\,(1.1)\,(1.15)\,wv\left(\frac{W}{L_2}\right)^s$$

B. Development of Equations Using Green's Values

The experimental observations were made using point sources considered to be isotropic. With expressions developed in Section 6 C, it should be possible to correct the above equation so that it will apply to the case of a plane isotropic source. Using the empirical arguments for Co^{60}, the suggested design formula for calculating the total attenuation factor with two-legged ducts is

$$T = \left[\frac{1.4(1.1)WH}{\pi L_1^2 \ln\left(1 + \frac{WH}{\pi}\right)}\right]\left[1.15(1.1)(2)(0.067)\left(\frac{W}{L_2}\right)^{2.8}\right]$$

or more simply

$$T = \left[\frac{0.083}{L_1^2}\right]\left[\left(\frac{W}{L_2}\right)^{2.8}\right]\left[\frac{WH}{\ln\left(1 + \frac{WH}{\pi}\right)}\right]$$

when the dimensions are measured in feet.

If multiple right-angle bends are involved, the total attenuation factor for n legs would be

$$T = \left[\frac{0.5\ WH}{L_1^2 \ln\left(1 + \frac{WH}{\pi}\right)}\right]\left[\prod_{i=2}^{i=n} 0.17\left(\frac{W}{L_i}\right)^{2.8}\right] \text{ for } i = 2, 3, \ldots, n$$

Thus, the total attenuation factor for a duct having three right-angle bends, for instance, should be

$$T = \left[\frac{0.5\,WH}{L_1^2 \ln\left(1 + \frac{WH}{\pi}\right)}\right]\left[(0.17)^3\left(\frac{W^3}{L_2 L_3 L_4}\right)^{2.8}\right]$$

If the radiation is incident such that broadbeam parallel ray transmission applied to the first leg of the tunnel, then the transmission factor for the first leg is equated to unity, so that the above equations become for a single bend

$$T = \left[1.15(1.1)(2)(0.067)\left(\frac{W}{L_2}\right)^{2.8}\right]$$

where T represents the transmission factor for the second leg and the bend[15] or for multiple bends

$$T = \prod_{i=2}^{i=n} 0.17\left(\frac{W}{L_i}\right)^{2.8} \qquad \text{for } i = 2, 3, \ldots, n$$

It is important to note that the above empirical equations were developed specifically for square concrete ducts using sources varying from 400 Kev to around 3 Mev. If nonsquare rectangular ducts or bends other than 90° are to be considered, variation between calculated and observed results using these empirical formulations should not be viewed with alarm, and the theoretical analysis presented in Section 9 should be considered[15].

C. Empirical Relation of Ingold and Huddleston[21]

Green's relation has in essence been included in an expression developed by Ingold and Huddleston[21], which is

$$T = \frac{\left(\frac{H}{W}\right)^{0.907} W^{2.864}}{L_1^{2.534} L_2^{2.667} E_o^{0.710}}$$

This empirical relation is limited by the following inequalities:

(1) $0.662 \leq E_o \leq 6$ Mev
(2) $1.0 \leq H \leq 6.0$ feet
(3) $1.0 \leq W \leq 6.0$ feet
(4) $2 \leq L_1 \leq 36$ feet
(5) $1 \leq H/W \leq 2$
(6) $L_1/H < 6$

(7) $L_2/H \leq 6$
(8) $L_1/W \leq 2$
(9) $L_2/W \leq 2$

The formula is substantiated by data from 6 × 6 ft concrete ducts to 1 × 1 ft concrete ducts. Some of these data are conveniently summarized by Huddleston and Wilcoxin and plotted with consistent parameters in Reference 22.

SECTION 9. LE DOUX-CHILTON METHOD FOR DETERMINING THE TRANSMISSION OF GAMMA RADIATION THROUGH TUNNELS HAVING BENDS

A. Assumptions and Principles

LeDoux and Chilton[10] have formulated an analysis of gamma transmission through two-legged tunnels from basic scattering principles, employing primarily the albedo concept discussed in Section 5. They considered the basic rectangular tunnel with perpendicular legs shown in Figure 26, where the leg lengths are assumed to be great compared to the widths and heights. Specifically, the length of the shorter leg should be at least three times the largest cross-sectional dimension of either leg. They further assumed that tunnel dimensions were equal to or greater than the mean free path of the radiation in the wall materials and less than the mean free path in air. (The mean free path is the average distance a "particle" of radiation travels between interactions.) These limitations imply that the analysis may be valid for concrete ducts as small as 3 or 4 inches in height or width and that the interaction of the radiation with air in the tunnel is negligible.

Basic calculations are based on a point source at the center of the tunnel entrance and consider scattering from the prime areas (Fig. 26) to a detector located in the middle of the tunnel exit. The prime areas are directly visible from the source and the detector, whereas the transmission areas are not visible due to the presence of the inside corner lip. Radiation arriving at the detector from these areas is considered to have penetrated the lip. Transmission through the lip is discussed in terms of an energy absorption coefficient. From Figure 26, it is seen that a portion of the radiation is scattered before it penetrates the lip while another portion is transmitted through the lip and then scattered.

Aside from being translucent to gamma radiation, the corner lip also scatters some of the radiation which would have missed the detector so that it impinges on the detector. This effect is called in-scatter and causes the detector to see the corner lip as a bright line. The calculation for this effect has been simplified by assuming that scattering through two or more angles of appreciable amount is of negligible proportion.

B. Computational Procedure

The formats in Tables IV and V can be used as a guide for the Le Doux-Chilton computations for transmission of radiation from a point source through rectangular tunnels having a 90° bend. The required information is leg length, width and height, which are to be expressed in centimeters. From these values, the β's are computed (Table IV). It is then necessary to assume a source strength. The partitioning of initial gamma from a nuclear

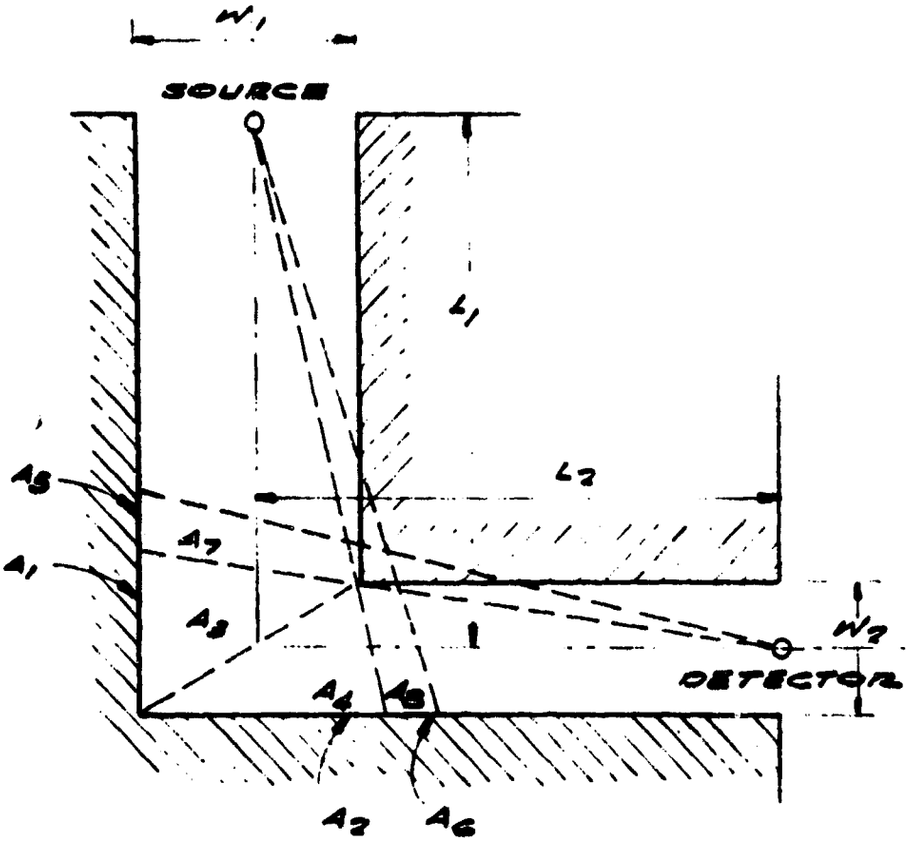

{ H = TUNNEL HEIGHT PERPENDICULAR TO PLANE OF PAPER
W = SAME FOR BOTH LEGS

PRIME AREAS
{ A_1 = WALL AREA
A_2 = WALL AREA
A_3 = ROOF & FLOOR AREA
A_4 = ROOF & FLOOR AREA

TRANSMISSION AREAS
{ A_5 = WALL AREA
A_6 = WALL AREA
A_7 = ROOF & FLOOR AREA
A_8 = ROOF & FLOOR AREA

FIGURE 26. BASIC TUNNEL GEOMETRY FOR THE LE DOUX-CHILTON METHOD, INDICATING PRIME AND TRANSMISSION SCATTERING AREAS[10]

TABLE IV. FORM FOR DOSE COMPUTATION[10]

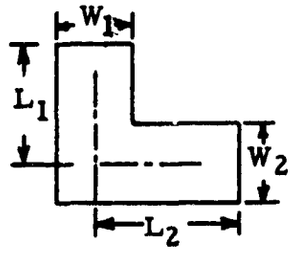

L_1 = _____ cm

L_2 = _____ cm

W_1 = _____ cm

W_2 = _____ cm

H = _____ cm

$\beta_1 = \frac{W_1}{2L_2}$ β_1 = ___

$\beta_2 = \frac{W_2}{2L_1}$ β_2 = ___

$\beta_3 = \frac{H}{2L_2}$ β_3 = ___

	$1+\beta$	$1-\beta$	$(1-\beta)^2$	$(1-\beta)^3$
β_1				
β_2				

Source Energy, E = _____ Mev

Scatt. Area	Cos θ_o Formula		Value
1	$\frac{W_1}{2L_1}$	=	____
2	1.00		1.00
3	$\frac{H}{2L_1}$	=	____
4	$\frac{H}{2L_1}$	=	____
5	$\frac{W_1}{2L_1(1-\beta_2)}$	=	____
6	1.00		1.00
7	$\frac{H}{2L_1(1-\beta_2)}$	=	____
8	$\frac{H}{2L_1}$	=	____

Enter curves (Fig. 38) for values of a using arguments of E and cos θ_o

a_1 = ___

a_2 = ___

a_3 = ___

a_4 = ___

a_5 = ___

a_6 = ___

a_7 = ___

a_8 = ___

TABLE V. FORM FOR DOSE COMPUTATION[10]

$$G_b = \frac{a_1}{1+\beta_1} + \frac{a_2}{\beta_2(1+\beta_2)} + \frac{a_3}{1-\beta_1} + \frac{a_4}{1-\beta_2}$$

$$= (\quad) + (\quad) + (\quad) + (\quad)$$

a, β, L from Table IV

G_b = _____

$$G_t = \frac{(1-\beta_1)a_5 + 2a_7}{2\mu_a' L_2 (1-\beta_1)^2 (1-\beta_2)^3}$$

$$+ \frac{(1-\beta_2)a_6 \quad 2\beta_2 a_8}{2\mu_a L_1 \beta_2 (1-\beta_1)^2 (1-\beta_2)^2}$$

$$= \frac{(\quad)}{(\quad)} + \frac{(\quad)}{(\quad)}$$

$$= (\quad) + (\quad)$$

μ_a, μ_a' from Table VI

G_t = _____

$(ZN/\mu_a^2) r_o^2$ = _____ From Table VI

$$a_1 = \tan^{-1}\left[\frac{W_1}{2L_1(1-\beta_2)}\right] = \_\_\_\_\_$$

$$a_2 = \tan^{-1}\left[\frac{W_2}{2L_2(1-\beta_1)}\right] = \_\_\_\_\_$$

$a_1 + a_2$ = _____

$\theta_s = 90° - (a_1 + a_2)$ = _____

$(K/r_o^2)_{\theta_s}$ _____ From Fig. 39

$$G_s = \left(\frac{ZNK}{\mu_a^2}\right) \frac{1}{2L_2(1-\beta_1)^3(1-\beta_2)^3}$$

G_s = _____

G_{TOT} = _____

$T_2 = 4\beta_1\beta_2\beta_3 G_{TOT}$

T_2 =

explosion into discrete energy levels is rather tedious, involves uncertainties, and complete data for all the weapons of interest are, understandably, not available. It is convenient to use 1.25 Mev as an energy level for the calculation outlined in Tables IV and V.

Cos θ_o is defined by Figure 21 and is the angle of incidence with respect to the normal at the centroids of the various areas indicated in Figure 26. With cos θ_o and the source energy, it is possible to obtain albedo coefficients a_1 through a_8 from Figure 27. In this figure, a is termed the differential directional dose albedo, which is the total albedo divided by 2π. It would be desirable to have the data of Figure 27 extended to higher energy levels, so that an energy level of 1.25 Mev would not have to be used in conjunction with Tables IV and V.

Values of a and β from Table IV are used to solve for the prime gamma factor G_p, as shown in Table V. The gamma transmission factor G_t is then calculated with a, β, and L from Table IV, and absorption coefficients (μ_a, μ_a') from Table VI. It is to be noted that the absorption coefficients have units of "per centimeter," which requires that L be measured in centimeters as stated in Table IV.

Table VI also contains a column for $\left(\frac{ZN}{\mu_a^2}\right)r_o^2$. This quantity, when multiplied by K/r_o^2 from Figure 28, gives $\left(\frac{ZNK}{\mu_a^2}\right)$ which is used in the computation of the scattering coefficient G_s. K is called the Klein-Nishina coefficient for scattering probability. (A detailed substantiation for its use in corner lip effects is given in the Appendix of Reference 10.) From Figure 28, the appropriate value of K/r_o^2 is found at θ_s which is determined from

$$\theta_s = 90° - a_1 - a_2$$

where

$$a_1 = \tan^{-1} \frac{W_1}{2L_1(1-\beta_2)}$$

$$a_2 = \tan^{-1} \frac{W_2}{2L_2(1-\beta_1)}$$

The G factors are then summed in Table V and multiplied by the β's to give the transmission factor T_2. It is to be noted that T_2 is the ratio of the dose at the end of the second leg to that at the intersection of the leg centerlines. As noted in Section 6, the transmission factor for the first leg, T_1, equals $1/L_1^2$.

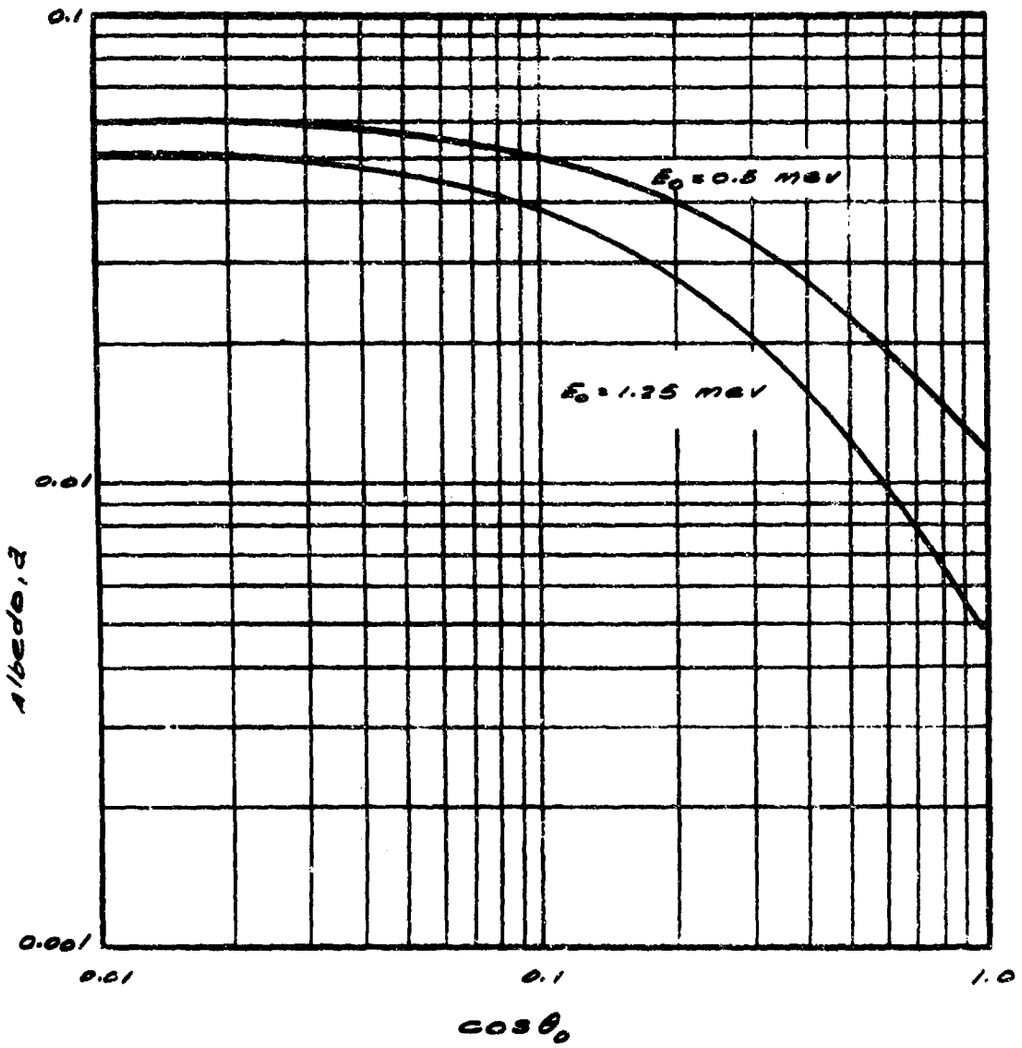

FIGURE 27. DIFFERENTIAL DIRECTIONAL DOSE ALBEDO FOR 1.25 MEV AND 0.5 MEV GAMMA PHOTONS FROM CONCRETE (ISOTROPIC ASSUMPTION)[10]

TABLE VI. NUCLEAR QUANTITIES USED IN TUNNEL ATTENUATION FORMULAS[10]

E, Mev	μ'_a, cm^{-1}	μ_a, cm^{-1}	$\left(\frac{ZN}{\mu_a^2}\right) r_o^2$	Material
0.50	0.0473	0.0473	17.00	Earth
1.25	0.0473	0.0434	20.10	(100 pcf)
6.00	0.0473	0.0300	45.70	
0.50	0.0695	0.0695	11.55	Concrete
1.25	0.0695	0.0630	13.70	(145 pcf)
6.00	0.0695	0.0442	31.30	
0.50	0.3140	0.2240	3.38	Iron
1.25	0.2450	0.1700	4.68	(475 pcf)
6.00	0.2260	0.1747	5.47	
0.50	6.260	1.120	1.68	Lead
1.25	2.545	0.375	1.51	(705 pcf)
6.00	1.318	0.422	1.19	

μ_a = Energy absorption coefficient for primary radiation

μ'_a = Energy absorption coefficient for reflected radiation

Z = Number of electrons per atom of scattering material

N = Number of atoms per unit volume of the scattering material

r_o^2 = Classical radius of electron = 2.8×10^{-13} cm

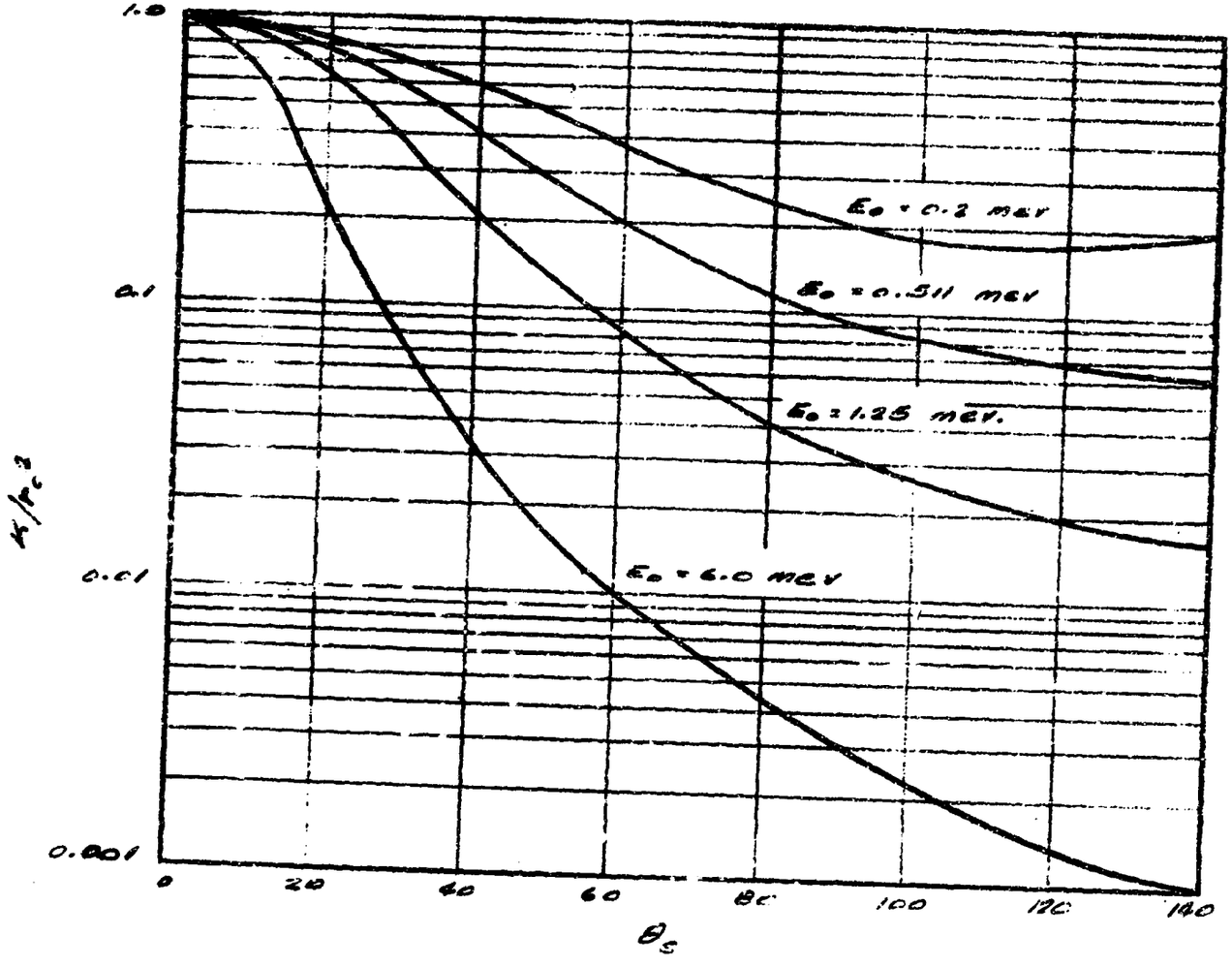

FIGURE 28. KLEIN-NISHINA COEFFICIENT FOR SCATTERING PROBABILITY PER ELECTRON(10)

C. Conversion from Point to Plane Isotropic Source for One Bend

The general procedure for transforming the expression for attenuation from a point isotropic source to a plane isotropic source is given in Section 6C. In Section 6B, it was noted that theory differs from experiment by about 40 percent for the first leg of a tunnel. Section 7B notes a discrepancy of 15 percent for the second leg. These observations have been combined in Section 8B along with an accuracy factor of 10 percent to convert observations from a point isotropic source to those that should be obtained from a plane isotropic source.

Noting that the total transmission factor for a tunnel with two legs is given by the product

$$T = T_1 T_2,$$

one obtains for a two-legged rectangular tunnel

$$T = \left\{\left[\frac{(1.4)(1.1)}{L_1^2}\right]\left[\frac{WH}{\pi \ln\left(1+\frac{WH}{\pi}\right)}\right]\right\}\left\{(1.15)(1.1)\,T_2\right\}$$

which reduces to

$$T = \frac{0.62\,WH\,T_2}{L_1^2 \ln\left(1+\frac{WH}{\pi}\right)}$$

T_2 is obtained from Figure 29, which shows plots of calculations from Tables IV and V, or from direct calculations following the format in the tables.

D. Transmission Factors for Multiple Right-Angle Bends

If the source is distributed across the entrance of the tunnel, a correction factor is applied to the transmission factor for the first leg, but the scattering principles used for calculating the factor for the second leg are assumed to be generally applicable to both point and distributed sources. Consequently, in Section 9C, the formulas for T_2 were considered to be reasonably valid for the plane isotropic source; that is, no correction factor was applied to T_2 for a change in source configuration.

For tunnels with multiple bends, the calculation for T_2 can be applied to legs past the second by letting L_2 in Figure 26 be increased by half the tunnel width. (This increase is actually insignificant since it is assumed that L is large compared to W.) Thus, if L is the leg length between the

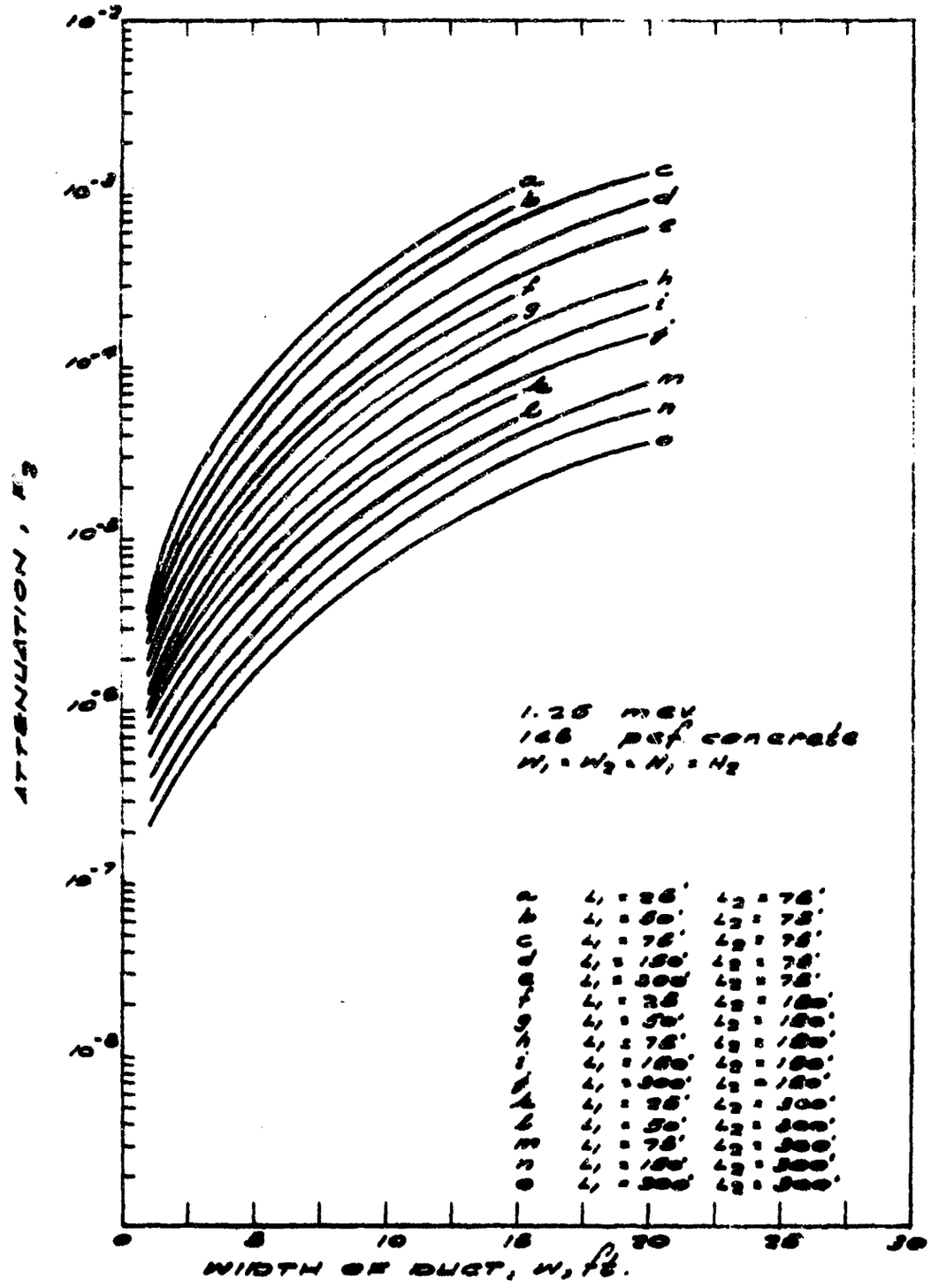

FIGURE 29. THEORETICAL ATTENUATION OF GAMMA RADIATION IN SHELTER LEG OF A TUNNEL HAVING A 90° BEND

intersection of centerlines at the corners, the total transmission factor for a tunnel with n legs can be written in the form

$$T_{TOT} = \left[kT_1\right]\left[(CT_2)(CT_3)\ldots(CT_n)\right]$$

where k is a factor to be applied to the transmission factor of the first leg and C is a constant to be applied to factors of subsequent legs. Actually, C is nothing more than the product of the 15-percent backscatter factor and the 10-percent accuracy figure, both of which have been used previously. (It is interesting to note that Reference 10 considers the theory accurate to within 10 percent and Reference 20 considers that experimental measurements are also accurate to within 10 percent.) T_2 through T_n can be obtained from repeated application of Figure 29 or calculated by repeated application of the format in Tables IV and V. If a tunnel has n legs with leg length = l_n, then, in general, L_1 (in Table IV) = $l_n - 1$ and $L_2 = l_n$.

T_{TOT} = can be expressed as

$$T_{TOT} = \left[kT_1\right] \prod_{i=2}^{i=n} (1.3T_i) \text{ for } i = 2, 3, \ldots, n$$

where

$$C = (1.15)(1.1) \cong 1.3$$

For example, the transmission factor for a four-legged tunnel with three right-angle bends would be

$$T_{TOT} = \left[kT_1\right] \left[(1.3)^3 T_2 T_3 T_4\right]$$

It remains to establish the conditions for T_1. If the incident radiation is plane isotropic, then $T_1 = 1/L_1^2$ and $k = \dfrac{(1.4)(1.1)WH}{\pi \ln\left(1 + \frac{WH}{\pi}\right)} = \dfrac{0.5\,WH}{\ln\left(1 + \frac{WH}{\pi}\right)}$

so that

$$T_{TOT} = \left[\frac{0.5\,WH}{L_1^2 \ln\left(1 + \frac{WH}{\pi}\right)}\right] \prod_{i=2}^{i=n} (1.3T_i) \text{ for } i = 2, 3, \ldots, n$$

If the radiation is incident as parallel ray broadbeam, then the transmission factor for the first leg is unity or $kT_1 = 1$. The scattering at the corner is still considered to be valid. Thus, for burst angles less than 40°

$$T_{TOT} = \prod_{i=2}^{i=n} (1.3T_i) \text{ for } i = 2, 3, \ldots, n$$

The procedure developed in the LeDoux-Chilton analysis may be considered to apply when the empirical relations of Section 8 are not valid. That is, if the cross section of the tunnel is not square or if the walls are not concrete, the calculational procedures outlined in Tables IV and V will at least offer a method to estimate transmitted radiation if computerized programs or machine computation are not available.

SECTION 10. PENETRATION OF FALLOUT RADIATION INTO TUNNELS

A. General

Penetration of fallout radiation into buildings and structures has received special attention in the literature because of its importance in civil defense. Fundamental information has been compiled in Reference 5. The use of this information in engineering applications has been explained in References 11 and 23. Reference 11 presents a procedure used by the Office of Civil Defense for calculating the penetration of radiation into building passageways and shafts, which can be considered to be equivalent to the tunnels and ducts of interest here.

The OCD method utilizes the concept of "solid angle fraction" to discuss the effect of tunnel geometry on the reduction of radiated intensity. A solid angle is defined to be the area projected (radially) on the surface of a unit sphere. A solid angle fraction is defined to be the solid angle divided by 2π (the surface area of a hemisphere). This compares to the 4π steradians normally encountered in the surface area of a unit sphere. Solid angle fractions can be determined from basic tunnel dimensions expressed in terms of normality ratio, n, and eccentricity ratio, e, in Figure 3[illegible] where

$$n = 2L/H$$

$$e = W/H$$

Transmission factors (termed reduction factors in References 11 and 23) are expressed as the ratio of the dose rate at the point of interest to the dose rate three feet from an infinite plane isotropic source. This factor is shown as a function of solid angle fraction in Figure 31, where three positions of a tunnel opening relative to a fallout source are shown. Case 1 involves the accumulation of source particles on a tunnel cover which affords no barrier protection. This case represents direct transmission only. It is to be noted that in this case the transmission factor equals unity for $\omega = 1$ and corresponds to the separation of a detector from the source by 3 feet of air[11].

Case 2 in Figure 31 represents a horizontal passageway receiving radiation from a semi-infinite plane source. At $\omega = 1$, it is seen that $T = 1/2$, which corresponds to the placement of a detector in the vertical plane of the aperture[11]. This factor is predicated on the basis of direct and reflected radiation.

Case 3 represents the radiation reflected into a vertical shaft due to an infinite plane source around the aperture. At $\omega = 1$, $T = 0.1$. This

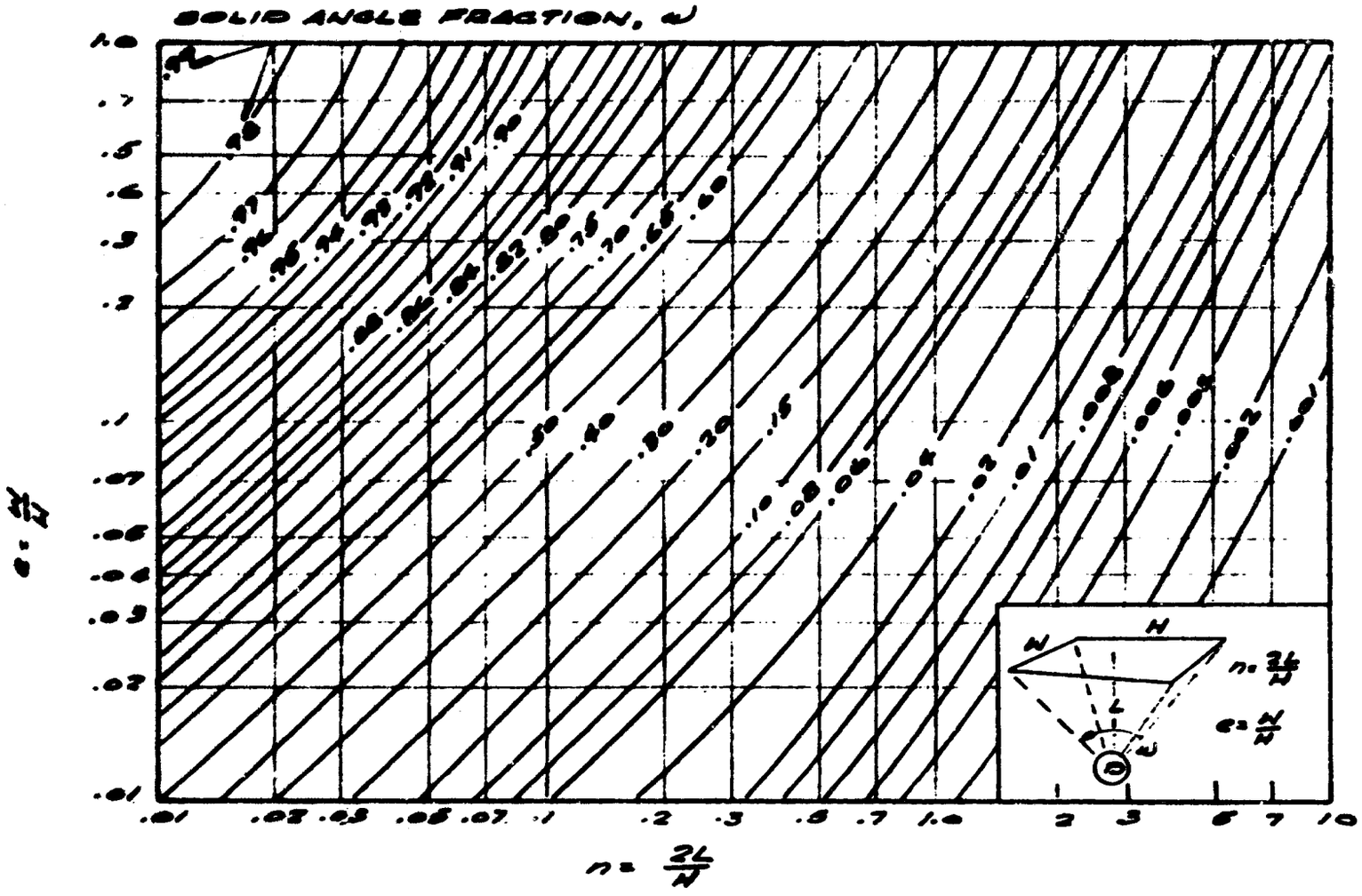

FIGURE 30. SOLID ANGLE FRACTION[11]

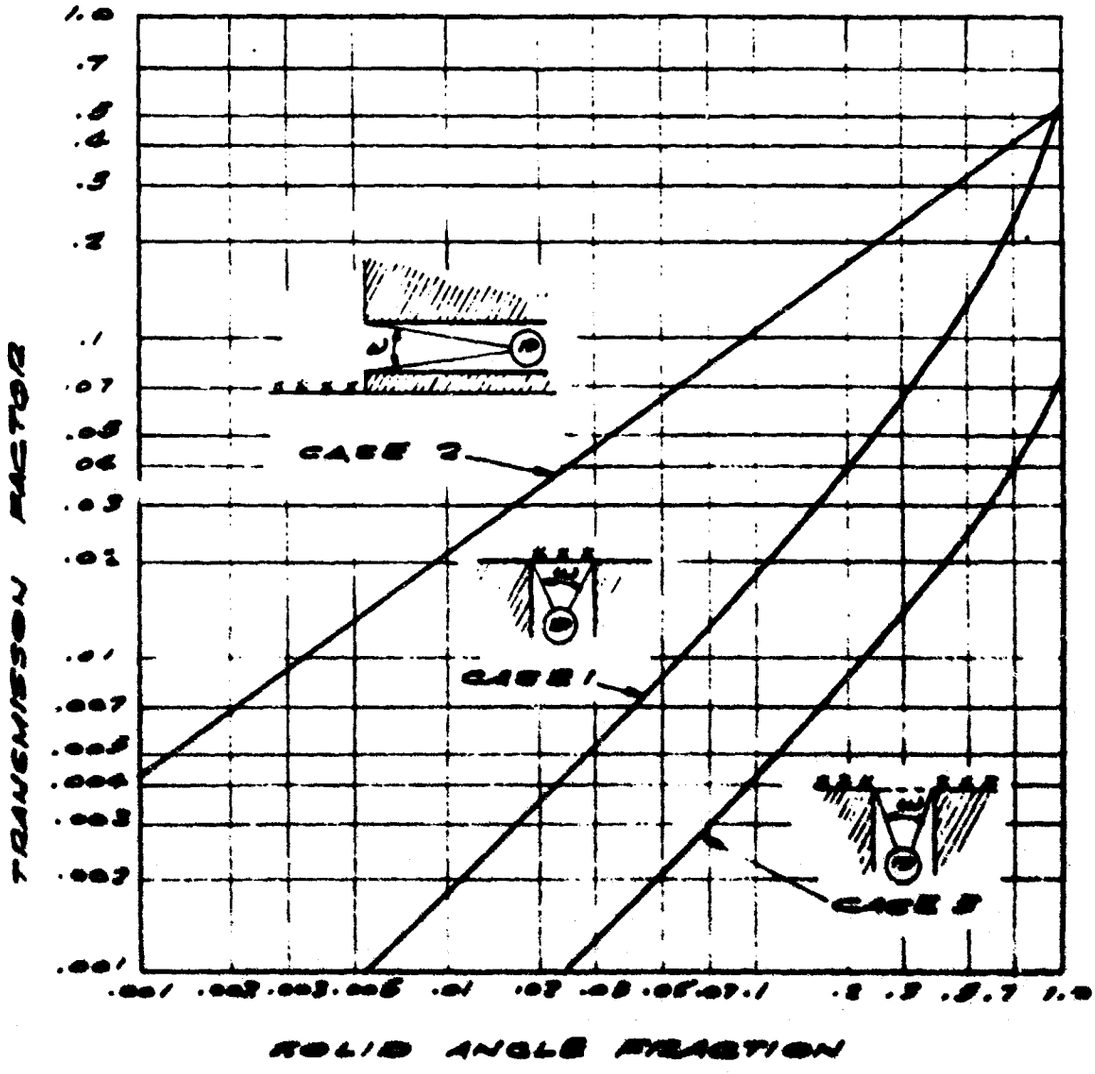

FIGURE 31. TRANSMISSION FACTOR FOR RADIATION FROM FALLOUT INTO PASSAGEWAYS AND SHAFTS[11]

indicates that a detector placed in the vertical plane and receiving only reflected radiation, sometimes termed skyshine, will record an intensity of 1/10 that indicated by a detector placed 3 feet above the infinite plane[11].

B. Calculations Using the OCD Method

Consider the horizontal passageway shown in Figure 32a. The eccentricity ratio for the cross section of both legs is $5/7.5 = 0.67$ or $e_1 = e_2 = 0.67$. The normality ratio for $L = AB = 15$ ft is $2 \times 15/7.5$ or $n = 4$. From Figure 30, ω_1 is about 0.024, and, from Figure 31, for this value of the solid angle fraction, the transmission factor, T_1, is seen to be 0.038 for Case 2. With the LeDoux-Chilton method (Section 9D), a factor of 0.033 is obtained; but it is to be noted that the two methods define transmission factors differently.

To obtain the total transmission factor from A to C, it is necessary first to obtain $n_2 = 2(10 - 7.5)/7.5 = 2$. Since $e_2 = e_1$, we obtain from Figure 30 a value of $\omega_2 = 0.09$. An experimental approximation factor of 0.1 is used for the corner reduction effects. The total transmission factor is defined to be

$$T_{TOT} = T_{AB}(0.1)(\omega_2) = 0.038(0.1)(0.09) = 0.00034$$

Application of the method to a vertical shaft (shown in Fig. 32b) is as follows:

$$e_1 = \frac{3}{3} = 1 \text{ and } n_1 = 2 \times (6/3) = 4$$

From Figure 30, $\omega_1 = 0.039$

From Figure 31, for skyshine (Case 3), $T = 0.0016$
and for direct (Case 1) $T = 0.0068$
so that the total is $T_1 = 0.0084$

$$e_2 = 1, \text{ and } n_2 = \frac{2(16-1/2 - 1-1/2)}{10} = 3$$

From Figure 30, $\omega_2 = 0.062$

The corner effect is assumed to be 0.1.

Thus, $T_{TOT} = T_1 \text{ (corner effect)} (\omega_2) = 0.0084\ (0.1)(0.062) = 0.000052$.

The important facets of the OCD method as it pertains to penetration of fallout radiation into shafts and tunnels are:

(1) The transmission factor for the first leg is determined as a function of a solid angle.

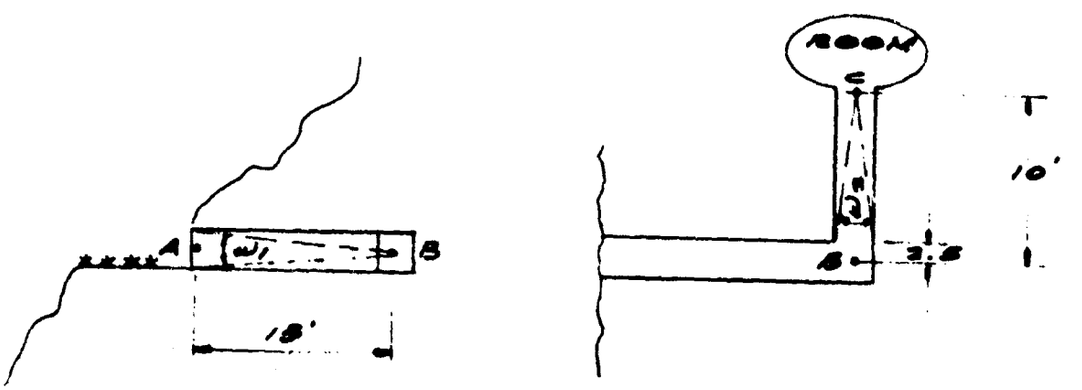

* = SOURCE

4. HORIZONTAL PASSAGEWAY W/ONE BEND, CROSS SECTION = 5'X7.5'

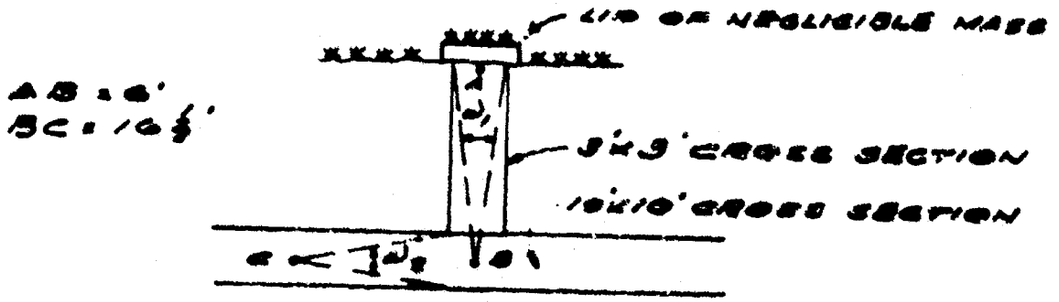

* = SOURCE

6. VERTICAL SHAFT INTERSECTING HORIZONTAL TUNNEL

FIGURE 32. SCHEMATIC FOR SAMPLE CALCULATION OF FALLOUT RADIATION USING OCD CHARTS(11)

(2) Each corner attenuates the radiation by a factor of 10.

(3) The attenuation in the second leg equals the solid angle subtended by the second leg.

(4) Transmission in legs past the second leg equals one-half the subtended solid angle.

Thus, for a tunnel with n legs and n - 1 corners,

$$T_{TOT} = (0.1)^{n-1} T_1 \omega_2 \prod_{i=3}^{i=n} (0.5\,\omega_i) \text{ for } i = 3, 4, \ldots, n$$

A special case arises when a vertical shaft does not have a cover, because fallout particles will accumulate at the intersection of the shaft with a horizontal tunnel. The absence of a lid in Figure 32b, for example, would cause a source to accumulate under point B. Relative to point C, this source would approximate Case 2 in Figure 31. Case 2 is not considered to apply, however, as it represents a source distributed over a semi-infinite plane. Case 1 in Figure 31 represents direct transmission from a spot source in a plane perpendicular to the point of interest. Since, in Figure 32b, C is at an oblique angle to the plane containing the spot source, Case 1 will give a transmission factor that overestimates the intensity of the radiation incident at C from the source below point B. Thus, for the case of an uncovered vertical shaft, the transmission factor from A to C will be the sum of a skyshine factor (Case 3) from A to C and a direct factor (Case 1) from the beginning of the second leg to C, or in equation form

$$T_{AC} = T_{AB(\text{Case 3})}\, \omega_2 (0.1) + T_{BC\ (\text{Case 1})}$$

where T_{BC} is evaluated at ω_2 in Figure 31.

For subsequent legs,

$$T_{TOT} = T_{AC} (0.1)^{n-2} \prod_{i=3}^{i=n} (0.5\omega_i) \text{ for } i = 3, 4, \ldots, n$$

C. Recommendations for Use of OCD Method

The OCD method (requiring the use of Figs. 30 and 31) is recommended only for determining transmission factors for the first leg or from an isolated spot at the bottom of a vertical shaft. For subsequent legs and corners, it should be regarded as a preliminary calculation.

Both the OCD method and the LeDoux-Chilton method assume plane isotropic sources, but the OCD method is based on observations and does

not attempt to calculate corner albedo. The methods also differ in their discussion of the problem of theoretically distributing a source across the tunnel opening. The OCD method considers a spherical surface saturated with point sources at the tunnel opening and utilizes the concept of a solid angle fraction to determine the transmission through the first leg. The LeDoux-Chilton method considers the transmission from a point source at the opening and then integrates or sums the effect for a disk source equivalent in area to the tunnel opening.

SECTION 11. EXPERIMENTAL RESULTS FOR TRANSMISSION OF GAMMA RADIATION

A. Simulation Experiments at the ORNL Tower Facility

Some experiments for observing the attenuation of radiation in a particular tunnel geometry have been reported by Cain[24]. The data are applicable only for the given geometry, but are considered valuable in that they indicate trends. It is to be noted that the tunnel sizes are not especially suited for the tunnels under consideration due to the low length to width (or length to height) ratio of the first cubicle. Also, a circular opening in the ceiling of the middle tunnel undoubtedly affected the measured transmission.

A point source was suspended by cable between some steel towers at Oak Ridge National Laboratory. (The facility is described in detail in References 24 and 25.) The specific tunnels used in the experiment are shown schematically in Figure 33. The orientation of the source relative to the tunnel is shown at the top of the schematic. Two 12-foot cubicles, concrete lined, were connected by a three-legged, concrete-lined tunnel with a 3' × 8' cross section. Tunnel legs connecting the cubicles with the middle leg of the tunnel were perpendicular to both the cubicles and the middle leg. The connecting legs measured 6-1/3 feet from the bunker to the centerline of the middle tunnel which had a total length of 15-1/6 feet. A vertical, circular concrete tunnel, 3 feet in diameter, opened into the center of the ceiling of the center leg and was covered by a concrete hatch, one foot thick.

The bunkers or cubicles were constructed in such a manner that the effectiveness of concrete slabs of various thicknesses for shielding the bunker could be determined. Radiation penetrating the overburden was considered negligible. The front bunker was protected by vertical shields and the top bunker by horizontal shields. After initial tests, the reactor, simulating the point source, was placed at a height of 100 feet, such that a line from the center of the source to the center of the shield of the front bunker was perpendicular to the shield. A similar line to the center of the shield of the top bunker formed an angle of 9-1/2° with the plane of the shield.

Figure 34 shows results obtained with 20 inches of concrete shielding on the front bunker and no shielding on the top bunker. Figure 35 shows the dose rate for 20 inches of shielding on the top bunker and no shielding on the front bunker. Since the presence of the vertical shaft in the center leg could introduce an unknown factor, it is convenient to consider primarily the transmission of gamma radiation around the intersection of the first and second legs.

In Figure 34, the dose rate at I is about 3.8×10^{-5} and at H is around 1.2×10^{-5}. At E, it has decreased to 1×10^{-6}. Consequently, the transmission factor from the cubicle to the first leg is about 0.316. The transmission

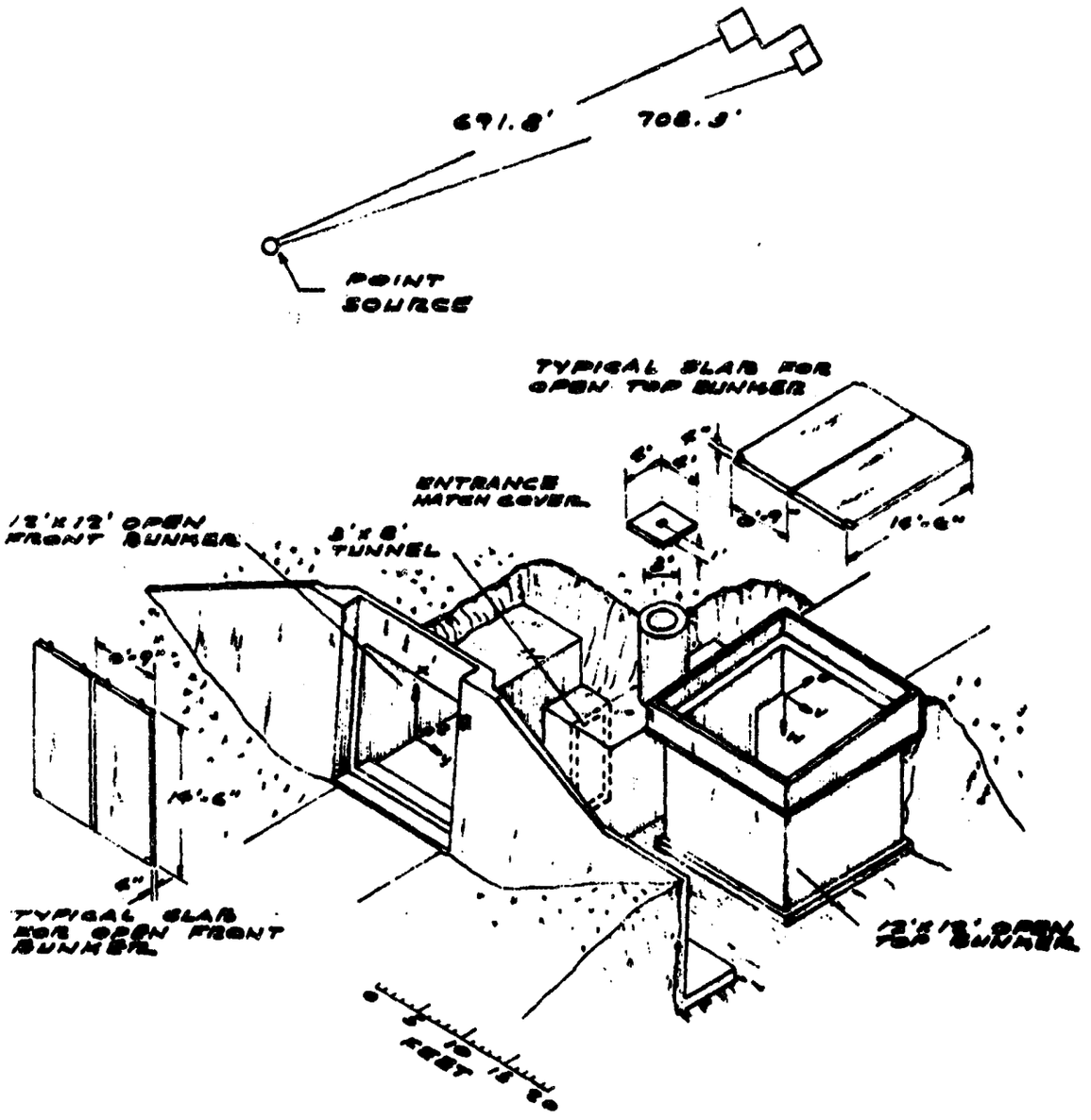

FIGURE 33. SCHEMATIC OF BUNKER-TUNNEL ARRANGEMENT, SHOWING THE COORDINATE SYSTEMS[24]

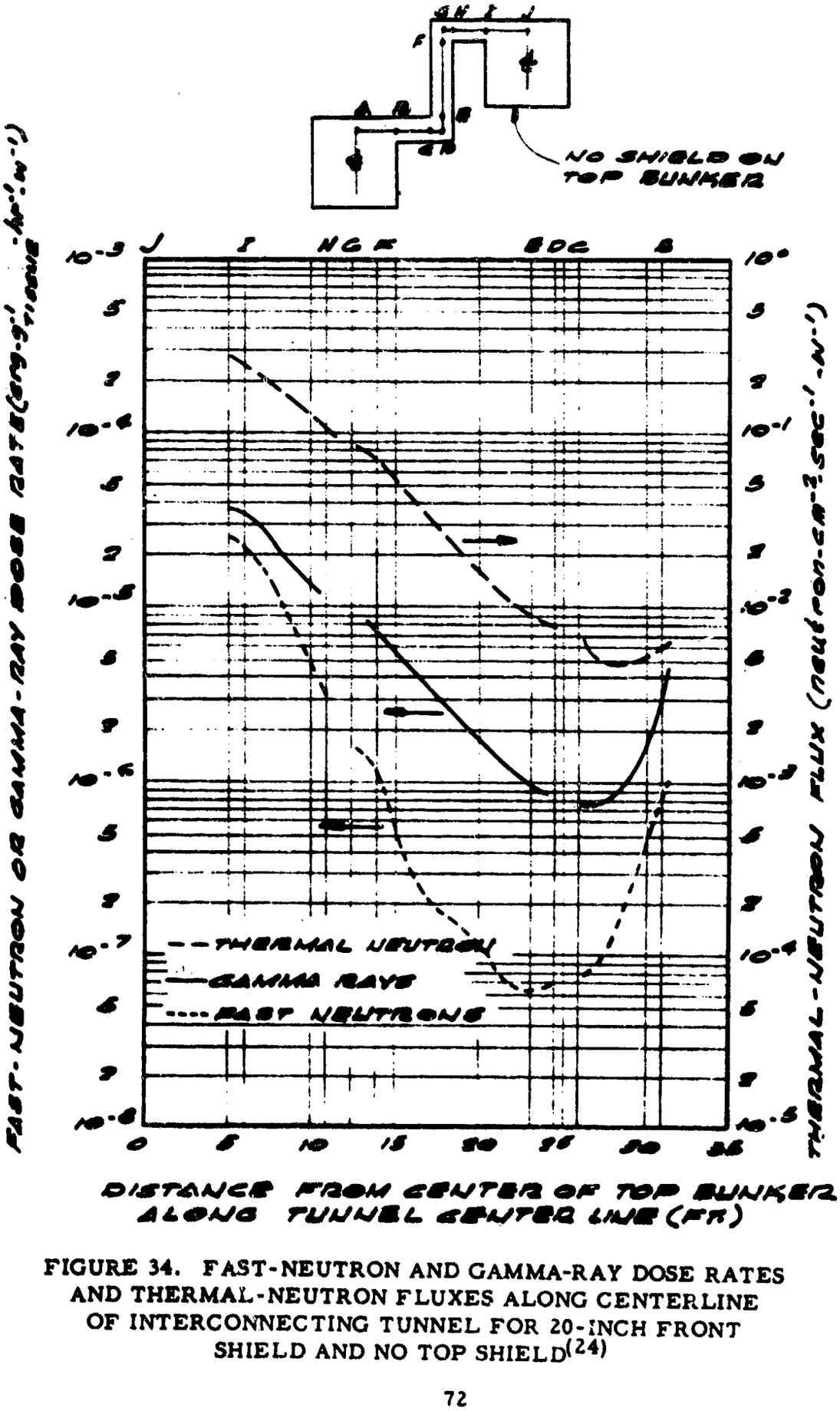

FIGURE 34. FAST-NEUTRON AND GAMMA-RAY DOSE RATES AND THERMAL-NEUTRON FLUXES ALONG CENTERLINE OF INTERCONNECTING TUNNEL FOR 20-INCH FRONT SHIELD AND NO TOP SHIELD[24]

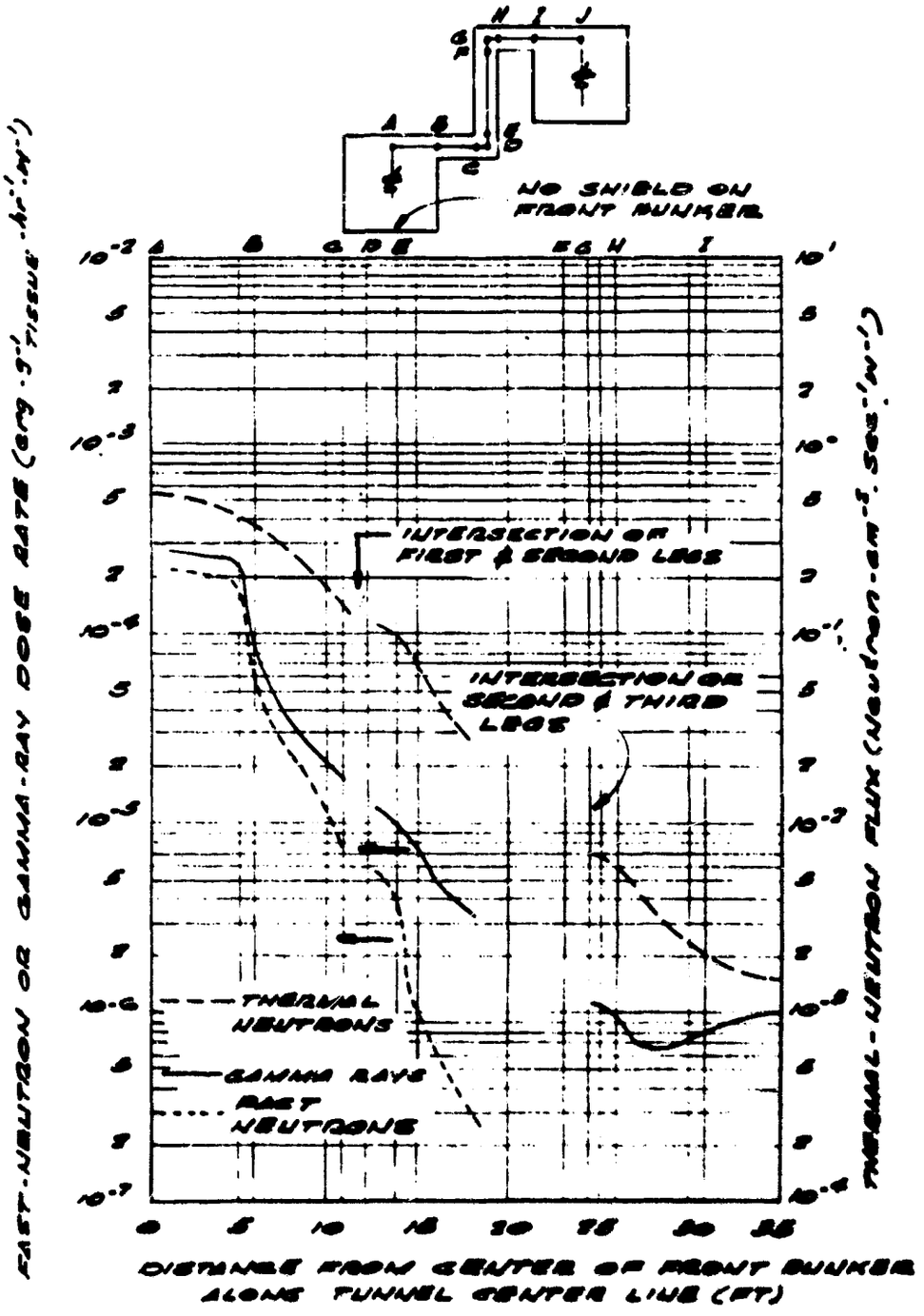

FIGURE 35. FAST-NEUTRON AND GAMMA-RAY DOSE RATES AND THERMAL-NEUTRON FLUXES ALONG CENTERLINE OF INTERCONNECTING TUNNEL FOR 20-INCH TOP SHIELD AND NO FRONT SHIELD[24]

factor for the intersection of the first and second legs would be $(1.0 \times 10^{-6})/(1.2 \times 10^{-5}) = 0.0835$. This, which was given previously as a good rule of thumb, corresponds to attenuation by a factor of 10 around a corner. It should be noted that the intersection of the cubicle with the tunnel does not afford the average corner protection, since the cubicle does not have a long length compared to its width. In Figure 35, the factor from the front cubicle to the first leg is $(1.8 \times 10^{-5})/(2.8 \times 10^{-4}) = 0.064$, which again deviates from the usual corner. The protection afforded by the intersection of the first and second legs is the ratio of the dose rate at D to that at G or $(1.2 \times 10^{-6})/(1.2 \times 10^{-5}) = 0.1$, which is again the factor of 10 for an "average" corner.

Another study was conducted at the ORNL Tower Facility in which three concrete-lined holes, 4 feet in diameter and 20 feet deep were used. A horizontal concrete-lined tunnel, 6 feet high, 2-1/2 feet wide and 20 feet long, was constructed so that its ceiling would intersect one of the tunnels 10 feet below ground level, as shown in Figure 36. The reactor was positioned 100 feet from the center of the top of the hole, and the angle formed by the line from the reactor to the center of the hole was varied. (Data from angle variation were presented in Section 6C). Again, it is noted that the geometry is not a standard type for the tunnels under consideration, especially at the corner intersection.

Typical results from these tests are shown in Figure 37, where the dose rate 27 inches above the tunnel floor is plotted versus distance from the hole centerline. Dose rates in the tunnel when an iron shield is placed over the hole are compared with those obtained for the case of no shield. It is seen that for a burst angle of 0° the radiation reflected around the corner three feet from the hole axis is less than one-tenth of that in the vertical hole, for both a shielded and an unshielded case. For greater burst angles, however, it is necessary to go about 8 to 10 feet into the tunnel to reduce the dose rate by a factor of 10. Similar results are obtained for concrete shielding as shown in Figure 38. It is to be remembered that the tunnel geometry for Figures 37 and 38 is for the case of intersecting circular and rectangular tunnels. Also, even though a true corner situation is not represented in that the vertical hole goes beyond the 6-foot intersection with tunnel, it is interesting to note that the radiation transmitted is attenuated by a factor of at least 10 when the second leg equals almost twice the greatest cross-sectional dimension of the intersecting tunnel. Difficulties in assessing the accuracy of the experiments are pointed out but are conservatively quoted as being ± 28%[25].

B. Full-Scale Experiments

The difficulties in obtaining accurate transmission data even when experiments and geometry are designed and performed under the best of conditions are indicative of the complexities encountered in full-scale testing. Results from full-scale tests, which are limited not only by technical difficulties but also by testing restrictions or bans, are useful primarily for

UNCLASSIFIED
2-01-056-330-1218

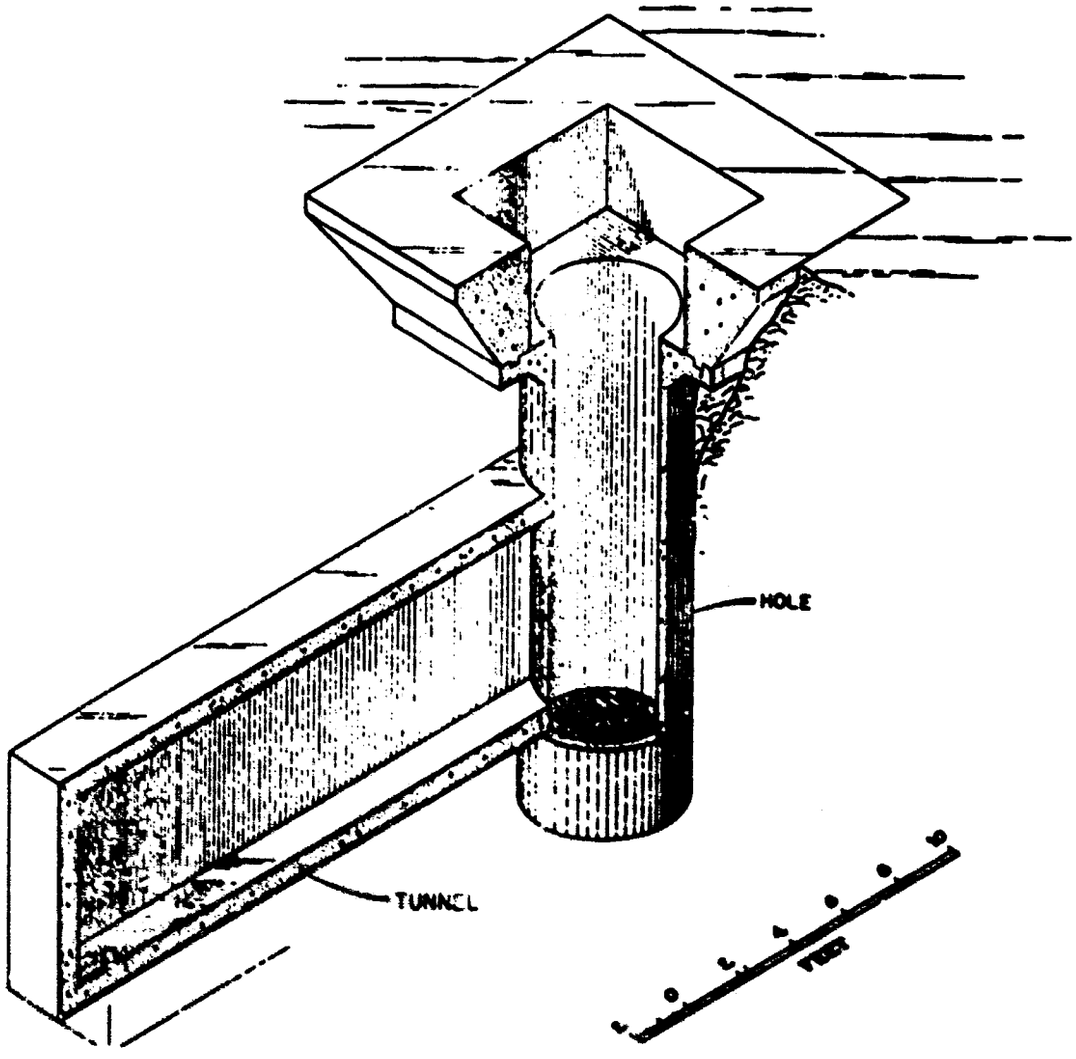

FIGURE 36. CUTAWAY VIEW OF HOLE NO. 1 AND TUNNEL[25]

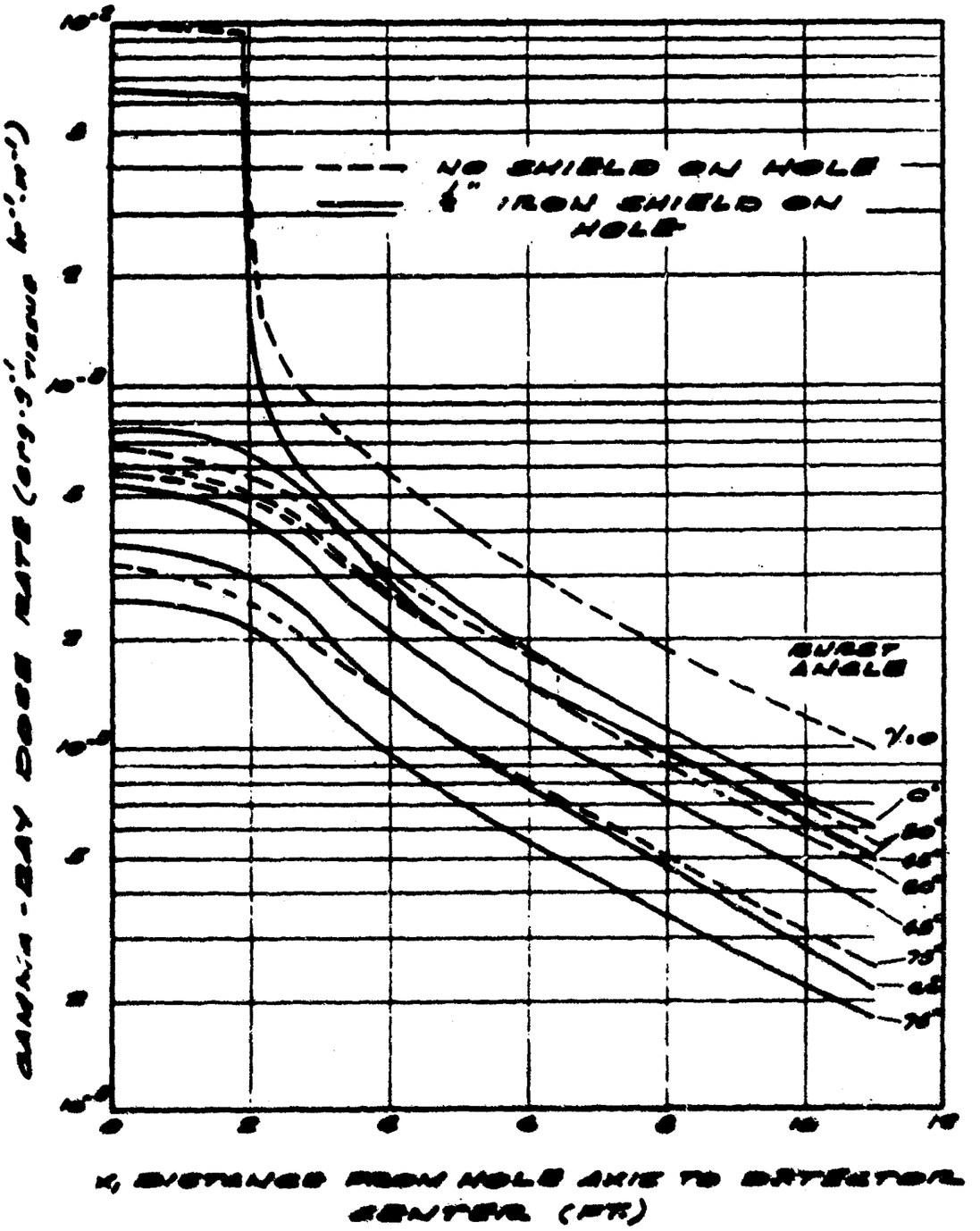

FIGURE 37. GAMMA-RAY DOSE RATE IN TUNNEL AS A FUNCTION OF THE DISTANCE FROM THE AXIS OF HOLE NO. 1 WITH AND WITHOUT A ONE-HALF-INCH THICK IRON SLAB OVER THE HOLE (ANGLE OF BURST EQUAL 0°, 30°, 45°, 60°, 75°)[25]

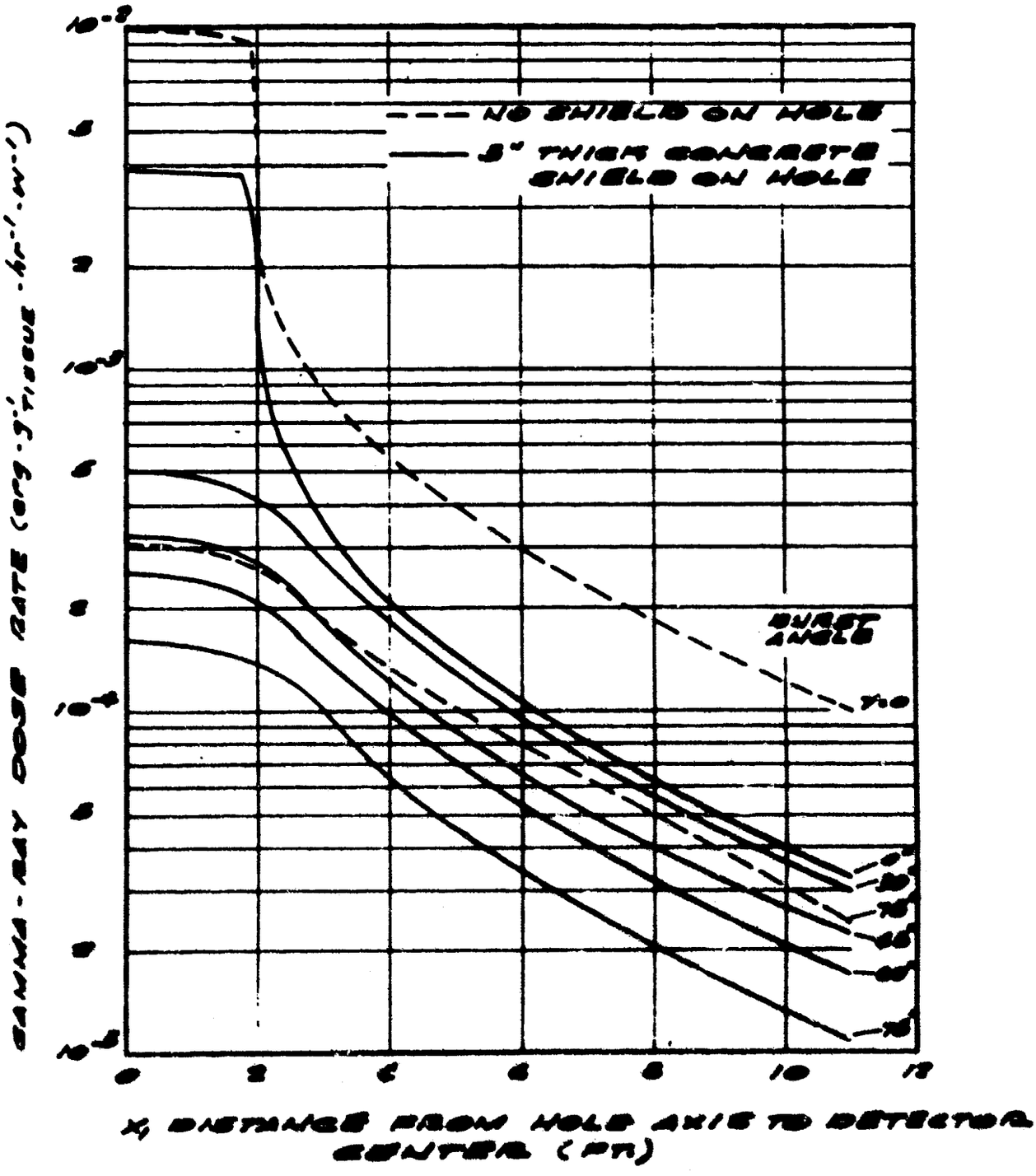

FIGURE 38. GAMMA-RAY DOSE RATE IN TUNNEL AS A FUNCTION OF DISTANCE FROM THE AXIS OF HOLE NO. 1 WITH AND WITHOUT A THREE-INCH THICK CONCRETE SHIELD OVER THE HOLE (ANGLE OF BURST EQUAL 0°, 30°, 45°, 60°, 75°)[25]

comparative purposes. Since such results are not specific enough for design purposes, but do point out weaknesses, limitations and inaccuracies in existing methods, the results from some of the tests conducted during Operation Plumbob are presented.

Radiological attenuation in entranceways to buried shelters was measured during one of the Plumbob tests[26]. The yield from a weapon detonated at an altitude of 700 feet was 36.6 KT. Radiation doses incident at four buried shelters, 1360, 1360, 1040, and 860 feet from ground zero, are shown in Figures 39 through 42, respectively. A schematic of the shelter profile is superposed on the curves. These shelters were reinforced concrete arch structures with their crown 4 feet below ground level. Three of the structures were 20 feet long, while the fourth was 32 feet long. The entrance shaft was a little over 6 feet long with a 2-1/2-foot square cross section.

Radiation exposures were measured 3 feet above the floor as indicated by the encircled letters A through F in Figures 39 through 42. Instruments at position A were under the center of the shaft. In Figure 40, instruments D, E, and F were located across the structure, all being about 15 feet from B. Transmission factors of total gamma radiation dose are shown in Table VII. They are based on the free field readings. It is interesting to note the variation in readings between the film badge determination and the chemical dosimeter readings for the transmitted gamma.

Considerable radiological attenuation data for various types of field fortifications were also collected by Davis[27] with the Priscilla Shot at Frenchman Flat (Exercise Desert Rock 7, Operation Plumbob). The weapon was a 37-KT yield and the burst height was 700 feet. Unfortunately, much of the data were inconsistent, varying with the type of detection device, and insufficient to permit many conclusions for the present purposes. We can, however, derive benefit from the foxhole measurements (see Fig. 43). For point A inside the horizontal tunnel of the offset foxhole, the transmission factor relative to the outside dose for initial gamma ranged from 0.006 to 0.008 at 2280 feet from GZ and from 0.003 to 0.005 at 3900 feet from GZ.

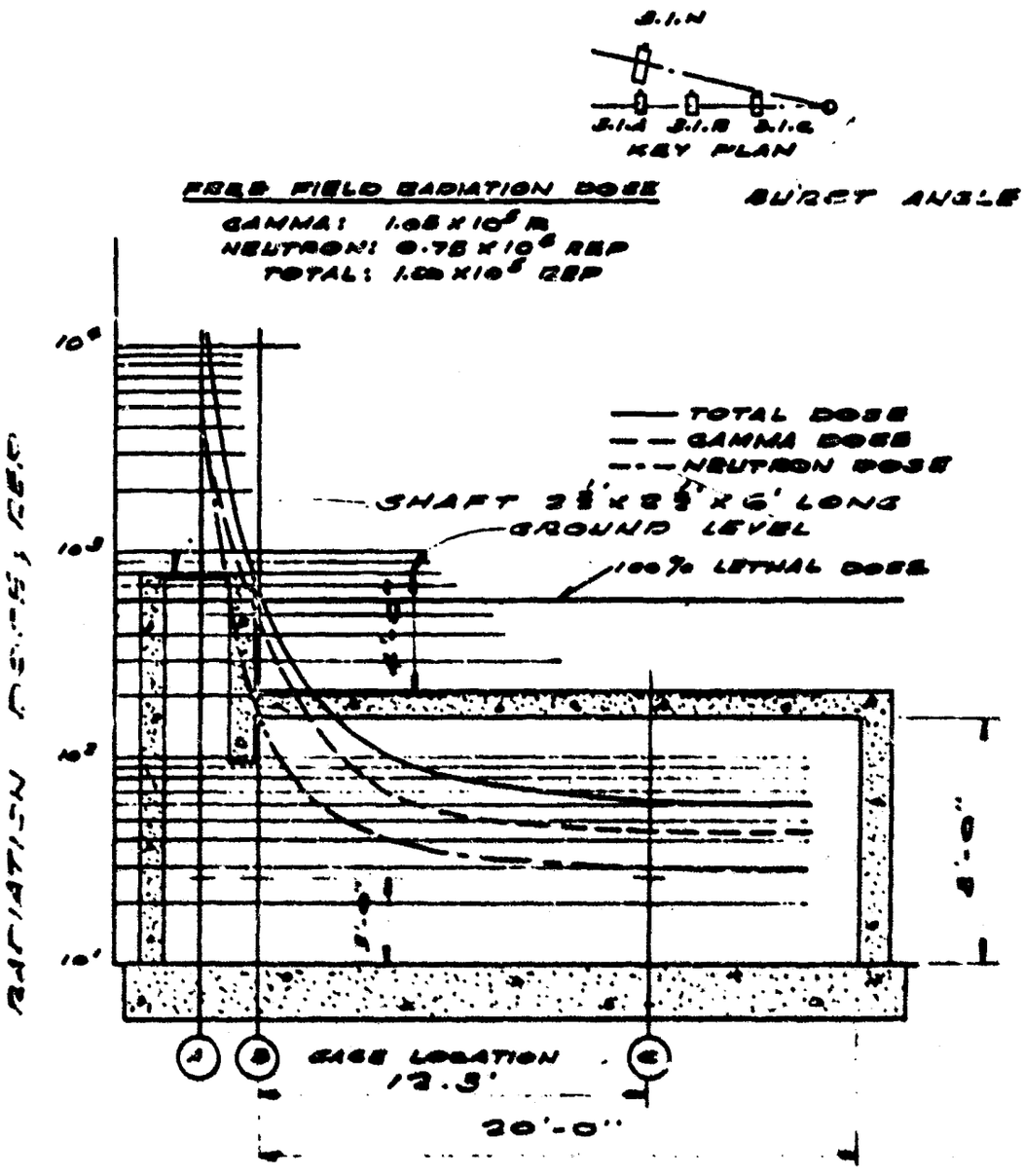

FIGURE 39. TOTAL NUCLEAR RADIATION DOSE PROFILE, STRUCTURE 3.1.A[26]

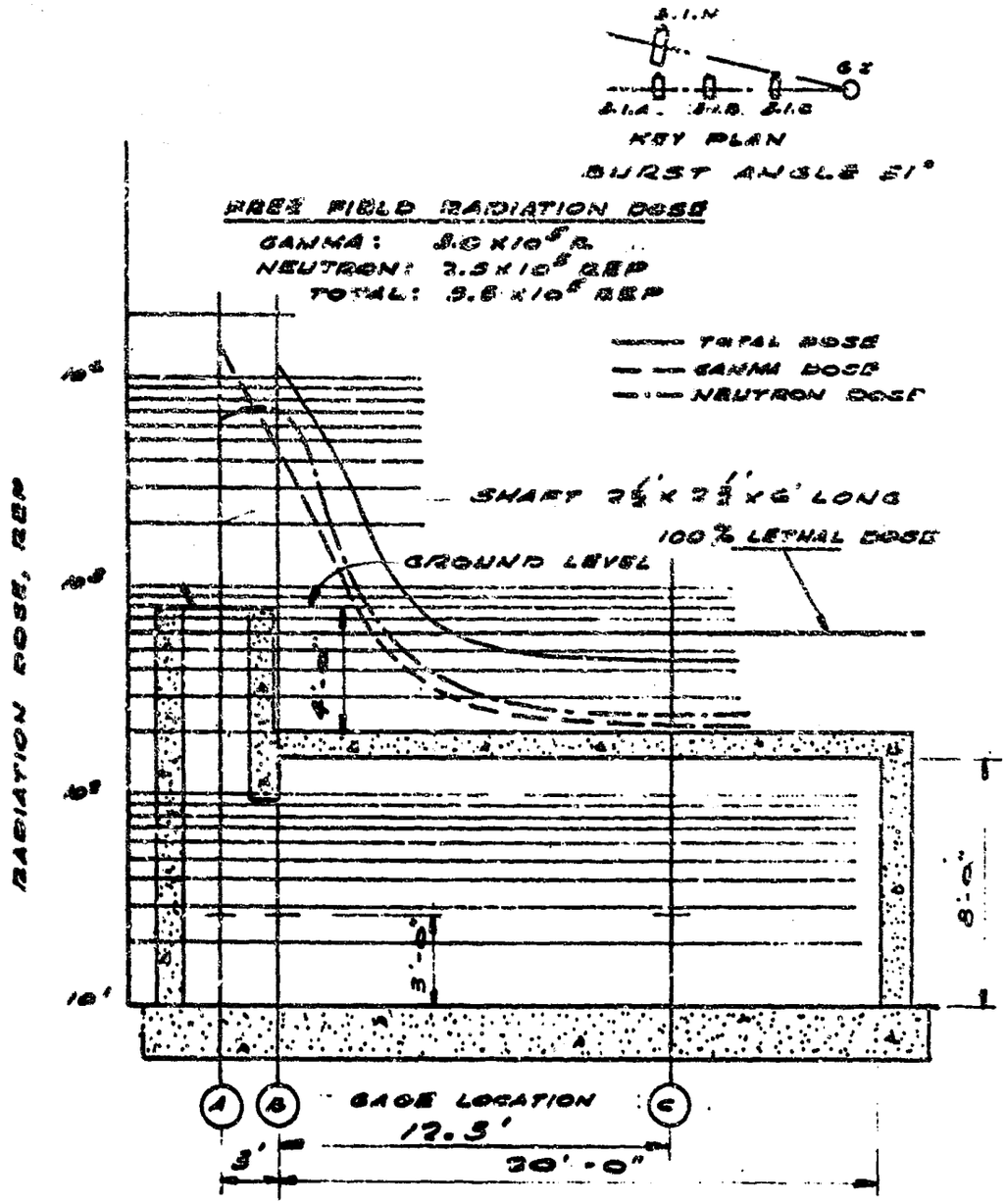

FIGURE 42. TOTAL NUCLEAR RADIATION DOSE PROFILE, STRUCTURE 3.1.C[26]

TABLE VII. SHIELDING CHARACTERISTICS OF PROJECT 3.1 STRUCTURES: PRISCILLA SHOT, FRENCHMAN FLAT, OPERATION PLUMBOB[26]

Yield: 36.6 KT

Height of Burst: 700 ft

Type		Earth Cover	Horizontal Range	Slant Range	Dose		Transmission Factor (Di/Do)	
					Film Badge	Chemical Dosimeter	Film Badge	Chemical Dosimeter
Concrete arches		ft	yd	yd	r	r		
3.1.a	A	4	453	510	$> 10^3$	3.5×10^3	$> 9 \times 10^{-3}$	3.4×10^{-2}
	B				4.2×10^2	7.7×10^2	4×10^{-3}	7.6×10^{-3}
	C				4.4×10^1	5.0×10^1	4.2×10^{-4}	4.9×10^{-4}
3.1.b	A	4	347	418	$> 10^3$	9.3×10^3	$> 5 \times 10^{-3}$	4.9×10^{-4}
	B				$> 10^3$	3.5×10^3	$> 5 \times 10^{-3}$	1.9×10^{-2}
	C				1.25×10^2	1.35×10^2	6.2×10^{-4}	7.1×10^{-4}
3.1.c	A	4	287	370	$> 10^3$	1.5×10^4	$> 3 \times 10^{-3}$	5.0×10^{-2}
	B				$> 10^3$	4.3×10^3	$> 3 \times 10^{-3}$	1.4×10^{-2}
	C				2.1×10^2	4.55×10^2	7.0×10^{-4}	1.5×10^{-3}
3.1.n	A	4	453	510	$> 10^3$	3.75×10^3	$> 9 \times 10^{-3}$	3.7×10^{-2}
	B				5.7×10^2	1.2×10^3	5.4×10^{-3}	1.2×10^{-2}
	C				1.65×10^2	< 50	1.6×10^{-4}	$< 5 \times 10^{-4}$
	D				3.5×10^1	8.4×10^1	3.1×10^{-6}	8.2×10^{-4}
	E				3.9×10^1	4.6×10^1	3.7×10^{-6}	6.5×10^{-4}
	F				4.0×10^1	8.8×10^1	3.8×10^{-4}	8.6×10^{-4}

Structure	Horizontal Range	Slant Range	Gamma Dose		Neutron Dose	
			Film Badge	Chemical Dosimeter	Foil Method	Chemical Dosimeter
	yd	yd	r	r	rep	rep
3.1.c	287	370	3.0×10^5	3.00×10^5	2.5×10^5	2.49×10^5
3.1.b	347	418	2.0×10^5	1.89×10^5	1.6×10^5	1.62×10^5
3.1.a and n	453	510	1.05×10^5	1.02×10^5	7.5×10^4	7.65×10^4

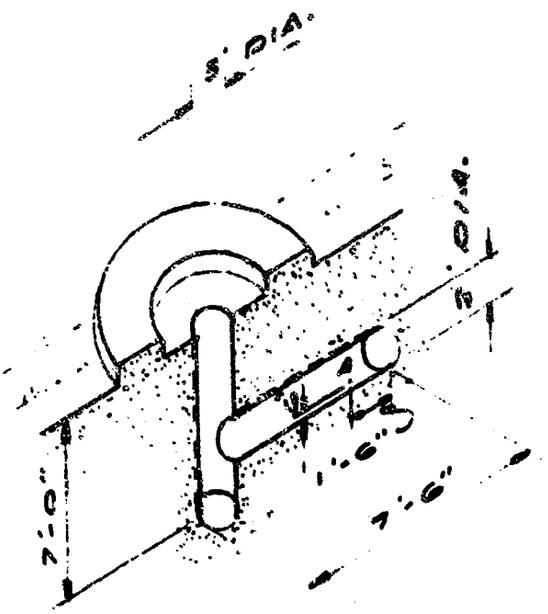

FIGURE 43. OPEN OFFSET FOXHOLE[27]

SECTION 12. COMPARISON BETWEEN THEORETICAL AND EXPERIMENTAL RESULTS FOR GAMMA TRANSMISSION

Having observed the difficulties in formulating theoretical approaches for the determination of transmission factors and the variations in transmission factors obtained from experiment, it is useful to compare results from Sections 7, 8, 9, 10, and 11 in order to indicate the usefulness and limitations of the currently available methods and data. The empirical observations of Section 11 will be used as a basis for comparison, since these tests were not used for the development of any of the calculational procedures. The tunnel geometry used in the tests reported in Section 11 is not necessarily ideal, and, consequently, it is almost impossible to establish that agreement with computational predictions exists. Even under controlled conditions, such as those mentioned in Section 8, the formulation of a desirable expression for predicting the effect of tunnel geometry on the transmission of gamma radiation is exceedingly difficult.

Table VIII shows a comparison between the results measured in the facility shown in Figure 33 and those that would be calculated using the procedures applicable to that geometry. It should be noted that the 12-foot cubicle is not considered in the calculations. Also, the circular riser in the middle of the 3 × 8 tunnel probably affects attenuation in the tunnel and is responsible for the variation between measured and calculated results. It should be noted that the source used for the tests conducted on the tunnel shown in Figure 33 was 100 feet from the tunnel opening, whereas the source used for some of the tests from which the Ingold-Huddleston formula was obtained was located in a tunnel and surrounded by three walls.

Table IX compares the measured and predicted attenuation due to the intersection of the circular hole with the rectangular tunnel shown in Figure 36. Again, the source was in the air and not surrounded by the tunnel. In the instance under consideration, the burst angle was 0°, so that no attenuation is attributed to the circular hole. Consequently, the factors compared in the table are T_2 plus the corner effect. Area equivalence was used to get values for W and H for the circular first leg in order that calculations could be carried out. Also, the width of the second leg is parallel to the length of the first leg, so that the 6-foot height of the rectangular tunnel is considered to be the width of the second leg. The values quoted in the table were calculated for the distances indicated. It should be noted that this introduces an error in the approximate method, since in this method tunnel lengths are defined only to the corner. The values shown in parentheses for the approximate method were calculated using shorter leg lengths; that is, with the corner dimension subtracted.

The transmission factor obtained in a full-scale test on a buried concrete arch structure is compared with the factor that would be calculated with the approximate method in Table X. The geometry of the structure

TABLE VIII. COMPARISON OF TRANSMISSION FACTORS FOR GAMMA RADIATION IN A RECTANGULAR CONCRETE TUNNEL OBTAINED EXPERIMENTALLY AT ORNL WITH THOSE THAT WOULD BE PREDICTED BY THE LE DOUX-CHILTON METHOD GREEN'S METHOD, THE APPROXIMATE METHOD, THE EMPIRICAL EORMULA OF INGOLD AND HUDDLESTON, AND THE OCD METHOD

Refer to: Figures 33, 34 (Points I and D) and 35 (Points B and G)

Method	Transmission Factors
ORNL	$10\text{-}25 \times 10^{-3}$
LeDoux-Chilton	0.50×10^{-3}
Green's	0.47×10^{-3}
Approximate*	1.06×10^{-3}
Ingold-Huddleston	0.13×10^{-3}
OCD	0.16×10^{-3}

Dimensions (Except for Approximate Method)

$L_1 = 6.3$ $W_1 = W_2 = 3$

$L_2 = 12.1$ $H_1 = H_2 = 8$

*Dimensions for Approximate Method

$L_1 = 4.8$ $W_1 = W_2 = 3$

$L_2 = 9.1$ $H_1 = H_2 = 8$

TABLE IX. COMPARISON OF GAMMA RADIATION TRANSMISSION FACTORS OBTAINED EXPERIMENTALLY AT ORNL FOR A RECTANGULAR TUNNEL INTERSECTING A CIRCULAR HOLE WITH THE TRANSMISSION FACTORS THAT WOULD BE CALCULATED USING THE LE DOUX-CHILTON METHOD, THE APPROXIMATE METHOD, AND GREEN'S METHOD

Refer to: Figures 36, 37, and 38

Method	T_2 + Corner Effect	Dimensions
ORNL	80×10^{-3}	$L_1 = 13$ $L_2 = 3$ $W_1 = 2\sqrt{\pi}$ $W_2 = 6$ $H_1 = 2\sqrt{\pi}$ $H_2 = 2.5$ *For approximate only: W_1, W_2, H_1, H_2 same as above. $L_1 = 10$, $L_2 = 1$
LeDoux-Chilton	364×10^{-3}	
Approximate*	312.3×10^{-3}	
Green	--	
ORNL	29×10^{-3}	Same as above except $L_2 = 6$ *For approximate only: W_1, W_2, H_1, H_2 same as above. $L_1 = 10$, $L_2 = 4$
LeDoux-Chilton	11.8×10^{-3}	
Approximate*	19.5×10^{-3}	
Green	170×10^{-3}	
ORNL	15×10^{-3}	Same as above except $L_2 = 9$ *For approximate only: W_1, W_2, H_1, H_2 same as above. $L_1 = 10$, $L_2 = 7$
LeDoux-Chilton	3.94×10^{-3}	
Approximate*	6.39×10^{-3}	
Green	54.8×10^{-3}	

TABLE X. COMPARISON OF GAMMA TRANSMISSION FACTORS OBTAINED IN FULL-SCALE TESTS ON BURIED CONCRETE ARCH STRUCTURES WITH THE TRANSMISSION FACTORS THAT WOULD BE CALCULATED USING THE APPROXIMATE METHOD

Refer to: Figure 39 (Point C)

Method	T_1	T_2 + Corner Effect	T_{Total}
Full Scale	41.9×10^{-3}	10×10^{-3}	0.42×10^{-3}
Approximate*	70.6×10^{-3}	3.59×10^{-3}	0.253×10^{-3}

Dimensions (Except for Approximate Method)

$L_1 = 9$ $\quad L_2 = 15.3$

$W_1 = 2.5$ $\quad W_2 = \sqrt{32\pi}$

$H_1 = 2.5$ $\quad H_2 = \sqrt{32\pi}$

***Dimensions for Approximate Method**

$L_1 = 6$ $\quad L_2 = 13.3$

$W_1 = 2.5$ $\quad W_2 = \sqrt{32\pi}$

$H_1 = 2.5$ $\quad H_2 = \sqrt{32\pi}$

makes it difficult to estimate values for the other methods. It is seen that if T_1 is neglected, the radiation transmitted to point C in Figure 39 is calculated to be greater than the amount that was measured.

Transmission factors predicted by the various methods are compared with full-scale tests on an open offset foxhole in Table XI. The total factor, if multiplied by five, would give a larger factor than those that were measured. The factor calculated for the corner and the second leg is larger than the total measured factor.

The values for transmission factors in the full-scale test appear to indicate that factors predicted by theoretical methods or formulas developed in controlled experiments are not conservative unless the attenuation in the first leg is ignored. Consequently, it is not possible to recommend a straightforward design procedure for predicting transmission of gamma radiation into tunnels and entranceways with existing theories and data. The only procedure that could be suggested or recommended would consist of calculating the transmission by the applicable methods, ignoring attenuation in the first leg, multiplying the calculated factors for the corner and second leg by a safety or design factor of about 5, and choosing the largest of the factors. Comparison with results from full-scale tests on a similar geometry could in some instance allow for choosing other than the largest factor.

Again, it should be specifically noted that ideal tunnel geometries and sources were not used, either in laboratory tests or full-scale studies. Consequently, it is not possible, with current information, to adapt the theoretical or empirical formulations to any other tunnel arrangement with any degree of accuracy; and, in trying to use a given equation for a particular geometry, it may be expedient to use dimensions not necessarily consistent with the precise definitions used in the derivations. For engineering calculations, these approximations are small, especially for a design factor of 5 or more.

TABLE XI. COMPARISON OF GAMMA TRANSMISSION FACTORS MEASURED IN FULL-SCALE TESTS ON OPEN OFFSET FOXHOLE WITH THOSE THAT WOULD BE CALCULATED USING THE LE DOUX-CHILTON METHOD, THE APPROXIMATE METHOD, AND GREEN'S METHOD

Refer to: Figure 43 (Point A)

Method	T_1	T_2 + Corner Effect	T_{Total}
Full Scale	-	-	$3.1 - 8.1 \times 10^{-3}$
LeDoux-Chilton	103×10^{-3}	5.44×10^{-3}	0.56×10^{-3}
Approximate*	106.9×10^{-3}	18.43×10^{-3}	1.97×10^{-3}
Green	206×10^{-3}	4.95×10^{-3}	1.02×10^{-3}

Dimensions (Except for Approximate Method)

$L_1 = 6$ $\quad L_2 = 4.5$

$W_1 = 1.5\sqrt{\pi}$ $\quad W_2 = \sqrt{\pi}$

$H_1 = 1.5\sqrt{\pi}$ $\quad H_2 = \sqrt{\pi}$

*Dimensions for Approximate Method

$L_1 = 5$ $\quad L_2 = 3$

$W_1 = 1.5\sqrt{\pi}$ $\quad W_2 = \sqrt{\pi}$

$H_1 = 1.5\sqrt{\pi}$ $\quad H_2 = \sqrt{\pi}$

SECTION 13. FAST NEUTRON TRANSMISSION IN STRAIGHT TUNNELS

A. General

Since the energy spectrum from a nuclear weapon detonation changes very little with distance[2], it should be possible to allow representative ranges of energies for neutrons to apply over all distances. As mentioned in Section 2C, fast or high energy neutrons are arbitrarily defined to be those neutrons with energies in excess of 0.5 Mev. The relations given in this section are for high energy neutrons from a nuclear weapon.

B. Plane Isotropic Source

Price, Horton and Spinney[6] give the following relation for calculating the transmission of fast neutrons down straight cylindrical tunnels with non-reflecting walls:

$$\phi = \frac{J'}{2} \ln \left[1 + \left(\frac{R^2}{L} \right) \right]$$

where

ϕ = Neutron flux, neutrons per unit area per unit time

J' = Neutron current, neutrons per unit area per unit time

R = Radius of tunnel, ft

L = Tunnel length, ft

The neutron source is assumed to be isotropic. A net current of J' entering the tunnel will produce a neutron flux ϕ on the tunnel centerline a distance L from the source. J' is the number of neutrons crossing a unit area in unit time. The flux ϕ at a point is the number of neutrons passing in unit time through a sphere of unit cross-sectional area centered at that point; obviously, its magnitude is insensitive to the direction in which the quanta cross. It should be specifically noted that this relation is based on the assumption of nonreflecting walls, and as such, may introduce an error in practical cases.

The above equation can be used to give approximate values for a tunnel with a rectangular cross section if the rectangular tunnel has a cross-sectional area equal to the cross-sectional area for the circular one, or

$$R^2 = \frac{WH}{\pi}$$

Replacing R^2 by its equivalent yields

$$\phi = \frac{J'}{2} \ln\left(1 + \frac{WH}{\pi L^2}\right)$$

If the tunnel is long relative to its cross-sectional dimensions, the approximation

$$\ln\left(1 + \frac{WH}{\pi L^2}\right) \approx \frac{WH}{\pi L^2}$$

becomes valid so that

$$\phi \approx \frac{J'}{2}\left(\frac{WH}{\pi L^2}\right) \qquad \text{for } L \gg WH$$

The transmission factor is defined for isotropic sources as

$$T = \frac{\phi \text{ at distance L down the tunnel}}{\phi \text{ at unit distance down the tunnel}}$$

so that for long tunnels, when L is greater than three times the largest cross-sectional dimension, the transmission factor should be approximately

$$T = \frac{WH}{\pi L^2 \ln\left(1 + \frac{WH}{\pi}\right)}$$

for isotropic distribution across the tunnel mouth.

As an approximation, all neutron radiation can be treated as originating from a plane isotropic source regardless of distance, since neutrons have a short mean free path in air. Also, the fact that about 75 percent of the doses over distances of biological interest are derived from neutrons with energies in excess of 0.75 Mev[2] should allow one to approximate the percentage of dose transmitted down a tunnel due to the incidence of fast neutrons at the tunnel mouth. Since thermal neutrons are readily transmitted through tunnels due to the backscatter (discussed in Section 14), an assumption that only about 1/2 of the incident neutrons are fast should yield a conservative but reasonable value for the transmitted dose.

C. Cosine Source

A cosine source refers to the distribution of neutrons emergent from a medium at a surface and essentially states that the intensity is peaked in the direction of the normal to the surface[6]. This type of source is probably a more reasonable representation of a neutron source from a nuclear weapon

than is a plane isotropic source. For this reason, the following relation for cosine distribution, also taken from Reference (6), is presented. The symbols and tunnel geometry are the same as before and again it is assumed that the tunnel walls do not reflect.

$$\phi = 2J' \left[1 - \left(1 + \frac{R^2}{L^2} \right)^{-1/2} \right]$$

For long tunnels, this reduces to

$$\phi \cong J' \left(\frac{R}{L} \right)^2$$

In the case of cosine distribution, it is possible to evaluate ϕ for $L = 0$, which is not possible in the case of an isotropic source. It is expedient to define the transmission factor as

$$T = \frac{\text{flux at L}}{\text{flux at L = 0}}$$

For $L = 0$, the flux for a cosine source is

$$\phi = 2J'$$

so that

$$T = \left[1 - \left(1 + \frac{R^2}{L^2} \right)^{-1/2} \right]$$

and for long tunnels, $L \gg R$,

$$T = \frac{R^2}{2L^2}$$

The transmission factor for a rectangular tunnel would be

$$T = \left[1 - \left(1 + \frac{WH}{\pi L^2} \right)^{-1/2} \right]$$

or, for the case of a long tunnel

$$T = \frac{WH}{2\pi L^2}$$

The angular and energy distribution of neutrons from a nuclear burst is not well defined. For purposes of calculating transmission factors in tunnels, the assumption that 1/2 the incident neutrons are high energy and simulate a cosine distribution across the tunnel mouth may be as reasonable as any other assumption.

SECTION 14. THERMAL NEUTRON ATTENUATION IN A STRAIGHT TUNNEL

A. General

Some neutrons at every distance from the burst are thermal neutrons. Since the transmission of these neutrons down a tunnel can be determined approximately through the use of a plane isotropic source and can be determined more accurately through the use of a cosine source, the information contained in the following paragraph is presented. Fast neutron transmission is accounted for by line-of-sight analysis, with no allowance for scattering from the wall[6].

B. Backscatter Approximation

For calculating the transmission of neutrons streaming down a straight tunnel having a circular cross section, Price et al.[6] suggest multiplying the relations given in Section 13 for plane isotropic source and cosine source by

$$S_i = \frac{1}{1 - a} \qquad \text{for isotropic distribution of backscatter}$$

$$S_c = \frac{L - aL + 4Ra}{L(1 - a)} = 1 + \frac{4Ra}{L(1 - a)} \qquad \text{for cosine distribution of backscatter}$$

where a is the ratio of incident to reflected intensity, or the albedo. These multipliers can also be used for the transmission factors given for rectangular ducts; and, if so desired, they can be applied to fast neutrons.

Some experimental results for a uniform plane source obtained by Horton and Halliday[6, 28] are shown in Figure 44 for the case of a cylindrical steel duct running through a water shield.

It can be seen that a correction for cosine backscatter more nearly represents the case than does an isotropic correction. In determining values for all the computed curves, the albedo was taken to be 0.55. For concrete, the albedo would be 0.3. Although the neutron angular distribution from a nuclear weapon has not been measured, it appears that the assumption of a cosine distribution at the tunnel mouth for both fast and thermal neutrons, equally divided in intensity, should suffice for a practical estimation of the neutron radiation dose transmitted down a tunnel. A design factor of two is used to account for uncertainties. Thus for thermal neutrons

$$T = 2\left\{1 - \left[1 + \left(\frac{R}{L}\right)^2\right]^{-1/2}\right\}\left[\frac{L - aL + 4Ra}{L(1 - a)}\right]$$

for $3 \text{ or } 4 \leq L/R \leq 30$.

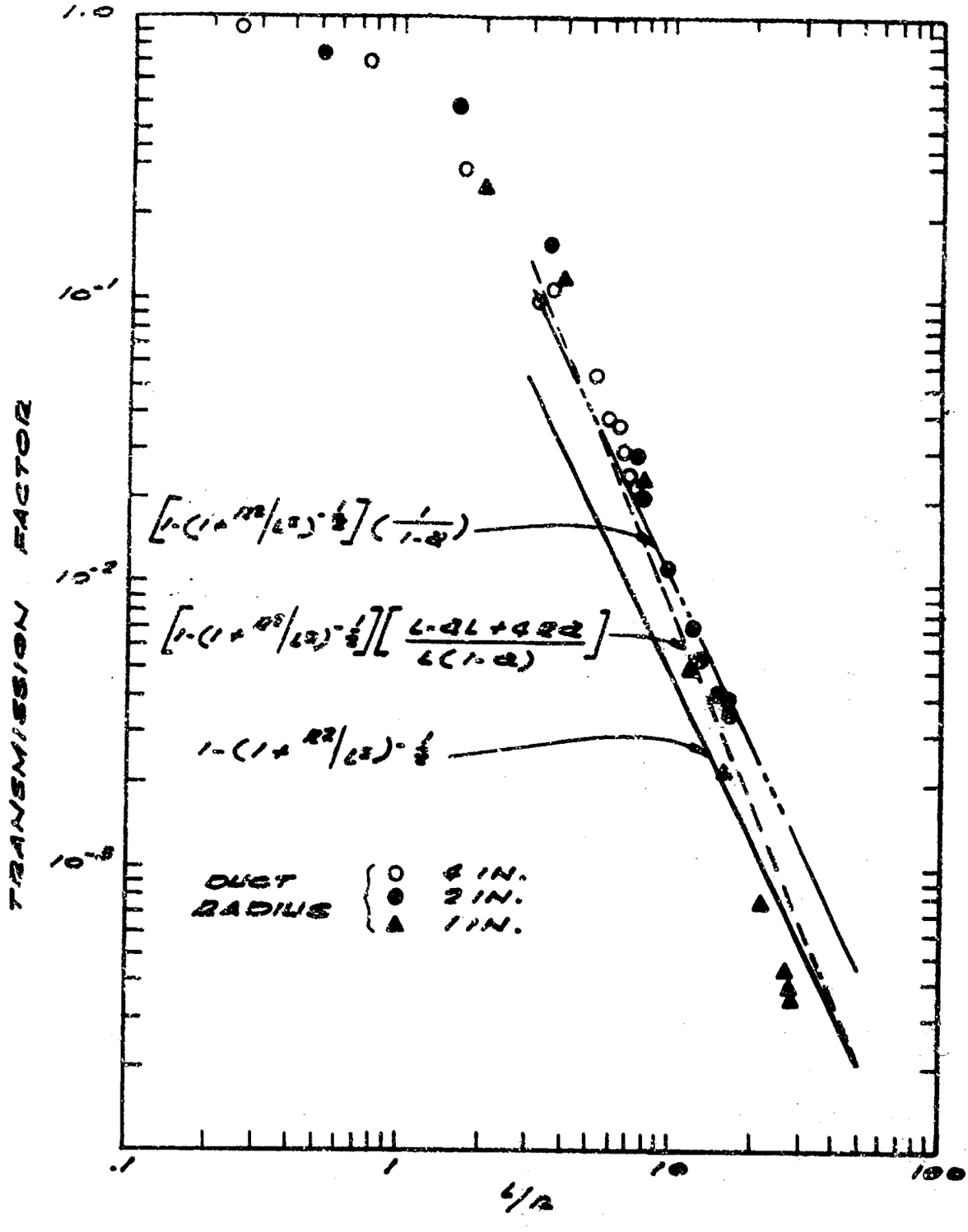

FIGURE 44. MEASURED THERMAL NEUTRON FLUX ALONG AXIS OF STEEL WALLED CYLINDRICAL DUCT THROUGH A WATER SHIELD, WITH ONE END OF DUCT IN CONTACT WITH EXTENDED UNIFORM PLANE SOURCE OF THERMAL NEUTRONS[6, 28]

For $L/R \geq 4$, not too much accuracy is lost by using the approximate substitution $R^2/2L^2$ for the quantity in the braces. The formula for a rectangular tunnel would be

$$T = \left\{\frac{WH}{\pi L^2}\right\}\left[\frac{L - aL + 4a\sqrt{\frac{WH}{\pi}}}{L(1 - a)}\right]$$

SECTION 15. AN EMPIRICAL RELATION FOR CALCULATING THE TRANSMISSION OF THERMAL NEUTRONS DOWN A STRAIGHT CYLINDRICAL TUNNEL

A. General

The analytical procedures available for computing the transmission of thermal neutrons down a straight cylindrical tunnel are founded on assumptions of considerable magnitude. For this reason, it is desirable to give careful consideration to experimentally determined transmission factors. Horton and Halliday have measured the attenuation of thermal neutrons in small diameter steel pipes running through water shields. The experimental data obtained are shown in both Figures 44 and 45. An extended uniform plane source of thermal neutrons was used in their experiments, and the estimated albedo of the pipe and water shield was 0.55.

B. Empirical Equations for Transmission Factors

The experimental points shown in Figure 44 are replotted in Figure 45. It was shown in Section 14 that for $4 \leq L/R \leq 30$, the assumption of cosine distribution and backscatter could be used to obtain a representative estimate of the thermal neutron radiation transmitted down a tunnel. Using the tunnel diameter as a basis, it can be seen in Figure 45 that for $2 \leq L/2R \leq 15$, a relation of the type

$$T = C_1(L/2R)^{C_2}$$

can be used to describe the experimental data very closely if C_1 and C_2 are 1.2 and minus 2.96. For design purposes, a value of minus 3 for C_2 can be used, and the empirical design equation becomes

$$T = 1.2(2R/L)^3$$

for cylindrical steel tunnels through water shields.

The albedo effect for tunnel walls other than steel can be included by multiplying the cubic relation by the ratio of the correction factors given in Section 14. If the albedo for the new material is a', then

$$T = 1.2(2R/L)^3\left[\frac{L(1-a)}{L - aL + 4Ra}\right]\left[\frac{1 - a' + 4a'(R/L)}{1 - a'}\right]$$

which is given for a' = 0.8 in Figure 45. (The value of 0.8 for a' is an arbitrary choice. Steel lining in the ducts reduced the albedo to an estimated value of 0.55, the value quoted in Section 15A.) It is seen that when a greater percentage of the incident radiation is reflected by the tunnel walls, the

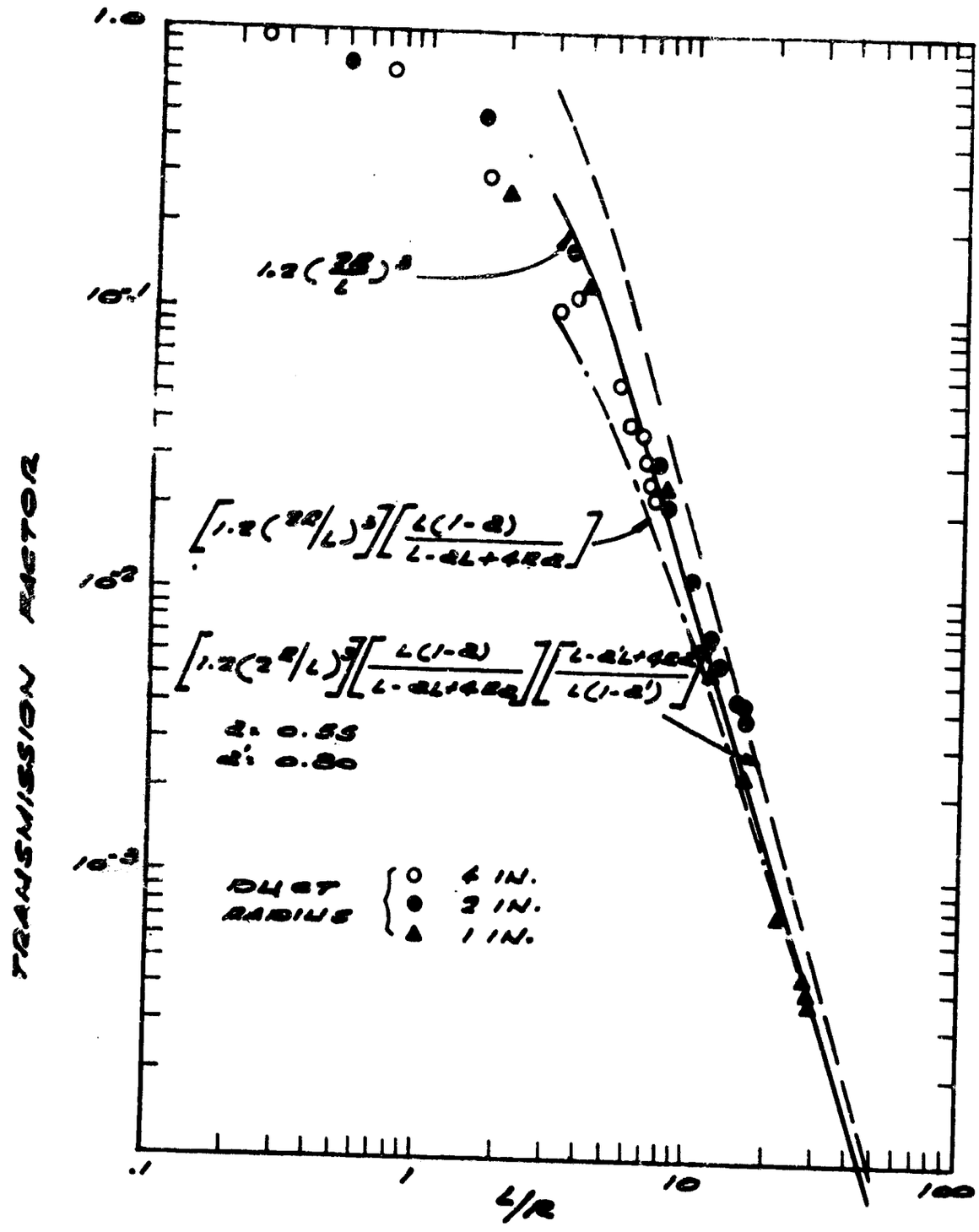

FIGURE 45. EMPIRICAL RELATIONS FOR MEASURED THERMAL NEUTRON FLUX[6, 28]

transmission factor increases. Thus, the expressions for thermal neutrons can be safely used for fast neutrons due to the fact that fast neutrons are reflected more often as thermal neutrons than as fast neutrons[6].

SECTION 16. TRANSMISSION RELATIONS BASED ON DIFFUSION APPROXIMATIONS FOR CALCULATING NEUTRON TRANSMISSION

A. General

Barcus[29] has developed a theory for the unscattered transmission of neutrons in cylindrical ducts in which it is assumed that the neutrons all have the same energy and that the neutron source is plane isotropic. His transmission equation for small values of R/L reduces to

$$T = [1/2](R/L)^2$$

which is the relation obtained from cosine distribution for flux at a distance L down the tunnel produced by unscattered neutrons from the source. This equation is applicable through the use of a reflection coefficient (albedo) to thermal and intermediate energy neutrons; therefore, the Barcus work should also be applicable to the transmission of thermal and intermediate energy neutrons.

The transmission equations developed by Barcus involve a diffusion approximation and do not appear to improve the accuracy with which the transmission of neutrons down straight tunnels can be computed. However, the application of his work to tunnels having obliquely intersecting legs is useful and is presented in this section.

B. Transmission Factors for Tunnels Having Obliquely Intersecting Legs

The transmission factor for a tunnel with two obliquely intersecting legs and no line of sight between the leg ends is

$$T = \frac{\sigma_s}{8\sigma_a}\left(\frac{R}{L_1}\right)^2\left(\frac{R}{L_2}\right)K^2R\lambda_{tr}\left[\frac{\exp(-KL_2)}{1-\lambda_{tr}K\cos\psi}\right]$$

where

σ_s = scattering cross section, barns

σ_a = absorbing cross section, barns

L_1, L_2 = length on tunnel legs along centerline, cm

R = tunnel radius, cm

K = inverse of diffusion length, 1/cm

λ_{tr} = transport mean free path, cm

$\exp(x) = e^x$

ψ = acute angle formed by intersection of tunnel legs

This expression applies only when R/L_1 and $R/L_2 \ll 1$. The parameters used to formulate the expression are explained in Appendix H (Glossary), and it should be noted that metric units of length are required in the expression.

The diffusion coefficient is given by[30]

$$D' = \frac{1}{3(\Sigma_t - \Sigma_s \bar{\mu}_o)}$$

where

D' = diffusion coefficient, cm

Σ_t = total macroscopic cross section, cm^{-1}

Σ_s = total macroscopic scattering cross section, cm^{-1}

$\bar{\mu}_o$ = average cosine of the neutron scattering angle

When absorption is small,

$\Sigma_t \cong \Sigma_s$

and

$$D' = 1/3\left[\frac{1}{\Sigma_s(1 - \bar{\mu}_o)}\right]$$

The quantity in the brackets is called the transport mean free path and denoted by λ_{tr}. Thus,

$$D' = \lambda_{tr}/3$$

If scattering is spherically symmetrical, then $\bar{\mu}_o = 0$ and $\lambda_{tr} = 1/\Sigma_s$. From Reference (30), $K^2 = \Sigma_a/D'$, where Σ_a is the total absorbing cross section in units per centimeter. Noting that $\Sigma = \sigma N$, where N is the number of atoms per cubic centimeter, it is possible to express the transmission factor as

$$T = \frac{\Sigma_s}{8\Sigma_a}\left(\frac{R^4}{L_1^2 L_2}\right)\frac{K^2}{\Sigma_s}\left[\frac{\exp(-KL_2)}{1 - K\cos\psi/\Sigma_s}\right]$$

From Reference (6), pages 168, 262, $1/K \cong 7$ cm and $\Sigma_a = 0.0044 \times 2.3 = 0.0101$ cm. Using $K^2 = 3\Sigma_a\Sigma_s$, we get $\Sigma_s = 0.67$, for concrete. These numbers are for thermal and intermediate energy neutrons, as is pointed out in Section 16A. By substitution

$$T = 4\left[0.254\left(\frac{R^4}{L_1^2 L_2}\right)\left(\frac{\exp(-0.143L_2)}{1 - 0.214\cos\psi}\right)\right]$$

where the safety factor 4 accounts for inherent inaccuracies resulting from required assumptions in the development of the equation. For a rectangular tunnel with dimensions in centimeters

$$T = 0.104\left(\frac{W^2H^2}{L_1^2 L_2}\right)\left(\frac{\exp(-0.143L_2)}{1 - 0.214\cos\psi}\right)$$

or for two legs intersecting at 90°

$$T = \left(\frac{0.104}{L_2}\right)\left(\frac{WH}{L_1}\right)^2 e^{-0.143L_2}$$

The restriction that $R/L \ll 1$ for this expression limits its application to small narrow tunnels. Transmission factors calculated through the use of this equation for large tunnels may be questionable.

SECTION 17. EMPIRICAL RELATIONS FOR DETERMINING THE TRANSMISSION OF THERMAL NEUTRONS DOWN A TUNNEL HAVING BENDS

A. General

The transmission of thermal neutrons around a bend has been studied experimentally by Horton and Halliday[6, 28]. They found that the constants expressing the decrease in transmission of neutron radiation around a bend were the same for the first and second bends, if the incident radiation was isotropic at both the first and second bends.

B. Transmission Equations

By experimental means, Horton and Halliday[6, 28] determined that if the angle between two cylindrical tunnel legs intersecting obliquely was reasonably large, as shown in Figure 46, then the transmission factor due to the bend only could be expressed by the relation

$$T_b = Ka_{DE} \operatorname{cosec} \psi$$

where K is a constant. In the experiments, Ka_{DE} was found to be 0.33. The albedo of the tunnel wall near the surface DE is denoted by a_{DE} and is determined by the wall material. Depending upon the angle with which the neutrons strike the surface, the albedo for concrete and water varies from about 0.1 to about 0.45[31]. An average value of 0.3 for concrete should suffice for most calculations considered here.

Since the experiments of Horton and Halliday have an estimated inaccuracy of about 20 percent, the design relation for a bend of any wall material is

$$T_b = \frac{1.2(0.33) \operatorname{cosec} \psi}{0.55} a_{DE}$$

or

$$T_b = 0.73\, a_{DE} \operatorname{cosec} \psi$$

where a_{DE} is the albedo of the material in region of the bend.

The attenuation down the second leg was found to vary in the same fashion as in the first leg. Thus, for a tunnel with n legs and n-1 equal-angled bends:

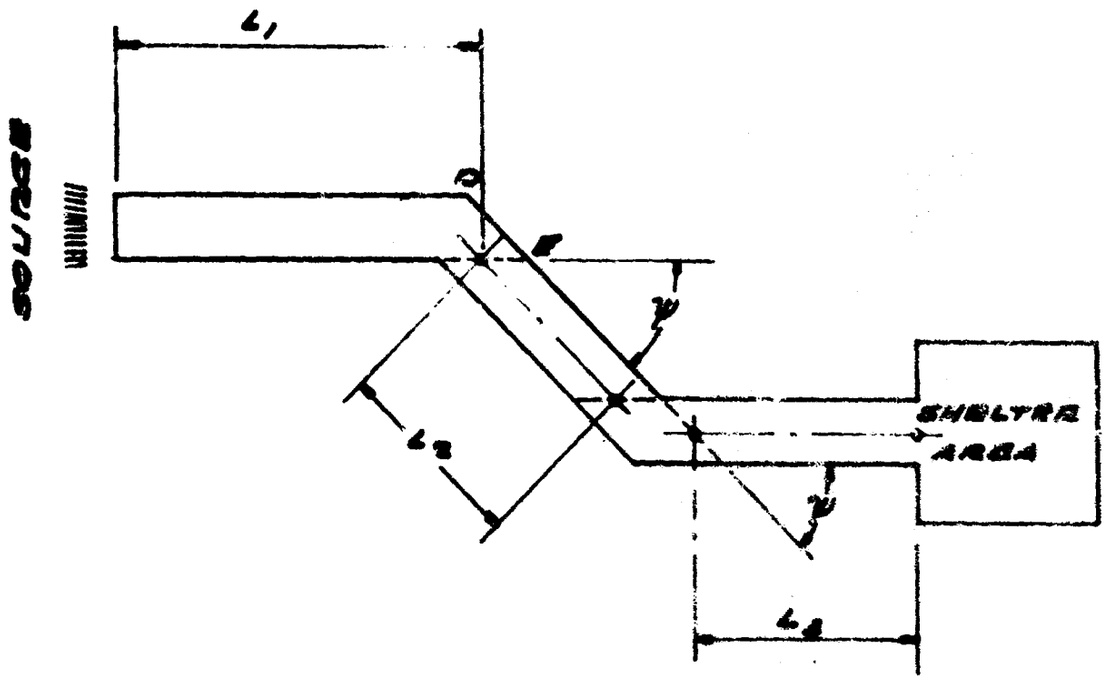

FIGURE 46. SCHEMATIC OF TUNNEL GEOMETRY FOR NEUTRON ATTENUATION STUDIES[6, 28]

$$T = \left[\prod_{i=1}^{i=n} \left(\frac{R_i}{L_i} \right)^2 \right] [0.73\, a_{DE}\, \text{cosec}\, \psi]^{n-1} \quad \text{for } i = 1, 2, \ldots, n$$

For this expression, the tunnel length are measured as shown in Figure 46. Comparison of this expression with data from full-scale and other simulation tests indicates that the value computed here should be quadrupled in order to give a conservative estimate of the transmitted neutron dose, as is indicated in Section 20.

SECTION 18. ENHANCED NEUTRON ATTENUATION IN TUNNELS WITH CORNER TRAPS

In some preliminary experiments[32], which were conducted for the guidance of further work, albedos of about 0.12 for concrete and 0.08 for water were found, using a Po - Be point neutron source. In similar experiments wherein the same type of source was used, Strickler, et al.[31], found albedos of 0.32 for aluminum and for concrete, and a value of 0.032 for water. Without indulging to the extent of ascertaining the discrepancies in the two pieces of work, which is not at all necessary for our purposes here, we can derive an important design concept from these facts. The variance between the test results was no doubt due to the different experimental conditions but, at any rate, we would intuitively suspect a larger albedo from concrete as compared to water.

Empirical observations[6, 33] of Shore and Schamberger indicate that a moderate reduction in neutron intensity can be obtained by just extending the first leg for a short distance past the intersection with the second leg. Their experiments were performed with tunnels intersecting at 45°. Specifically, they found that a space trap at location B in Figure 47 did not materially decrease the transmission around a corner, while a space trap at location A reduced the transmission to 1/3.

For a very small additional construction expense, it is possible that water traps can be deployed at the end of tunnel legs in multiple bend tunnels when the consideration of corner space traps becomes infeasible. Possible deployment of water traps is suggested by Figure 47. It is not known whether the protruding trap or a flush trap would be more advantageous.

Water traps would probably be less expensive than space traps for the case of tunnels having a very large cross section, whereas it would be expected that space traps would be more economical for the case of small cross sections. Also, water traps can be incorporated into existing designs with less difficulty than space traps.

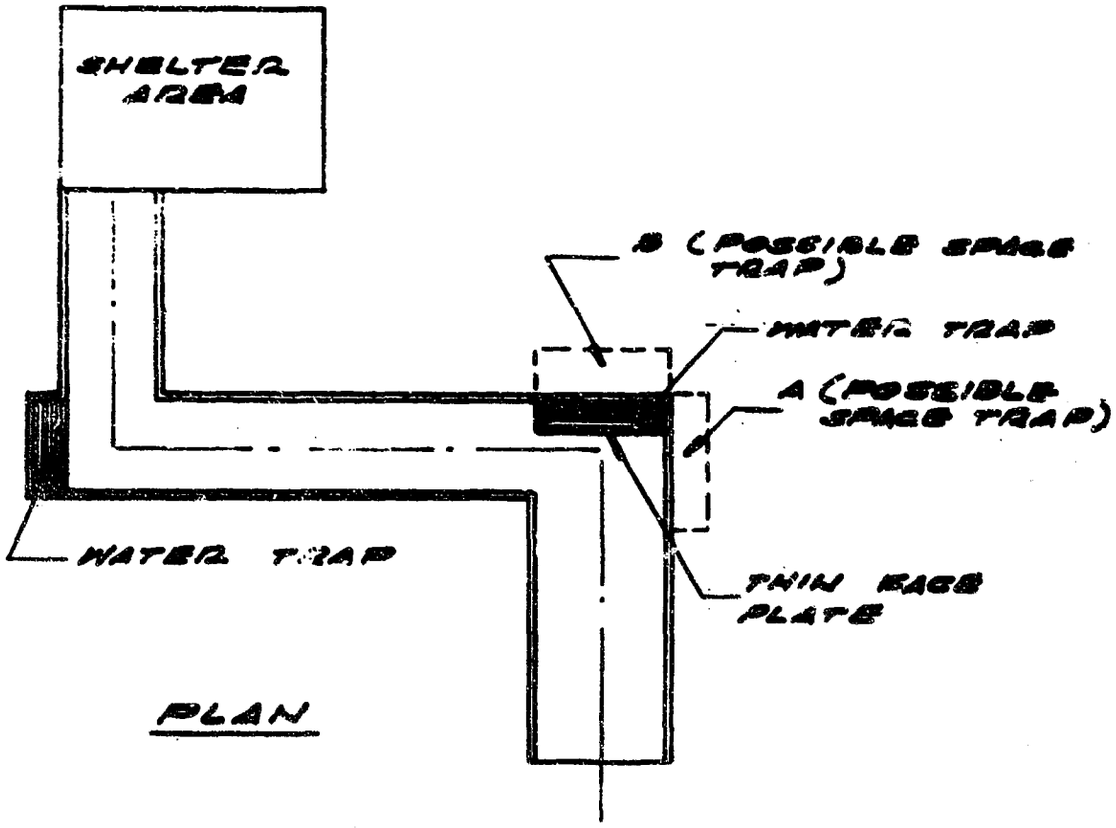

FIGURE 47. SCHEMATIC FOR LOCATION OF WATER AND SPACE TRAPS FOR NEUTRONS

SECTION 19. EXPERIMENTAL RESULTS FOR NEUTRON TRANSMISSION

A. Results from Simulation Experiments

Experimental observations of the transmission of thermal neutrons into tunnels have already been used in the empirical formulations of Sections 15 and 17. It appears that, in straight tunnels, the expressions for thermal neutrons overestimate the transmission of fast neutrons. For the case of obliquely intersecting tunnels, Shore and Schamberger[6, 33] have found that the number of fast neutrons transmitted around a bend decreases more rapidly than the cosecant of the angle of intersection indicated in Section 17. Thus, it appears that data for thermal neutrons may be used to estimate conservatively the transmission of fast neutrons down tunnels and around bends.

Terrell and Jerri[34] have reported the results shown in Figure 48 for transmission of thermal neutrons from both point isotropic and cosine sources into square ducts with a single right-angle bend. These data are for a number albedo, so that the transmitted dose cannot be determined without knowing the energy distribution. They are interesting for purposes of comparing the transmission characteristics of a cosine source and a point isotropic source. Comparison is limited, however, since the L/R ratios are not the same. For the point source $L_1/W = 9'/6' = 1.5$ while with cosine source $L_1/W = 17'/6' = 2.83$. (L_1 in this instance is measured from the tunnel mouth to the beginning of the corner, and L_2, the shelter leg, is measured from the end of the corner as shown in Figure 48.) Using $R = W/2$, it is seen that the ratios of L to R are 3 and 5.7, which is just about the limiting case for the tunnels under consideration.

In Figure 48, the data for the point source are normalized so that the counts for position B (intersection of leg centerlines) are the same as obtained for the cosine distribution. In the first leg, the attenuation varies approximately inversely with the distance. This is shown by the line with a slope of unity on the graph, which is a log-log plot. The transmission from B to A is fairly close to an inverse cubic relation as shown by the line with a slope of 3. For cosine distribution $T_{BA} = 0.0388$ while for the point source $T_{BA} = 0.0585$. The difference in transmission due to source variation can be accounted for by a factor of two. It is interesting to note that the slope of the data for the second leg is not in serious disagreement with the inverse cubic relations given by Reference (6).

The transmission of thermal neutrons into a particular tunnel geometry as reported by Cain is shown in Figures 34 and 35. He too observed that the neutron current leaving the wall had a cosine distribution.[24] Although the geometry used in his tests was not ideal for comparing with the tunnels of

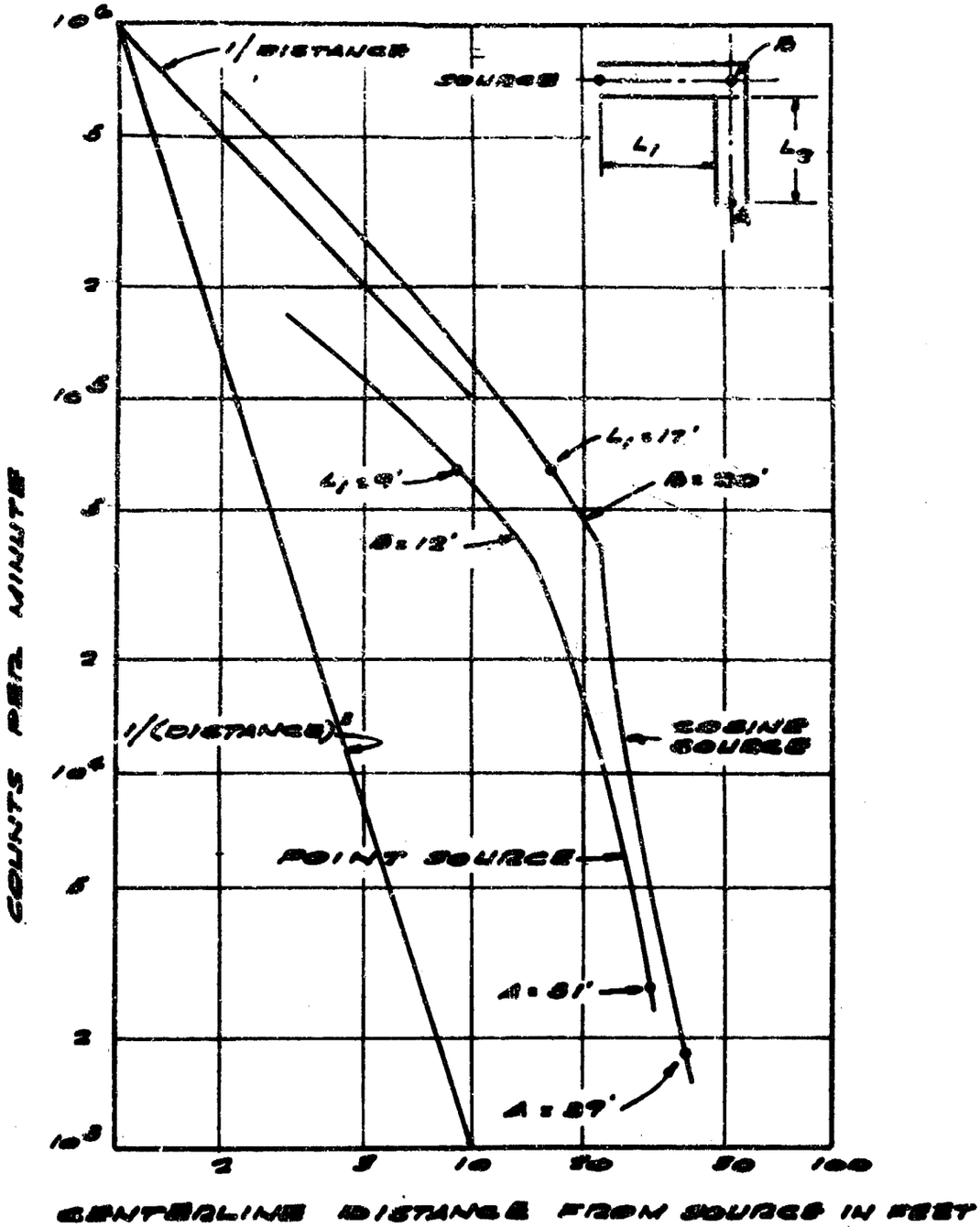

FIGURE 48. COMPARISON OF THERMAL NEUTRON FLUX CENTERLINE DISTRIBUTIONS FOR POINT ISOTROPIC AND COSINE THERMAL NEUTRON SOURCES[34]

importance here, it does indicate transmission characteristics in short tunnels with a low L/R ratio. It is important to note that, in both Figures 34 and 35, the fast neutrons decrease in intensity more quickly than do the thermal neutrons, which supports the observation in Section 15. These experiments were conducted at the ORNL tower facility described in Section 11.

Additional experiments at the ORNL tower facility have been conducted on neutron transmission into the tunnel arrangement shown in Figure 36[25]. The dose rate in the cylindrical hole as a function of L/R is shown in Figure 49 for various angles of incidence with the centerline of the hole. When the source was not directly over the hole, the attenuation did not depart drastically from the inverse cubic relation noted in Reference (6), especially for $L/R \geq 3$. Hole depth did not attenuate the dose rate any appreciable amount when the point source was directly overhead, except when a concrete shield was placed across the opening, in which case, the attenuation again approached the inverse cubic relation. The fast neutron dose rate 40 inches above the hole was about 3×10^{-2} erg $\cdot g^{-1}_{Tissue} \cdot hr^{-1} \cdot w^{-1}$.

Dose rate measurements of fast neutrons in the tunnel intersecting the vertical hole are shown in Figure 50. Again, the data agree reasonably well with an inverse cubic relation. For the data shown, the vertical hole extended below the floor of the tunnel. The addition of concrete blocks in the bottom of the hole to even the floor in the hole with that in the tunnel increased the dose rate only for an angle of incidence of 0°.

B. Results from Full-Scale Experiments

Transmission characteristics of neutron radiation from full-scale detonations are limited, but some data from Operation Plumbob are available in References (26) and (27). Neutron transmission into buried shelters is shown in Figures 39 through 42 along with data for gamma. (These tests are described in Section 11B.) Curves with approximate slopes of -3 are obtained when the neutron data are plotted on log-log graphs, so that there is some degree of agreement between these full-scale tests and simulation tests.

The neutron transmission factor for the open offset foxhole shown in Figure 43 was 0.003 at 2280 ft from ground zero[27]. These measurements were obtained in a different shot than the one used in the test on the buried shelters.

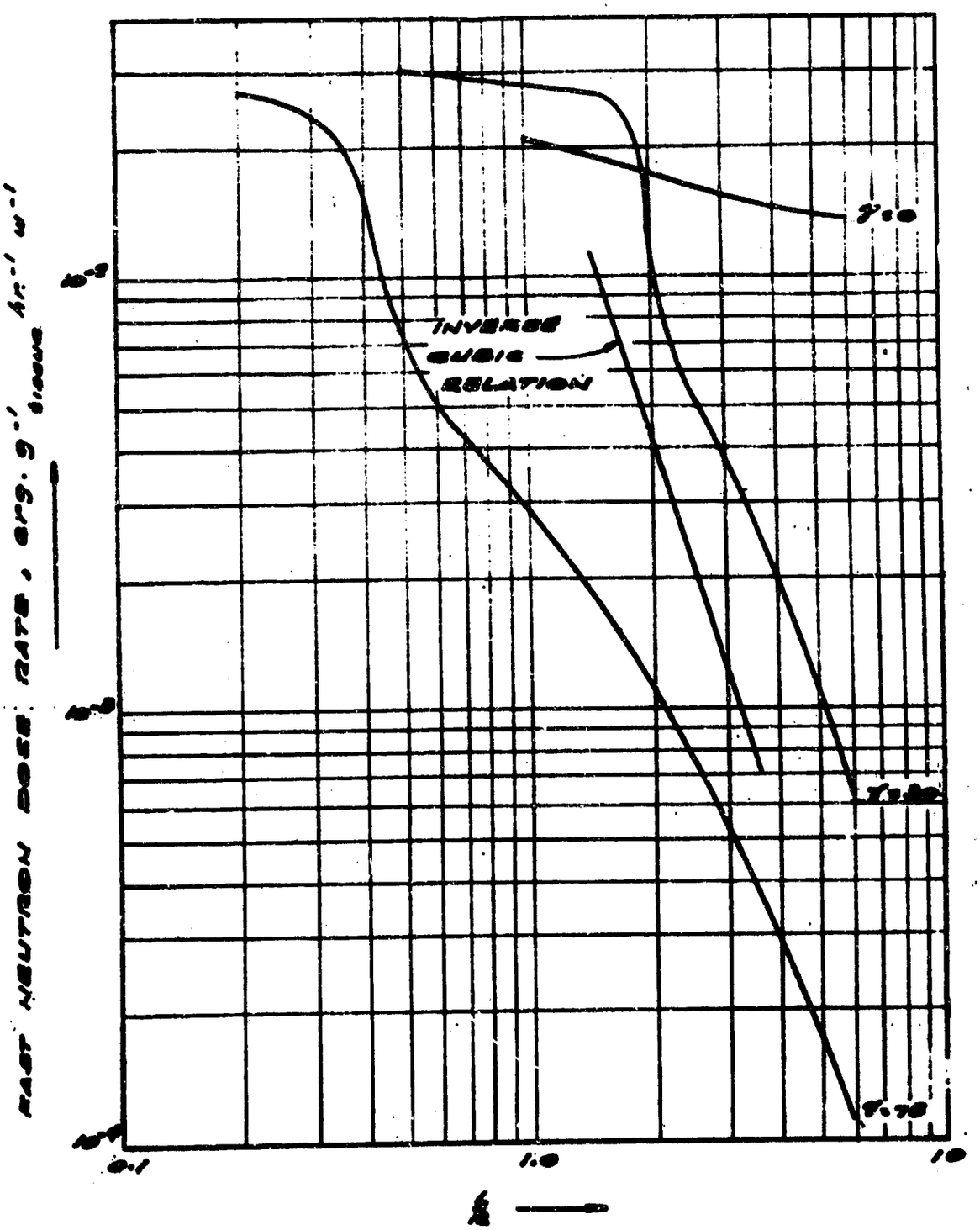

FIGURE 49. TRANSMISSION OF FAST NEUTRONS INTO A CYLINDRICAL HOLE WITH NO SHIELD (POINT SOURCE, 100' FROM OPENING)[25]

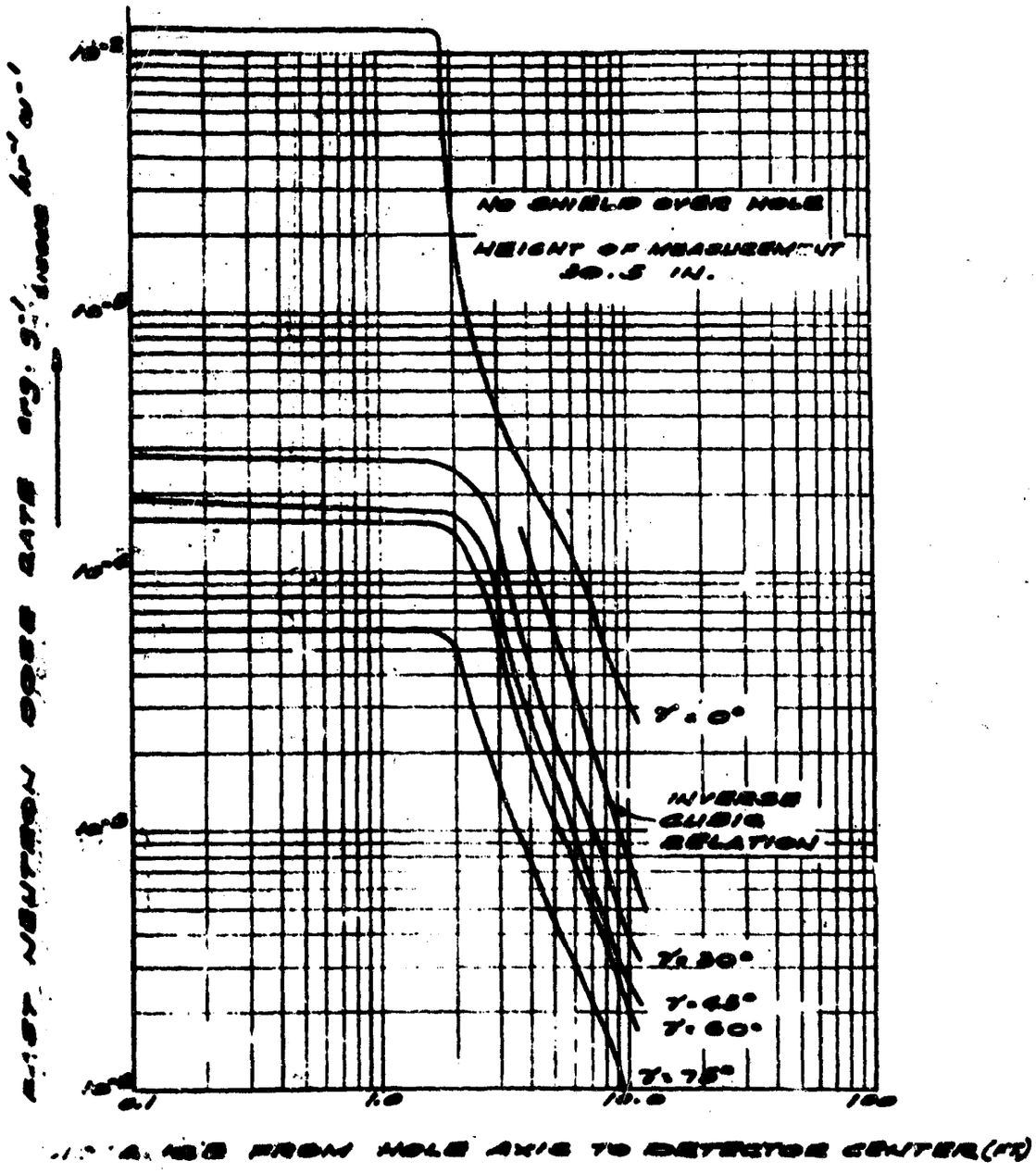

FIGURE 50. FAST NEUTRON DOSE RATE IN TUNNEL (POINT SOURCE, 100' FROM VERTICAL HOLE)[25]

SECTION 20. COMPARISON BETWEEN VARIOUS METHODS FOR DETERMINING NEUTRON RADIATION TRANSMISSION AND EXPERIMENTAL RESULTS

It is of interest to compare the methods of Sections 13 through 17 with the experimental observations in Section 19 in order to determine the usefulness and generality of the methods. It has already been observed in Section 19 that a negative slope of 3 on a log-log plot represents most of the data in a reasonable manner, especially past the initial portion of the individual legs. Use of this observation is impeded, however, by the fact that a different intercept on the "y-axis" is obtained for each set of data. It does point out a possible approach for future unification by letting the intercept be given as a function of geometry.

In the following, it is important to note that, for engineering purposes, with present knowledge, a design factor (or factor of uncertainty) of 4 or 5 is not unreasonable. Further research is expected to reduce the factor of uncertainty.

Calculations for the geometry used by Cain in Reference (24) are compared with measurements in Table XII. Values for the transmission factor for the first leg as calculated by the equations given in Section 13 and 14 are in reasonable agreement with the observed values for both the isotropic and cosine sources assumed in the equations. Values computed by the equations of Section 15 do not agree with the observed data. It is noted that the approximate formula for the "long tunnel" gives a larger value than the other relations. The method for calculating transmission around a corner evidently should be increased by a factor of 3 to 4. The computations for the total transmission factor using Section 16 do not agree with the experimental observations. Section 17 agrees within a factor of 2 for the fast neutrons and within a factor of 6 to 10 for the thermal neutrons. It is to be remembered that the geometry is not ideal, and measurements of interest are probably affected by the vertical cylindrical hole in the middle of the second leg.

The geometry under consideration in Table XIII is not ideal. Except for burst angles of 0°, the methods of Section 13 and 15 again give reasonable values for transmission into the vertical cylinder. For the 0° burst angle, there is essentially no protection afforded by tunnel length from the point source. Transmission into the rectangular tunnel, however, is less for the 0° burst angle than for the others. The methods of Section 13 give conservative values for the tunnel, whereas they give low values for transmission into the vertical cylinder. Section 15 gives a high value for both the cylinder and the tunnel. For the total transmission factor, Section 16 gives an inadequate value, just as it did for the calculations of Table XII. Section 17, however, gives a value which is much too large. Multiplication of the values computed using Section 16 would also indicate too much transmitted neutron radiation. An average area was used in the equation in Section 16.

TABLE XII. COMPARISON OF TRANSMISSION FACTORS FOR NEUTRON RADIATION IN A RECTANGULAR CONCRETE TUNNEL OBTAINED EXPERIMENTALLY AT ORNL WITH THOSE THAT WOULD BE PREDICTED BY THE METHODS OF SECTIONS 13, 14, 15, 16, AND 17

Refer to Figures 33, 34, and 35

TRANSMISSION IN FIRST LEG

$[L_1 = 6.3,\ R = (3 \times 8/\pi)^{1/2}]$

Method		Fast	Thermal
Experimental	Fig. 34	6.95×10^{-2}	3.40×10^{-1}
	Fig. 35	6.59×10^{-2}	3.16×10^{-1}
Section 13	Isotropic	8.94×10^{-2}	-
	Cosine	8.40×10^{-2}	-
	Long Tunnel	9.60×10^{-2}	-
Section 14		-	3.01×10^{-1}
Section 15		81.6×10^{-2}	4.55×10^{-1}

TRANSMISSION AROUND CORNER

Method	T_{Fast}	$T_{Thermal}$
Figure 34	4.17×10^{-1}	7.2×10^{-1}
Figure 35	5.48×10^{-1}	7.0×10^{-1}
Section 17	2.19×10^{-1}	2.19×10^{-1}

TOTAL TRANSMISSION

$(L_1 = 6.3,\ L_2 = 12.1)$

Method	T_{Fast}	$T_{Thermal}$
Figure 34	3.00×10^{-3}	3.20×10^{-2}
Figure 35	-	5.83×10^{-2}
Section 16	2.83×10^{-4}	2.83×10^{-4}
Section 17	2.19×10^{-3}	5.34×10^{-3}

TABLE XIII. COMPARISON OF NEUTRON RADIATION TRANSMISSION FACTORS OBTAINED EXPERIMENTALLY AT ORNL FOR A RECTANGULAR TUNNEL INTERSECTING A CIRCULAR HOLE WITH THE TRANSMISSION FACTORS THAT WOULD BE CALCULATED BY THE METHODS OF SECTIONS 13, 15, 16, AND 17

Refer to Figures 36, 49, and 50

TRANSMISSION INTO VERTICAL CYLINDER REFERENCED TO DOSE RATE 40 INCHES ABOVE GROUND

($L_1 = 13$, $R_1 = 2$)

Method	T at Burst Angles of 0	30	75
Figure 49	4.5×10^{-1}	1.73×10^{-2}	3.00×10^{-3}
Section 13 — Isotropic		1.47×10^{-2}	
Section 13 — Cosine		1.00×10^{-2}	
Section 13 — Long Tunnel		1.18×10^{-2}	
Section 15		2.52×10^{-2}	

TRANSMISSION INTO TUNNEL REFERENCED TO ONE FOOT FROM HOLE CENTER

($L_2 = 10$, $H_2 = 2.5$, $W_2 = 6$)

Method	T at Burst Angles of 0	30	45	60	75
Figure 50	2.07×10^{-3}	1.48×10^{-2}	1.57×10^{-2}	1.35×10^{-2}	1.50×10^{-2}
Section 13 — Isotropic			2.72×10^{-2}		
Section 13 — Cosine			2.00×10^{-2}		
Section 13 — Long Tunnel			2.39×10^{-2}		
Section 15			5.43×10^{-2}		

TOTAL TRANSMISSION REFERENCED TO 40 INCHES ABOVE GROUND

($L_1 = 13$, $L_2 = 10$)

Method	T at Burst Angles of 0	30	75
Figures 49 and 50	1.07×10^{-3}	1.33×10^{-4}	3.00×10^{-5}
Section 16		3.57×10^{-5} (avg area)	
Section 17		16.04×10^{-4}	

Measurements from full-scale tests are compared with prediction methods in Tables XIV and XV. In Table XIV, Section 17 gives a very conservative value and Section 16 gives a reasonable one. In Table XV, however, even the thermal correction indicated in Section 17 gives a value deficient by a factor of 2. The methods appear to predict results from full-scale tests more closely than they predict data from simulation tests, except for the ones from which they were developed.

In summary, with respect to full-scale tests, the relation for total transmission in Section 17 appears to predict transmission only to a reasonable degree, and needs improvement for prediction of transmission around corners. If, as in Section 16, a factor of four is included for corner transmission, Section 17 should give a conservative value when compared to measured values for both full-scale and simulation tests. Thus, in lieu of better information, the formula

$$T = \left[\prod_{i=1}^{i=n} \left(\frac{R_i}{L_i}\right)^2\right] \left[4(0.73)\, a_{DE} \cos\psi\right]^{n-1} \text{ for } i = 1, 2, \ldots, n$$

appears to be the more realistic of the possible expressions, but it also has shortcomings.

Of course, the total transmitted dose is the sum of initial gamma (Section 12), fallout (Section 10), and neutron (Section 20) doses. Variations in measurements from different experiments indicate the complexity in the problem of predicting doses transmitted through tunnels from the detonation of nuclear weapons. These variations further indicate that unifying experiments need to be undertaken. For any given calculation with a specific geometry, it is not unreasonable to use a factor of 10 to insure that a conservative estimate of the radiation transmitted into the geometry has been made.

TABLE XIV. COMPARISON OF NEUTRON TRANSMISSION FACTORS OBTAINED IN FULL-SCALE TESTS ON BURIED CONCRETE ARCH STRUCTURES WITH THE TRANSMISSION FACTORS THAT WOULD BE CALCULATED USING THE METHODS OF SECTIONS 16 AND 17

Refer to Figures 39, 40, 41, and 42

Dimensions		
$L_1 = 9$	$W_1 = 2.5$	$H_1 = 2.5$
$L_2 = 15.3$	$W_2 = \sqrt{32w}$	$H_2 = \sqrt{32w}$

Method	Total T	Notes
Figure 39	4.0×10^{-4}	
Figure 40	5.33×10^{-4}	
Figure 41	6.18×10^{-4}	
Figure 42	1.00×10^{-3}	
Section 16	3.38×10^{-4}	Average Area
Section 17	7.36×10^{-4}	Fast Neutrons

TABLE XV. COMPARISON OF NEUTRON TRANSMISSION FACTORS MEASURED IN FULL-SCALE TESTS OF AN OPEN OFFSET FOXHOLE WITH THOSE THAT WOULD BE CALCULATED USING THE METHODS OF SECTIONS 16 AND 17

Method	Total T	Notes
Reference 27	3×10^{-3}	
Section 16	0.132×10^{-3}	
Section 17	1.43×10^{-3}	Thermal
	0.676×10^{-3}	Fast

Dimensions		
$L_1 = 6$	$W_1 = 1.5\sqrt{\pi}$	$H_1 = 1.5\sqrt{\pi}$
$L_2 = 4.5$	$W_2 = \sqrt{\pi}$	$H_2 = \sqrt{\pi}$

SECTION 21. EFFECT OF TUNNEL GEOMETRY ON TRANSMISSION OF GAMMA AND NEUTRON RADIATION

A. Circular-Rectangular Intersection of Tunnel Cross Section

The effect of tunnel geometry has already been mentioned in previous sections in discussions of the length to radius (L/R) ratios used in the mathematical formulations. If it is necessary to transform from a rectangular to a circular cross section, the equivalent radius R is given by $R = \sqrt{WH/\pi}$. References (35) and (36) indicate that cross-sectional area, and not shape, affects transmission characteristics. No information exists, however, for a rectangular-circular intersection and its effect upon transmission characteristics.

B. Shelters Having Multiple Tunnels or Shafts

Vertical shafts are treated no differently than horizontal tunnels: for gamma radiation, transmission into the first leg is determined by the angle of burst, while, for neutrons, a cosine distribution is assumed across the mouth of the tunnel. In general, in providing a required amount of attenuation through a shaft or tunnel by employment of one or more bends, it can be assumed that little or no attenuation is offered by the exposed leg since, in the worst case, the incident radiation would be parallel to this leg. The attenuation afforded by remaining legs and bends can be calculated by use of methods and procedures presented in other parts of this report.

Multiple access is usually designed into underground shelters since there is a good possibility that one entrance may become inaccessible under attack conditions. In order for a design to be conservative, the fallout radiation dose at the shelter end of each entrance would be added with consideration of further attenuation inside. The initial radiation (in the case of multiple openings) would depend on angle of incidence, so that openings facing the burst could be treated as above with no attenuation afforded from gamma by the first leg and the neutrons having a cosine distribution. For openings not facing the burst, there will be a contribution from skyshine due to the scattering of the radiation; gamma may be considered as a plane isotropic source across the opening while neutrons still have a cosine distribution. This procedure should overestimate the transmission from the openings not facing the burst. It further points out the usual inadequacy of a single leg in attenuating radiation.

C. Two-Legged Tunnel with Obliquely Intersecting Legs

If legs of a tunnel intersect at an angle other than 90°, then the transmission around the bend only is given approximately by

$$T_\psi = T_{90}/\sin_\psi$$

This relation is equivalent to the cosecant variation found to hold experimentally for neutrons[6] and it may not be unreasonable to expect it to be valid for gamma, even though experimental confirmation has not been found in the literature.

D. Tunnels Having Multiple Bends

Since the attenuation down each leg of a tunnel having multiple bends varies in the same manner, except perhaps for the exposed leg, the total transmission factor can be written as

$$T_{TOT} = \left[\prod_{i=1}^{i=n} (T_{Li})\right] \left[\prod_{j=1}^{j=n-1} (T_{Bj})\right]$$

where

n = number of legs

T_{Li} = transmission factor for i^{th} leg

T_{Bj} = transmission factor for j^{th} bend

For a tunnel with four legs

$$T_{TOT} = T_{L1} T_{L2} T_{L3} T_{L4} T_{B1} T_{B2} T_{B3}$$

This product is applicable for 90° intersections or oblique bends. These factors for gamma are determined from Section 6, 7, 8, and 9 with the most conservative value being recommended if all sections are applicable. The factors for neutrons can be determined from Sections 13, 14, 15, 16, and 17, again using the highest value for indicated transmission.

As a matter of interest, Terrell, et al.[37], has experimentally observed that the transmission factors for Z- and U-shaped tunnels are essentially equal. In their experiments, the legs intersected at 90°.

REFERENCES

1. Rockwell, T. III, Editor, Reactor Shielding Design Manual, McGraw-Hill, New York, 1956.

2. Glasstone, S., Editor, The Effects of Nuclear Weapons, U.S. Atomic Energy Commission, 1962.

3. Corps of Engineers, Design of Structures to Resist the Effects of Atomic Weapons, EM 1110-345-413, 1959.

4. Departments of Army, Navy, and Air Force, Capabilities of Atomic Weapons (U), TM23-200, Washington, D.C., 1957. "Confidential."

5. Spencer, L. V., Structure Shielding against Fallout Radiation from Nuclear Weapons, NBS Monograph 42, 1961.

6. Price, B. T., Horton, C. C., and Spinney, K. T., Radiation Shielding, Pergamon Press, MacMillan Company, New York, 1957.

7. LeDoux, J. C., Nuclear Radiation Shielding Provided by Buried Shelters, Interim Report, U. S. Naval Civil Engineering Laboratory, Port Hueneme, California, 1959.

8. Spencer, L. V., and Hubbell, J. H., Report on Current Knowledge of Shielding from Nuclear Explosions, Report 5659, NBS, 1957.

9. Miller, C. F., Gamma Decay of Fission Products from the Slow Neutron Fission of U-235, USNRDL Tech Rept.-TR-187, 1957.

10. LeDoux, J. C , and Chilton, A. B., Attenuation of Gamma Radiation through Two-Legged Rectangular Ducts and Shelter Entranceways-An Analytical Approach, U. S. Naval Civil Engineering Laboratory, TN-383, Port Hueneme, California, 1961.

11. OCDM Engineering Manual, Design and Review of Structures for Protection from Fallout Gamma Radiation, U. S. Government Printing Office, 1961.

12. Blizard, E. P., and Abbot, L. S., Reactor Handbook, Shielding, Interscience Publishers, Div. of John Wiley & Sons, New York, 1962.

13. Chilton, A. B. and Huddleston, C. M., A Semiempirical Formula for Gamma Rays on Concrete, Tech. Rept. R228, U. S. Naval Civil Engineering Lab., Port Hueneme, California, 1962.

14. Hayward, E , and Hubbell, J., "The Albedo of Various Materials for 1-Mev Photons," Phys. Rev., 93, No. 5, 1954.

15. Green, D. W., Attenuation of Gamma Radiation in a Two-Legged 11-Inch Rectangular Duct, Technical Report R 195, U. S. Naval Civil Engineering Lab., Port Hueneme, California, 1962.

16. Sheehan, W. D., "Shielding Results from Weapons Effects Testing," Shielding Symposium Proc., U. S. Naval Radiological Defense Lab. and OCDM, San Francisco, California, 1960.

17. French, R. L., and Wells, M. B., "Calculations of the Spatial, Energy and Angular Distributions of Weapons Radiation," Shielding Symposium Proc., U. S. Naval Radiological Defense Lab. and OCDM, San Francisco, California, 1960.

18. Holland, L. B., et al., "Shielding Against Prompt Weapons Radiation," Annual Progress Report for Period Ending Sept. 1, 1962, Neutron Physics Division, Oak Ridge National Laboratory, ORNL 3360, 1962.

19. Chilton, A. B , Progress in Radiation Shielding Research for Protetive Shelters, Tech. Note N-385, U. S. Naval Civil Engineering Lab., Port Hueneme, California, 1960.

20. Chapman, J. M., Gamma Dose Rates and Energy Spectra in a Three-Foot Square Duct, Tech. Note N-443, U. S. Naval Civil Engineering Lab., Port Hueneme, California, 1962.

21. Ingold, W. C , and Huddleston, C. M., An Empirical Formula for Calculating Gamma-Ray Dose Attenuation in Concrete Ducts, Technical Report R 349, U. S. Naval Civil Engineering Lab., Port Hueneme, California, 1964.

22. Huddleston, C. M., and Wilcoxin, W. L., Gamma-Ray Streaming through Ducts, Technical Report R 289, U. S. Naval Civil Engineering Laboratory, Port Hueneme, California, 1964.

23. Eisenhauer, C., An Engineering Method for Calculating Protection Afforded by Structures against Fallout Radiation, NBS Report 7810, 1963; also NBS Monograph 76, 1964.

24. Cain, V. R., A Study of the Shielding Characteristics of Basic Concrete Structures at the Tower Shielding Facility, ORNL-3464, Oak Ridge National Laboratory, Oak Ridge, Tennessee, 1964.

25. Cain, V.R., Clifford, C.E., and Hallard, L.B., Measurements of Radiation Intensities in Vertical Concrete-Lined Holes and an Adjoining Tunnel at the Tower Shielding Facility, ORNL 3513, Oak Ridge National Laboratory, Oak Ridge, Tennessee, 1964.

26. Flathau, W. J., Breckenridge, R. A., and Wiehle, C. K., Blast Loading and Response of Underground Concrete Arch Protective Structures (U), Operation Plumbob-Project 3.1, WT-1420, DASA, 1959 (now Unclassified).

27. Davis, N. J., Jr., Protection Afforded by Field Fortifications Against Nuclear Weapons Effects (U), Report 1557-TR, Dept. of the Army, Corps of Engineers, Fort Belvoir, Virginia, 1950 (now Unclassified).

28. Horton, C. C., and Halliday, D. B., UKAE Report SWP/P28, 1956.

29. Barcus, J. R., Transmission of Neutrons by Cylindrical Ducts Penetrating Radiation Shields, AEC-TID-4500 (14th Edition), Physics and Mathematics, SCTM21-59(16), 1959.

30. Glasstone, S., and Sesonske, A., Nuclear Reactor Engineering, D. Van Nostrand Co., New York, New York, 1963.

31. Strickler T. D., Gilbert, H. E., and Auxier, J. A., "Fast Neutron Scattering from Thick Slabs," Nuclear Science and Engineering, Vol. 3, pp. 11-18, 1957.

32. Hungerford, H. E., Some Ground Scattering Experiments Performed at the Bulk Shielding Facility, CF-52-4-99, now Unclassified, ORNL, 1952.

33. Shore, F. J., and Schamberger, R. D., Rep WASH-292, Part 3, 1955, AEC.

34. Terrell, C. W., and Jerri, A. J., Radiation Streaming in Shelter Entranceways, Armour Research Foundation 1158A01-5, Final Report, 1961.

35 Ingold, W. C., Some Applications of a Semi-Empirical Formula for Differential Dose Albedo for Gamma Rays on Concrete, TN-469, U. S. NCEL, Port Hueneme, California, 1962.

36. Fowler, T. R., and Dorn, C. H., Gamma Ray Attenuation in a 12-Inch Diameter Round Concrete Duct, TN-465, U. S. NCEL, Port Hueneme, California, 1962.

37. Terrell, C. W., Jerri, A. J., Lyday, R. O., Jr., and Sperber, D., Radiation Streaming in Ducts and Shelter Entranceways, ARF 1158-12, June 1960, and ARF 1158A02-7, Final Rept., NCEL, Port Hueneme, California, 1962.

APPENDIX A. BIBLIOGRAPHY

1. Adams, S., "Interaction of Higher Temperature Air with Materials During Re-entry," Proc. Intl. Symposium on High Temperature Technology, 6 Oct 1959, McGraw-Hill Book Co.

2. Air Force Intelligence Center, "Nuclear Weapon Casualties - Effects on Personnel," 1 May 1961, E. H. Smith and Co., Inc., 901 Pershing Drive, Silver Spring, Maryland, ASTIA No. AD 261739

3. Albright, G. H., Beck, E. J., LeDoux, J. C., and Mitchell, R. A., "Evaluation of Buried Corrugated-Steel Arch Structures and Associated Components," NCEL Rep. WT-1422, Operation Plumb bob - Proj. 3.3 (Conducted May - Oct 1957), 28 Feb. 1961, DASA.

4. Allen, F. J., Futterer, A. T., and Wright, W. P., "Neutron Transmission versus Thickness for Some Common Materials," Dept. Army Proj. No. 512-10-001, BRL Rep. No. 1174, Sep 1962, ASTIA No. 295691.

5. Allen, F. J., "Neutron Reflection and Flux Versus Depth for Nevada Test Site Soil," BRL Rep. No. 1190, Jan 1963.

6. An Engineer Looks at Fallout Shelter, EMO Manual No. 1 (Rev.), Emergency Measures Organization, Privy Council Office, Ottawa, Canada.

7. Anderson, D. G., "Co^{60} Gamma Dose Measurements Inside Cylindrical Shields," 16 Dec 1957, USAF Nuclear Aircraft Research Facility operated by Convair, Div. of General Dynamics Corp., Fort Worth, Texas.

8. Anderson, F. E., Jr., et al., Design of Structures to Resist Nuclear Weapon Effects, Manual of Engineering Practice No. 42, ASCE, 1961, 345 East 47th St., New York, N. Y.

9. Anthony, A. E., Jr., "The Transport of Neutrons through the Atmosphere for a Burst Height of 500,000 Feet," Tech. Doc. Rep. No. AFSWC-TDR-62-17, Feb 1962, ASTIA AD No. 272546.

10. Auxier, J. A., et al., "Experimental Evaluation of the Radiation Protection Afforded by Residential Structures Against Distributed Sources," 19 Jan 1959, Civil Effects Test Operations, OTS, USDC.

11. Barker, E. C., "Final Report on Capture Gamma Ray Experiments Using Portable Neutron Sources and Coincidence Counting," 12 Dec 1949, NEPA Division, Oak Ridge, Tennessee.

12. Barker, R. R., General Handbook for Radiation Monitoring, LA-1835, Sep 1954, Los Alamos Sc. Lab.

13. Batter, J. F., et al., "An Experimental Evaluation of the Radiation Protection Afforded by a Large Modern Concrete Office Building," Civil Effects Test Operations, 22 Jan 1960, OTS, USDC.

14. Batter, J. F. and Starbird A. W., "Attenuation of Cobalt-60 Radiation from a Source Distributed Around a Concrete Blockhouse," 15 Jun 1961, prepare for NDL by Tech. Ops.

15. Batter, J. F., and Starbird A. W., "Attenuation of Cobalt-60 Radiation by a Simple Structure with a Basement," 25 Jul 1961, Tech. Ops.

16. Batter, J. F., and Starbird, A., "The Effect of Limited Strips of Contamination on the Dose Rate in a Multistory Windowless Building, 20 psf Wall and Floor Thickness," Vol. I, submitted to OCD-DOD, 30 Apr 1962, Tech. Ops.

17. Batter, J. F., and Starbird, A. W., "The Effect of Limited Strips of Contamination on the Dose Rate in a Multistory Windowless Building, 80 psf Wall and Floor Thickness," Vol. II, submitted to OCD-DOD, 15 May 1962, Tech. Ops.

18. Batter, J. F., et al., "The Effect of Limited Strips of Contamination on the Dose Rate in a Multistory Windowless Building, 0 psf Wall and 20 psf Floor Thickness," Vol. III submitted to OCD-DOD, 30 Jun 1962, Tech. Ops.

19. Batter, J. F., et al., "The Effect of Limited Strips of Contamination on the Dose Rate in a Multistory Windowless Building," Final Report, Aug 1962, submitted to OCD-DOD, Tech. Ops.

20. Bebbs, E. H., Vogt, R. H., and Faust, W. R., "Effect of Angle of Incidence Upon Penetration of Gamma Radiation," Rep. 4165, 16 Apr 1953, NRL, ASTIA AD No. 7358.

21. Begley, J. J., "Plastic Materials in Lightweight Neutron Shields: General Theory and Practice," Aug 1962, Picatinny Arsenal, Dover, New Jersey, ASTIA No. AD 284982.

22. Beissner, R. E., and Smith, D. R., "Studies in Shielding, II Single Scattering and Capture Theory in Air and Ground," 30 Sep 1957, U.S. Air Force Nuclear Aircraft Research Facility operated by Convair, Div. of General Dynamics Corp., Fort Worth, Texas.

23. Berger, M., and Lamkin, J. C., "Sample Calculations of Gamma Ray Penetration into Shelters: Contributions of Skyshine and Roof Contamination," NBS J. Res., RP 2827, Vol. 60, p. 109, 1957.

24. Berger, M. J., and Raso, D. J., "Backscattering of Gamma Rays," TR 5982, Jul 1958, NBS.

25. Berger, M. J., and Raso, D. J., "Monte Carlo Calculations of Gamma Ray Backscattering," Radiation Research, Vol. 12, 1960, p. 20.

26. Berger, M. J., and Spencer, L. V., "Penetration of Gamma Rays from Isotropic Sources through Aluminum and Concrete," TN 11, 1959, NBS.

27. Berger, M. J., "Penetration of Gamma Radiation from a Plane Monodirectional Oblique Source," NBS J. Res., Vol 56, No. 3, Mar 1956, Paper 2656, p. 111-128.

28. Bethe, H. A., Tonks, L., and Hurwitz, H., "Neutron Penetration and Slowing Down at Intermediate Distances Through Medium and Heavy Nuclei," Phys. Rev., Vol. 80, Oct 1950, p. 11.

29. Bethe, H. A., et al., Blast Wave, LA-2000, OTS, USDC.

30. Biram, M. B., and Tait, J. H., "The Scattering of Neutrons by the Walls of a Laboratory," AERE T/R 563, 1950.

31. Blizard, E., TM 253, 30 Aug 1962, Classified, ORNL, Available from AEC.

32. Blizard, E. P., and Miller, J. M., "Radiation Attenuation Characteristics of Structural Concrete," 29 Aug 1958, ORNL.

33. Bloxsom, D. E., "Cooling of Solid Surfaces with Heat Power Inputs Over 10^5 watts/cm^2," 1957, Heat Transfer and Fluid Mechanics Institute, Stanford University Press.

34. Bolles, R. C., and Ballou, N. E., "Calculated Activities and Abundances of U235 Fission Products," TR-456, 1956, NRDL.

35. Bonin, J. H., Drice, C. F., and Halle, H., "Determination of Factors Governing Selection and Application of Materials for Ablation Cooling of Hypervelocity Vehicles," WADC-TR-59-87, Feb 1960, WADC.

36. Bost, W. E., et al., "Radioactive Fallout," Apr 1959, AEC.

37. Brodeur, R. J., and Batter, J. F., "Radiation Reflected into an Underground Shelter by a Projecting Air Vent," submitted to OCDM, Tech. Ops., 15 Mar 1962.

38. Brown, F. W., III, "Ignition of Fires and Fire Spread by Thermal Radiation," TN 442, 25 Jun 1962, NCEL.

39. Brown, F. W., III, and Eliason, A. Y., "Protection of Exposed Parts of Shelters Against Thermal Radiation from Megaton Weapons," TR 150, 28 Jul 1961, NCEL.

40. Burson, Z., and Borella, H., "Experimental Evaluation of the Radiation Provided by an Earth-Covered Shelter," Civil Effects Test Operations, AEC, AEC Category: HEALTH AND SAFETY, Feb 1962.

41. Carslow, H. W., and Jaejer, J. C., Conduction of Heat in Solids, 2nd Ed., Oct 1959, Oxford University Press, London, p. 63.

42. Cashwell, E. D., and Everett, C. J., A Practical Manual on the Monte Carlo Method for Random Walk Problems, Pergamon Press, 1959.

43. Chandrasekhar, S., Radiation Transfer, Oxford Press, 1956.

44. Chappell, D. G., "Gamma Ray Scattering from Thin Scatterers," Nucleonics, Vol. 14, No. 7, Jul 1956, pp. 36-37.

45. Clare, A. B., "The Measurement of Neutron Dose," AERE-R2924 United Kingdom Atomic Energy Authority Research Group Report, 1959.

46. Clarke, E. T., et al., "Measurement of Attenuation in Existing Structures of Radiation from Simulated Fallout," OCDM, 27 Apr 1959, Tech. Ops.

47. Clifford, C. E., "Gamma Dose in a Hole in a Uniformly Contaminated Plane: Contribution by Ground Penetration," DRCL Rep. No. 310A, Defense Research Chemical Laboratories, Dept. of National Defense, Ottawa, Canada (or Can. J. Phys., Vol. 39, No. 4, 1961, p. 604-608).

48. Collins, D. G., "A Monte Carlo Procedure for Calculating Penetration of Neutrons through Straight Cylindrical Ducts," Sec. 2, Task 1, Item 8 of FZM-2386, Contract No. AF 33(657)-7201, Doc. No. NARE6L 33T, MR-N-286, 24 Nov 1961, General Dynamics, Fort Worth, ASTIA AD No. 267085.

49. Cook, C. S., "Energy Spectrum of Gamma Radiation from Fallout," TR-318, 26 Oct 1959, NRDL.

50. Davison, B., Neutron Transport Theory, Int. Series of Monographs on Physics, Oxford University Press, London, 1957.

51. Donovan, L. K., and Chilton, A. B., "Dose Attenuation Factors for Concrete Slab Shields Covered with Fallout as a Function of Time after Fission," TR-137, 1 Jun 1961, NCEL, ASTIA AD No. 258246.

52. Dyson, J. A., and Harrison, J. R., "The Dependence of Fast Neutron Attenuation in Portland Cement Concrete on its Hydrogen Content," 11 Apr 1956, AERE R/R 1942, AERE, Harwell (U.K.).

53. Fermi, E., Rep. NP-2385, 1951, AEC.

54. Fitzsimons, N., "Integrated Design for Comprehensive Protection from the Effects of Nuclear Weapons," Review Draft, 27 Dec 1960, OCDM.

55. Flügge, S., Editor, Handbuch der Physik, Vol. 38/2, "Neutrons and Related Gamma Ray Problems," 1959, Springer Verlag, Berlin.

56. French, R. L., "Fast Neutron Free Field Environment and Unshielded Dose Rates for the TSF Bunker Experiment," Res. Note No. 63-2, Feb 1963, Radiation Research Associates.

57. Fundamentals of Nuclear Warfare, Jan 1961, Special Text 3-154, U. S. Army Chemical Corps School, Fort McClellan, Alabama.

58. Georgiev, S., Hildago, H., and Adams, M. C., "On Ablation for the Recovery of Satellites," 1959, Heat Transfer and Fluid Mechanics Institute, Stanford University Press, p. 171.

59. Glasgow, D. W., "Neutron Scattering from the Walls and Air of a Laboratory," HW-32086, Jun 1954.

60. Glasstone, S., Source Book on Atomic Energy, 1950, D. Van Nostrand Co., Inc., Princeton, N. J.

61. Haggmark, L. G., "Ship Shielding Factors - Computational Method Compared to Experimental Results," 7 Jun 1961, NCEL, ASTIA No. AD 259677.

62. Handbook of Chemistry and Physics, 36 Ed., 1955, Chem. Rubber Publ. Co., Cleveland, Ohio.

63. Hayward, E., and Hubell, H., "An Experiment on Gamma-Ray Scattering," TR-2264, Feb 1954, NBS.

64. Heitler, W., The Quantum Theory of Radiation, 3rd Ed., Oxford, Clarendon Press, 1954.

65. Holland, L. B., "Measurements of Radiation Intensities in Vertical Concrete-Lined Holes and an Adjoining Tunnel at the Tower Shielding Facility," ORNL 3513, to be published.

66. Holland, L. B., Cain, V. R., Maerker, R. E., Stern, H. E., Clark, F. H., Hull, J. L., Manning, J. J., and Ward, D. R., "Shielding Against Prompt Weapons Radiation," ORNL 3360, Jan 1963, AEC.

67. Horton, C. C., Halladay, D. B., Lakey J. R. A., and Harrison, J. R., "The Transmission of Thermal Neutrons in a Straight Annular Duct," AERE Report SWP/P 27, Jan 1956.

68. Hyodo, T., "Back Scattering of Gamma Rays," Nuc. Sci. and Engr., Vol. 12, No. 1, 1962, pp. 178-184.

69. Ingold, W. C., "Some Applications of a Semiempirical Formula for Differential Dose Albedo for Gamma Rays on Concrete," 30 Nov 1962, NCEL, ASTIA No. AD 291133.

70. Jarrett, A. A., "Statistical Methods Used in the Measurement of Radioactivity," AECU-262, 17 Jun 1946.

71. Johansson, S. A. E., "On the Possibility of Using Model Experiments to Study Shielding Problems," Dept. of Phys., Univ. of Lund, Lund, Sweden.

72. Judge, J., "High Temperatures Spur Novel Graphite Development," Missiles and Rockets, 7 Nov 1960, Vol. 7, No. 19, pp. 21-22.

73. Kessler, J., and Levoy, L., "A Study of Blast-Closure Devices," Tech. Doc. Rep. No. AFSWC-TDR-62-10, Final Rep., Feb 1962, AFSWC, ASTIA No. AD 274646.

74. Kinder, M. B., "Design of Rectangular Underground Structures to Resist Nuclear Weapons," M. S. Thesis, Civil Engr., 1961, University of Colorado, ASTIA AD No. 264553.

75. King, R. A., "Materials and Techniques for Thermal Transfer and Accomodations," Proc. Intl. Symposium on High Temperature Technology, 6 Oct 1959, McGraw-Hill Book Co.

76. "Lead Shielding," Prepared for Navy, Bureau of Aeronautics, submitted by Storchheim Research and Development Corp., Woodside, N. Y., 30 Jun 1958 through 30 Jun 1959, ASTIA No. AD 227423.

77. LeDoux, J. C., "Analysis of the Critical Shielding Volume for Underground Shelters," TN-381, Proj. Y-F011-05-329, Ntel.

78. LeDoux, J. C., and Donovan, L. K., "Shielding Factors for Underground Shelters of Various Geometric Shapes," Y-F011-05-329, NCEL, ASTIA AD No. 254344.

79. Launderfer, M., "The Backscattering of Gamma Radiation from Plane Concrete Walls," RFA-84, 3 Jul 1962.

80. Laupanskiu, O. I., "Gamma-Radiation of an Atomic Explosion," TR-4516 (Moscow, 1959), AEC.

81. Levy, A. V., "Extrema High Temperature," 9 Oct 1961, Lecture at UCLA under the series, "Materials for Missiles and Spacecraft."

82. Litz, L. M., "Graphite, Carbide, Nitride, and Sulfide Refractories," Proc. of Intl. Symposium on High Temperature Technology, 6 Oct 1959, McGraw-Hill Book Co., p. 90.

83. Marcum, J. I., "A Comparison of Monte Carlo Code Computations," RAND, Los Alamos, and Sandia, RM-2556. Jul 1961.

84. Maerker, R. E., ORNL Rep. No. 3288, AEC.

85. Mather, R. L., "Gamma Ray Collimator Penetration and Scattering Effects," J. Appl. Phys., Vol. 28, No. 10, Oct 1957, p. 1200-1207.

86. "Measurement of Absorbed Dose of Neutrons, and of Mixtures of Neutrons and Gamma Rays," NBS Hdbk. 75, 3 Feb 1961, GPO.

87. Merrill, M., and Cowell, W. L., "Literature Survey of Concretes for Nuclear Radiation Shielding," Y-R011-01-005, Type C, Final Report, 28 Jun 1960, NCEL, ASTIA AD No. 239871.

88. Merritt, J. L., and Newmark, N. M., Design of Underground Structures to Resist Nuclear Blast, Civil Engineering Studies, Structural Research Series, Vol I and II, No. 149, Revised Edition, Jul 1962, Dept. of Civil Engr., Univ. of Ill., Urbana, Ill.

89. Monk, C. B., Jr., Resistance of Structural Clay Masonry to Dynamic Forces, Rep. No. 7, Nov 1958, Structural Clay Products Research Foundation, Geneva, Illinois.

90. Morgan, R. H., and Corrigan, K. E., Handbook of Radiology, 1955, The Year Book Publ., Inc., Chicago, Ill.

91. Moteff, J., "Miscellaneous Data for Shielding Calculations," APEX-134, 1953, AEC, (or Nucleonics, Vol. 13, No. 5, 1955, pp. 28-31).

92. Moteff, J., "Miscellaneous Data for Shielding Calculations," APEX-176, 1954, General Electric Atomic Products Div., Cincinnati, Ohio.

93. Murray, R. L., Introduction to Nuclear Engineering, 1954, Prentice-Hall Inc.

94. Ntl. Res. Council, A Glossary of Terms in Nuclear Science and Technology, 1955, ASME, New York, N. Y., Individual sections available: I, Physics; II, Reactor Theory; III, Reactor Engineering; IV, Chemistry; V, Chemical Engineering; VI, Biophysics and Radiobiology; VII, Instrumentation; VIII and IX, Isotopes Separation and Metallurgy.

95. Newmark, N. M., and Haltwanger, J. D., Principles and Practices for Design of Hardened Structures (Air Force Design Manual), Tech. Doc. Rep. No. AFSWC-TDR-62-138, Dec 1962 (Proj. No. 1080, Task No. 10802), AFSWC.

96. Newmark, N. M., and Hansen and Associates, Protective Construction Review Guide (Hardening), Vol I and II, Jun 1961, Office of the Assistant Secretary of Defense, (Installations and Logistics), Office of the Deputy Assistant Secretary, (Properties and Installations).

97. "Nuclear Data," NBS Circular 499 and Supplements No. 1, 2, and 3, 1950-1951, USDC.

98. Nuclear Defense Measures, Jul 1959, Special Text 3-155. U. S. Army Chemical Corps School, Fort McClellan, Alabama.

99. Patterson, H. W., Hess, W. N., Moyer, B. J., and Wallace, R. W., "The Flux and Spectrum of Cosmic-Ray Produced Neutrons as a Function of Altitude," Health Physics, Vol. 2, 1958, pp. 69-72.

100. Peebles, G. H., "Gamma-Ray Transmission through Finite Slabs," NCEL TR-240, Dec 1952, Rand Corp., Santa Monica, Calif., ASTIA AD-8200.

101. Perkins, J. F., "Monte Carlo Calculation of Gamma Ray Albedo of Concrete and Aluminum," J. Appl. Phys., Vol. 26, No. 6, Jun 1955, pp. 655-658.

102. "Proceedings of the Shielding Symposium Held at NRDL," Vol. I, 17-19 Oct 1956, ASTIA No. AD 132830.

103. Purrus, W. R., "Gamma Removal Dose Calculations," Jul 1958, ASTIA No. AD 202 301.

104. Putz, R. R., and Broido, A., "A Computation Method for Gamma Radiation Intensity in the Presence of General Shielding and Source Configurations," Dec 1957, Proj. Civil, Univ. of Calif.

105. Radiological Monitoring Methods and Instruments, NBS Hdbk. 51, 1952, USDC.

106. Report of the International Commission on Radiological Units and Measurements, 1956, Handbook 62, (Supercedes Recommendations of the International Commission on Radiological Protection, NBS Hdbk. 47, 1951) USDC.

107. Roberts, L., "Stagnation Point Shielding by Melting and Vaporization," NASA R-10, 1959, p. 14.

108. Rockwell, T., Ed., Reactor Shielding Design Manual, 1956, McGraw-Hill Book Co., New York.

109. Rossi, B., "High-Energy Particles," Prentice-Hall, Inc., Englewood Cliffs, N. J., 1952.

110. Sax, N. I., and Associates, "Radiation and Radiation Hazards," Handbook of Dangerous Materials, 1951, Reinhold Publ. Corp., N. Y.

111. Schamberger, R. D., et al., "The Transmission of Neutrons and Gamma-Rays through Air Slots," Part III, "The Transmission of Gamma-Rays through Straight Air Slots in Water," 1 Sep 1954, Brookhaven National Laboratory under contract with the United States Atomic Energy Commission.

112. Schmoke, M. A., and Rexroad, R. E., "Attenuation of Simulated Fallout Radiation by the Roof of a Concrete Blockhouse," Aug 1961, NDL.

113. Segre, E., Editor, Experimental Nuclear Physics, Vol. I, John Wiley and Sons, Inc. New York, 1953.

114. Shore, F. J., and Schamberger, R. D., "The Transmission of Neutrons through Ducts in Water," BNL 390 (T-74), 1 Mar 1956.

115. Shumway, B. W., et al., "The Dose Distribution within an Aircraft Carrier Exposed to Uniform Co^{60} Contamination on the Flight Deck," 4 Oct 1960, NRDL, ASTIA No. AD 250710.

116. Simon, A., and Clifford, C. E., Rep. ORNL-1217 Rev., 1954, AEC.

117. Smith, R. J., and Benck, R. F., "Effect of Neutron Interactions with Blast and Thermal Shields on Measured Gamma Dose," Nov 1961, NDL-TR-18 (ASTIA AD No. 273253) and NDL-TR-19 (ASTIA AD No. 269264).

118. Smith, R. J., and Benck, R. F., "Effect of Neutron Interaction with Soil on Gamma Dose," NDL-TR-18, Mar 1961, ASTIA.

119. Spielberg, D., "Shielding Characteristics of Air, Soil, Water, Wood, and Other Common Materials," Attenuation of Gamma Rays and Neutrons, V. 2, WKNL-89, Feb 1957, Walter Kidde Nuclear Lab., Inc., Garden City, N. Y.

120. Spielberg, D., "Dose Attenuation by Soils and Concrete for Broad, Parallel-Beam Neutron Sources," AN-108, May 1958, Associated Nucleonics, Garden City, N. Y.

121. Spencer, L. V., and Diaz, J., "Neutron Penetration in Cylindrical Ducts," to be published.

122. Spencer, L. V., and Lamkin, J. C., "Slant Penetration of Gamma Rays in Concrete," 1959, NBS Unpublished Report.

123. Spencer, L. V., and Lamkin, J. C., "Slant Penetration of Gamma Rays: Mixed Radiation Sources," 1959, NBS Unpublished Report.

124. Spencer, L. V., and Lamkin, J. C., "Slant Penetration of Gamma Rays in Water," 1958, NBS Unpublished Report.

125. Starbird, A. W., et al., "Modeling Techniques as Applied to Fallout Simulation on Residential-Type Structures and Some Preliminary Results," 8 Jul 1961, prepared for OCDM, Tech. Ops.

126. Starbird, A. W., et al., "The Effect of Interior Partitions on the Dose Rate in a Multistory Windowless Building," 31 Jan 1963, prepared for OCDM, Tech. Ops.

127. Stephenson, R., Introduction to Nuclear Engineering, McGraw-Hill Book Co., 1958.

128. Steurer, W. H., "Materials for Thermal Protection," 16 Jan 1961, Lecture at UCLA under the series, Materials for Missiles and Spacecraft.

129. "Studies in Atomic Defense Engineering," Doc. P-290 and P-290.1, 1957 and 1958, Bureau of Yards and Docks.

130. Symposium on Survival Shelters, 25-27 Jun 1962, ASHRAE.

131. Terrell, C. W., "Radiation Streaming in Shelter Entranceways," NRDL-OCDM-Shielding Symposium Proc., 30 Oct 1960, San Francisco, Calif.

132. Terrell, C. W., and Jerri, A. J., "Comparison of Theory and Measurement of Photon Streaming in a Straight Rectangular Concrete Duct," Trans. Am. Nuc. Soc., Vol. 20, No. 2, Nov 1961.

133. Terrell, C. W., Jerri, A. J., and Lyday, M. O., "Measured Radiation Distributions in Shelter Entranceways," Trans. Am. Nuc. Soc., Vol 20, No. 3, Nov 1961.

134. "The Nature of Radioactive Fallout and Its Effects on Man," Summary Analysis of Hearings, May 27-29, and Jun 3-7, 1957, Joint Committee on Atomic Energy, 85th Cong., 1st Session, Joint Committee Print, Aug 1957, GPO.

135. Theus, R. B., and Beach, L. A., "Gamma-Ray Albedo from Iron," TR-4701, 1956, NRDL.

136. Titus, F., "Penetration in Concrete of Gamma Radiation from Fallout," Rep. ITR-1477, 22 Oct 1957, AEC.

137. Wells, M. B., "Air and Concrete Scattering of Gamma Rays," 20 Mar 1959, Proj. 6(1-9964), Contract AF 33(600)-32054, DCL, ASTIA AD No. 214 571.

138. Wells, M. B., "Analysis of the Measurements of Fast Neutron Dose Rates in Hole No. 1," Note No. 63-3, Feb 1963, Radiation Research Associates Res.

139 Whitcombe, D. W., "A Diffusion Solution for the Cylindrical Ducting Problem in Infinite Geometry," AFCD-3413.

140. Zerby, C. D., "Preliminary Report on the Penetration of Composite Slabs by Slant Incident Radiation," Rep. CF-54-9-120, 1954, ORNL.

141. Zobel, W., and Love, T. A., "Short Lived Fission Product Gamma Radiation," presented at Symposium of the Shorter-Term Biological Hazards of a Fallout Field, Washington, D. C., 1956.

APPENDIX B. NOMENCLATURE

Symbol	Description	Units
a	Albedo	Numeric
A	Area	ft^2, cm^2
C, C_1, C_2	Constants	Numeric
D	Dose rate	Roentgen/hr, r/sec, ...
D'	Diffusion coefficient	cm
D	Diameter	ft, cm, ...
e	Eccentricity ratio	Numeric
E	Total exposure dose	Roentgen
E_o	Source energy	mev
exp	Base of natural logarithm e	Symbolic
G_b	Factor for gamma transmission around bend from prime areas	Numeric
G_t	Factor for gamma transmission around corner through corner lip	Numeric
G_s	Factor for gamma transmission around bend through in scattering	Numeric
H	Tunnel height	ft, cm, ...
J'	Neutron current	Number/cm^2-sec
k, K	Constant	Numeric
K	Inverse of diffusion length	cm^{-1}
K	Klein-Nishina scattering probability	Numeric
$\ln$	Natural logarithm	Operating symbol

Symbol	Description	Units
L	Tunnel length	ft, cm, . . .
n	Normality ratio	Numeric
n	Number of tunnel legs	Numeric
N	Number of atoms per unit volume of scattering material	cm^{-3}
r_o	Classical radius of electron	cm
r	Distance	Feet
R	Radius	ft, cm, . . .
s	Empirical constant	Numeric
t	Time	Hour, sec, . . .
T	Transmission factor	Numeric
v	Empirical constant	Numeric
V_s	Average velocity of neutron	cm/sec
w	Empirical constant	Numeric
W	Tunnel width	ft/cm, . . .
Z	Number of electrons per atom of scattering material	Numeric
α_1	Angle that gamma photons strike corner lip	Degrees
α_2	Angle that gamma photons leave corner lip	Degrees
β	Ratio of leg height or width to length	Numeric
γ	Burst angle	Degrees
θ_o	Polar angle of incidence	Degrees
θ	Polar angle of reflection	Degrees
θ_s	Scattering angle	Degrees

Symbol	Description	Units
λ_{Tr}	Transport mean free path	cm
$\bar{\mu}_o$	Average cosine of neutron scattering angle	Numeric
μ_a	Absorption coefficient	cm^{-1}
μ'_a	Coefficient of radiation reflected from surfaces	cm^{-1}
π	Ratio of circumference to diameter	Numeric
$\prod$	Multiplication of terms	Operating Symbol
ρ	Neutron density	Number/cm^3
Σ_t	Total macroscopic cross section	cm^{-1}
Σ_s	Total macroscopic scattering cross section	cm^{-1}
σ_s	Scattering cross section	Barns
σ_a	Absorbing cross section	Barns
ϕ	Azimuthal angle	Degrees
ϕ	Neutron flux	Number/cm^2-sec
ϕ_T	Total or integrated neutron flux	Neutron/cm^2
ψ	Acute angle between centerline of adjacent tunnel legs	Degrees
ω	Solid angle fraction	Steradians

Subscripts

o	Source point or reference point
p	Specific point of interest
1, 2, . . .	Different points
s	Scattering

Symbol	Description	Units
DE	Area associated with two lines shown as points in tunnel cross section	
i	Number of values for a parameter occurring repeatedly as a factor in a given expression	
j	Number of bends	

APPENDIX C. UNITS OF DOSE MEASUREMENT

The rhm is a unit used to define quantitatively the strength of a gamma radiation source. One rhm is the quantity of gamma-ray source that gives a dosage rate of 1 roentgen per hour in air, at a distance of 1 meter from the source.

The rem and rep are quantitative units of any type of ionizing radiation. One roentgen equivalent man, rem, is the amount of absorbed radiation which produces an effect equivalent to the absorption by man of 1 roentgen of x- or γ-radiation. One roentgen equivalent physical, rep, is the amount of radiation causing the absorption of 93 ergs per gram of tissue.

The radiation unit, rad, is an absorbed dose unit corresponding to an energy absorption of 100 ergs/gm of any medium. The rad differs from the rep in that it can be applied to any medium. For soft tissue, the rad equals 93 percent of the dose in units of rep. These radiation dose units are summarized in Table XVI.

TABLE XVI. RADIATION DOSE UNITS

Radiation	Roentgen	Energy Absorbed, REP	Biological Damage, REM	RBE
X-Ray	1	1	1	
Gamma	1	1	1	1
Beta		1	1	1
Thermal Neutron		1	5	5
Fast Neutron		1	10	10
Proton		1	10	10
Alpha Particle		1	20	20

1 R = 1 esu/cc std air
= 2.083 × 10^9 ion pairs/cc std air
= 1.61 × 10^{12} ion pairs/gm air
= 6.77 × 10^4 Mev/cc std air
= 5.24 × 10^7 Mev/gm air
= 83.8 erg/gm air

R = Roentgen
REP = Roentgen Equivalent Physical
REM = Roentgen Equivalent Man
RBE = Relative Biological Effectiveness

1 REP = 93 ergs/gm tissue

1 REM = 93/RBE erg/gm tissue

APPENDIX D. LIST OF ILLUSTRATIONS

APPENDIX E. LIST OF TABLES

APPENDIX F. ABBREVIATIONS

AEC	U. S. Atomic Energy Commission
AFSWC	Research Directorate, U. S. Air Force Special Weapons Center, Air Force Systems Command, Kirtland Air Force Base, New Mexico
ANL	Argonne National Laboratory, University of Chicago, Argonne, Illinois
ARF	Armour Research Foundation of Illinois Institute of Technology, Chicago, Illinois
ASHRAE	American Society of Heating, Refrigeration, and Air-Conditioning Engineers, 345 East 47th Street, New York 17, New York
ASTIA	Armed Services Technical Information Agency
BRL	U. S. Army Ballistic Research Laboratory
CRL	Chemical and Radiological Laboratories, Army Chemical Center, Maryland
DA	Department of the Army
DASA	Defense Atomic Support Agency
DOD	Department of Defense
ERDL	U. S. Army Engineer Research and Development Laboratories, Corp of Engineers, Fort Belvoir, Virginia
ESL	Evans Signal Laboratory, Fort Monmouth, New Jersey
GPO	Superintendent of Documents, U. S. Government Printing Office, Washington, D. C.
KAPL	Knolls Atomic Power Laboratory, General Electric Company, Schenectady, New York
NASA	National Aeronautics and Space Administration
NBS	National Bureau of Standards

NCEL	The Navy Department, Bureau of Yards and Docks, U. S. Naval Civil Engineering Laboratory, Port Hueneme, California
NDL	Nuclear Defense Laboratory, Army Chemical Center, Maryland
NRDL	U. S. Naval Radiological Defense Laboratory, San Francisco, California
OCDM	Office of Civil and Defense Mobilization
ORNL	Oak Ridge National Laboratory, Oak Ridge, Tennessee
OTS	Office of Technical Services
SRI	Stanford Research Institute, Stanford University, Stanford, California
SwRI	Southwest Research Institute, San Antonio, Texas
Tech. Ops.	Technical Operations, Inc., Burlington, Massachusetts
USDC	U. S. Department of Commerce
WADC	Wright Air Development Command, Chicago, Illinois

APPENDIX G. CONVERSION FACTORS

ENERGY

Energy	Kw hr	Btu	ft lb	cal	Mev
1 Kw hr	1	3415	2.66×10^{6}	8.60×10^{5}	2.24×10^{19}
1 Btu	2.93×10^{-4}	1	778.1	252	6.58×10^{15}
1 ft lb	3.77×10^{7}	1.29×10^{-3}	1	0.324	8.46×10^{13}
1 cal	1.16×10^{-6}	3.97×10^{-3}	3.088	1	2.61×10^{13}
1 Mev	4.45×10^{-20}	1.52×10^{-16}	1.18×10^{-13}	3.83×10^{-14}	1

MASS ENERGY

Mass Energy	Mass Unit	Mev	Erg	Calorie
1 Mass Unit (mu)	1	931	1.49×10^{-3}	3.56×10^{-11}
1 Mev	1.07×10^{-3}	1	1.59×10^{-6}	3.80×10^{-14}
1 Ery	671	6.28×10^{5}	1	2.39×10^{-8}
1 Calorie	2.81×10^{10}	2.62×10^{13}	4.186×10^{7}	1

POWER

Power	Hp	Kw	Btu/hr	cal/sec	Mev/sec
1 Hp	1	0.7457	2547	178.26	4.65×10^{15}
1 Kw	1.341	1	3415	239	6.24×10^{15}
1 Btu/hr	3.93×10^{-4}	2.93×10^{-4}	1	0.070	1.82×10^{12}
1 cal/sec	5.61×10^{-3}	4.18×10^{-3}	14.29	1	2.61×10^{13}
1 Mev/sec	2.15×10^{-16}	1.60×10^{-16}	5.47×10^{-13}	3.83×10^{-14}	1

Multiply	By	To Obtain
atmospheres	14.70	lbs/sq in
"	76.0	cm Hg
barns	10^{-24}	cm^2
British thermal units	1.055×10^3	joules
" " "	0.2520	kg-cal
Btu/lb	0.556	gm-cal/gram
centimeters	0.3937	inches
"	3.28×10^{-2}	feet
coulombs	6.28×10^{18}	electronic charges
"	2.997×10^9	statcoulombs
curies	2.22×10^{12}	distintegrations/min
"	3.7×10^{10}	dis/sec
"	10^3	millicuries
"	10^6	microcuries
"	10^{-3}	kilocuries
disintegrations/min	4.55×10^{-10}	millicuries
" "	4.55×10^{-7}	microcuries
dis/sec	2.7×10^{-8}	millicuries
" "	2.7×10^{-5}	microcuries
dynes	1.02×10^{-3}	gms
"	2.248×10^{-6}	lbs
electron volt (ev)	10^{-6}	Mev
" "	1.6×10^{-12}	ergs
" "	1.6×10^{-19}	joules
ergs	10^{-7}	joules
"	6.24×10^5	Mev
"	6.24×10^{11}	ev

Multiply	By	To Obtain
roentgen	1	esu/cm^3 (air, s.c.)*
"	2.083×10^9	ion prs/cm^3 (air, s.c.)*
"	1.61×10^{14}	ion prs/gm (air)
"	6.77×10^4	Mev/cm^3 (air, s.c.)*
"	5.24×10^7	Mev/gm (air)
"	83.8	erge/gm (air)
"	2.0×10^{-6}	cal/gm (air)
statcoulomb	3.34×10^{10}	coulombs
"	2.095×10^9	electronic charge

*Standard conditions -- 0 deg C (32 deg F.) and 760 mm Hg.

APPENDIX H. GLOSSARY

-A-

ABSORPTION: The process by which radiation imparts some or all of its energy to any material through which it passes.

ABSORPTION COEFFICIENT: Fractional decrease in the intensity of a beam of X- or gamma radiation per unit thickness (linear absorption coefficient), per unit mass (mass absorption coefficient), or per atom (atomic absorption coefficient) of absorber, due to deposition of energy in the absorber.

ALBEDO: A reflection coefficient. It is the ratio of reflected radiation with particular properties to the incident radiation. Reflection in a particular direction is termed differential or directional albedo. Albedo can be expressed in terms of dose, energy or counts (number of particles).

ALPHA PARTICLE: A helium nucleus, consisting of two protons and two neutrons, with a double positive charge.

ALPHA RAY: Stream of fast-moving helium nuclei (alpha particles); a strongly ionizing and weakly penetrating radiation.

ANGLE OF BURST: The angle subtended by a line between the center of a tunnel opening and the point of burst and the centerline of the tunnel.

ANGLE OF INCIDENCE: The minimum angle subtended by a ray of radiation impinging on a plane surface and a line in the plane of that surface.

ANGSTROM UNIT: Abbreviated Å. One Angstrom unit equals 10^{-8} cms.

ATOMIC NUMBER: Number of protons in the nucleus; hence the number of positive charges on the nucleus. Also the number of orbital electrons surrounding the nucleus of a neutral atom.

ATOMIC WEIGHT: The weighted mean of the masses of the neutral atoms of an element expressed in atomic weight units.

ATTENUATION: The process by which a beam of radiation is reduced in intensity when passing through some material. It is the combination of absorption and scattering processes and leads to a decrease in flux density of the beam when projected through matter.

ATTENUATION COEFFICIENT, PAIR PRODUCTION: That fractional decrease in the intensity of a beam of ionizing radiation due to pair production in a medium through which it passes.

-B-

BACKSCATTER: The deflection of radiation by scattering processes through angles greater than 90° with respect to the original direction of motion.

BARN: Unit expressing the probability of a specific nuclear reaction taking place in terms of cross-sectional area. Numerically it is 10^{-24} cm^2.

BEAM: An unidirectional or approximately unidirectional flow of electromagnetic radiation or particles.

BETA PARTICLE: Charged particle emitted from the nucleus of an atom and having a mass and charge equal in magnitude to those of the electron.

BETA RAY: A stream of high speed electrons or positrons of nuclear origin more penetrating but less ionizing than alpha rays.

BURST HEIGHT: Minimum distance from center of detonation to any point on the ground.

-C-

CAPTURE, RADIATIVE: The process by which a nucleus captures an incident particle and loses its excitation energy immediately by the emission of gamma radiation.

COLLISION: Encounter between two subatomic particles (including photons) which changes the existing momentum and energy conditions. The products of the collision need not be the same as the initial systems.

COUNT (Radiation measurements): The external indication of a device designed to enumerate ionizing events. It may refer to a single detected event or to the total registered in a given period of time. The term often is erroneously used to designate a disintegration, ionizing event or voltage pulse.

CROSS SECTION: A concept used to discuss quantitatively the interaction (absorption or scattering) of neutrons with atomic nuclei.

CROSS SECTION, MACROSCOPIC: Expresses the effectiveness of the total number of nuclei in a volume for providing a type of interaction (absorption or scattering).

CROSS SECTION, MICROSCOPIC: The cross section applying to a single nucleus.

CROSS SECTION, TOTAL: The sum of the possibility of absorption or scattering interaction between a neutron and the nuclei in a region.

CURIE: That quantity of a radioactive nuclide disintegrating at the rate of 3.700×10^{10} atoms per second. (Abbreviated: c.)

-D-

DIFFUSION LENGTH: A quantity appearing in the diffusion equation. The square of the diffusion length equals a sixth of the distance between the source and point of absorption by a neutron.

DOSE (DOSAGE): According to current usage, the radiation delivered to a specified area or volume or to the whole body. Units for dose specification are roentgens for X- or gamma rays, reps or equivalent roentgens for beta rays. In radiology the dose may be specified in air, on the skin, or at some depth beneath the surface; no statement of dose is complete without specification of location. In recent years, there has been an increasing tendency to regard a dose or radiation as the amount of energy absorbed by tissue at the site of interest per unit mass.

ABSORBED DOSE: The quantity of energy imparted to a mass of material exposed to radiation (see RAD).

AIR-DOSE: X-ray or gamma ray dose expressed in roentgens delivered at a point in free air. In radiologic practice, it consists of the radiation of the primary beam and that scattered from surrounding air.

CUMULATIVE DOSE (Radiation): The total dose resulting from repeated exposures to radiation of the same region, or of the whole body.

THRESHOLD DOSE: The minimum dose that will produce a detectable degree of any given effect.

TISSUE DOSE: Radiation dose received by a tissue in the region of interest. In the case of X-rays and gamma rays, tissue doses are expressed in roentgens. At the present time, the rep is the generally accepted unit of tissue dose for other ionizing radiation.

DOSE RATE (DOSAGE RATE): Radiation dose delivered per unit time.

DOSIMETER: Instrument used to detect and measure an accumulated dosage of radiation; in common usage, it is a pencil size ionization chamber with a built-in, self-reading electrometer; used for personnel monitoring.

-E-

ELECTRON VOLT: A unit of energy equivalent to the amount of energy gained by an electron in passing through a potential difference of one volt. Larger multiple units of the electron volt are frequently used, viz: Kev for thousand or kilo electron volts; Mev for million electron volts and Bev for billion electron volts. (abbreviated: ev) 1 ev = 1.18×10^{-19} foot-pounds.

ERG: Unit of work done by a force of 1 dyne acting through a distance of one cm. Unit of energy which can exert a force of one dyne through a distance of one cm; cgs units; dyne-cm or $gm\text{-}cm^2/sec^2$.

-F-

FISSION, NUCLEAR: A nuclear transformation characterized by the splitting of a nucleus into at least two other nuclei and the release of a relatively large amount of energy.

FISSION PRODUCTS: Elements or compounds resulting from fission.

FISSION YIELD: The percentage of fissions leading to a particular nuclide by direct formation and by decay of precursors.

FLUX: For electromagnetic radiation, the quantity of radiant energy flowing per unit time. For particles and photons, the number of particles or photons flowing per unit time.

> NEUTRON FLUX: A term used to express the intensity of neutron radiation. The number of neutrons passing through a unit area in unit time. For neutrons of a given energy, the product of neutron density with speed.

-G-

GAMMA, INITIAL: Gamma radiation emitted within one minute after initiation of detonation, including prompt gamma.

GAMMA, NITROGEN CAPTURE: Gamma radiation induced through the capture of a neutron by the nucleus.

GAMMA, PROMPT: Gamma radiation emitted at the time of fission of a nucleus.

GAMMA RAY: Short wavelength electromagnetic radiation of nuclear origin with a range of wavelengths from about 10^{-8} to 10^{-11} cm, emitted from the nucleus.

GRAM-ROENTGEN: A unit of integral dose; the real energy conversion when one roentgen is delivered to one gram of air (83.8 ergs).

GROUND ZERO: The point on the earth's surface immediately above or below the point of detonation.

-H-

HALF-LIFE, RADIOACTIVE: Time required for a radioactive substance to lose 50 percent of its activity by decay. Each radionuclide has a unique half-life.

-I-

IN-SCATTER: Radiation which would have missed a detector center but was scattered into the detector by an adjacent medium.

INTEGRATED NEUTRON FLUX: The product of neutron flux and exposure time, which equals the total number of neutrons passing through a unit area.

ION PAIR: Two particles of opposite charge, usually referring to the electron and positive atomic or molecular residue after the interaction of ionizing radiation with the orbital electrons of atoms.

-K-

KLEIN-NISHINA COEFFICIENT: The probability of an amount of energy being scattered through an appropriate angle into a detector, for a particular particle energy.

KLEIN-NISHINA FORMULA: A formula that expresses the cross section of an unbound electron for scattering of a photon in the Compton effect, as a function of the energy of the photon. The term usually refers to the integral Klein-Nishina formula, which gives the total cross section for the process. The differential Klein-Nishina formula gives the differential cross section for scattering at a given angle.

-M-

MILLIROENTGEN (mr): A submultiple of the roentgen equal to one one-thousandth (1/1000th) of a roentgen.

MONTE CARLO: A mathematical procedure for computing the interaction between a photon and the medium in which it is traveling. The procedure usually requires machine computation.

-N-

NEUTRON: Elementary nuclear particle with a mass approximately the same as that of a hydrogen atom and electrically neutral; its mass is 1.008986 mass units. Thermal neutrons are in thermal equilibrium with their surroundings. Fast neutrons have energies greater than 0.5 Mev.

NUCLEUS (NUCLEAR): That part of an atom in which the total positive electric charge and most of the mass are concentrated.

-P-

PAIR PRODUCTION: An absorption process for X- and gamma radiation in which the incident photon is annihilated in the vicinity of the nucleus of the absorbing atom with subsequent production of an electron and positron pair. This reaction only occurs for incident photon energies exceeding 1.02 Mev.

PHOTON: A quantity of electromagnetic energy.

-Q-

QUANTUM: Synonymous with PHOTON.

-R-

RAD: The unit of absorbed dose, which is 100 ergs/gram. The rad is a measure of the energy imparted to matter by ionizing radiation per unit mass of irradiated material at the place of interest. This unit was recommended and adopted by the International Commission on Radiological Units at the Seventh International Congress of Radiology, Copenhagen, July 1953.

RADIATION: 1. The emission and propagation of energy through space or through a material medium in the form of waves; for instance, the emission and propagation of electromagnetic waves, or of sound and elastic waves.

2. The energy propagated through space or through a material medium as waves; for example, energy in the form of electromagnetic waves or of elastic waves.

BACKGROUND RADIATION: Radiation arising from radioactive material other than the one directly under consideration. Background radiation due to cosmic rays and natural radioactivity is always present. There may also be background radiation due to the presence of radioactive substances in other parts of the building, in the building material itself, etc.

SCATTERED RADIATION: Radiation which, during its passage through a substance, has been deviated in direction. It may also have been modified by an increase in wavelength. It is one form of secondary radiation.

SECONDARY RADIATION: Radiation originating as the result of absorption of other radiation in matter. It may be either electromagnetic or particulate in nature.

RAY: The straight line path that a photon travels between interactions.

ROENTGEN: The quantity of X- or gamma radiation such that the associated corpuscular emission per 0.001293 grams (1 cm^3) of standard air produces, in air, ions carrying 1 electrostatic unit of quantity of electricity of either sign. Standard air is taken as dry air at 0° C and 760 mm Hg (1 atm) pressure.

ROENTGEN EQUIVALENT MAN (REM): That quantity of any type ionizing radiation which when absorbed by man produces an effect equivalent to the absorption by man of one roentgen of X- or gamma radiation (400 KV).

ROENTGEN EQUIVALENT PHYSICAL (REP): The amount of ionizing radiation which will result in the absorption in tissue of 83 ergs per gram. (Recent authors have suggested the value 93 ergs per gram.)

-S-

SCATTERING: Change of direction of subatomic particle or photon as a result of a collision or interaction.

SHIELD: A body of material used to prevent or reduce the passage of particles or radiation. A shield may be designated according to what is intended to absorb, as a gamma-ray shield or neutron shield, or according to the kind of protection it is intended to give, as a background, biological, or thermal shield. It may be required for the safety of personnel or to reduce radiation sufficiently to allow use of counting instruments for research or for locating contamination or airborne radioactivity.

SLANT RANGE: Distance from point of interest directly to center of detonation.

SOURCE: The initiating point for photons.

POINT ISOTROPIC SOURCE: A source from which radiation emanates equally in all directions.

PLANE ISOTROPIC SOURCE: A plane array of point isotropic sources.

BROADBEAM PARALLEL SOURCE: A plane source from which all rays emerge monodirectionally; that is, the rays are all parallel.

COSINE SOURCE: A plane source in which the intensity in any angular direction varies as the cosine of that angle from the normal.

SPECTRUM: An array of the components (energies or frequencies) of radiation.

-T-

TRANSPORT MEAN FREE PATH: A term with units of length which is related to the macroscopic scattering cross section and the average cosine of the scattering angle.

-Y-

YIELD: The energy in a nuclear explosion, usually expressed in terms of tons of TNT.